Aerobic methane production from organic matter

Ivan Vigano

Author: Ivan Vigano (registered in Italy as Ivan Aronne Viganó)
ISBN: 978-90-393-52540
Printing: Ipskamp Drukkers BV, Enschede

Atmospheric Physic and Chemistry Group
Institute for Marine and Atmospheric research Utrecht (IMAU)
Department of Physic and Astronomy
Faculty of Science
Utrecht University

Aerobic methane production from organic matter

Aerobe methaan productie uit organisch materiaal

(met een samenvatting in het Nederlands)

Proefschrift

ter verkrijging van de graad van doctor aan de Universiteit Utrecht op gezag van de rector magnificus, prof.dr. J.C. Stoof, ingevolge het besluit van het college voor promoties in het openbaar te verdedigen op vrijdag 8 januari 2010 des ochtends te 10.30 uur

door

Ivan Vigano

geboren op 23 december 1978 te Bergamo, Italy

Promotor: Prof.dr. T.Röckmann

Dedicated to: Giuseppe Spreafico

Teresa Moroni

Alberto Consonni

"It doesn't matter how beautiful your theory is, it doesn't matter how smart you are. If it doesn't agree with experiment, it's wrong"

Richard Feynman

contents

Chapter 4

Chapter 5

Chapter 6

Chapter 7

Chapter 8

Samenvatting (in Dutch)

De doelstelling van het onderzoek dat in dit proefschrift gepresenteerd wordt is aerobe methaanproductie uit organisch materiaal te karakteriseren door gebruik te maken van verschillende experimentele technieken.
Samen met H_2O, CO_2 en N_2O speelt methaan (CH_4) een grote rol in de stralingsbalans van de atmosfeer en is dus een belangrijk broeikasgas. Het is al decennia lang bekend dat de productie van het volledig gereduceerde methaan bijna uitsluitend plaatsvind onder zuurstofarme omstandigheden, met name door productie door micro-organismen uit het rijk der *Archaea*. Methaan kan ook ontstaan bij onvolledige verbranding van organisch materiaal. De productie van CH_4 in een zuurstofrijk milieu onder omstandigheden die representatief zijn voor die in de atmosfeer is een nieuwe ontdekking die in 2006 door Keppler et al. werd gedaan. Verrassend genoeg hebben zij methaanemissies van planten gemeten in een afgesloten kamer met lucht die 20% zuurstof bevatte. Hoewel de schattingen van de totale wereldwijde productie uit deze bron nog onderwerp van discussie zijn, worden in dit proefschrift resultaten gepresenteerd waaruit duidelijk naar voren komt dat het mogelijk is om methaan te vormen uit afgestorven plantenresten wanneer er zuurstof voorhanden is. Temperatuur en het UV licht zijn zeer belangrijke factoren voor de productie van CH_4 uit plantaardig materiaal in een zuurstofrijke omgeving. Metingen aan levende planten worden in dit proefschrift niet behandeld.
Verscheidene belangrijke ontdekkingen zijn gedaan dankzij geavanceerde meettechnieken:

1. Dat methaanproductie uit plantenbiomassa kan plaatsvinden in aerobe processen is nu bevestigd.
2. Bacteriën zijn niet verantwoordelijk voor deze processen.
3. UV-straling en temperatuur zijn zeer belangrijke parameters die de intensiteit van de emissies bepalen.
4. Zelfs in het donker en bij kamertemperatuur worden zeer kleine hoeveelheden CH_4 uitgestoten.
5. De isotoopsamenstelling van het aerobe methaan is nu bepaald.
6. Ook is de rol van water op het deuteriumgehalte van het plantmateriaal en het uitgestoten methaangas bestudeerd.

In het eerste hoofdstuk wordt de rol van methaan in de atmosfeer uitgelegd.

Eerst wordt de rol van methaan als broeikasgas verklaard. Met name de sterke toename van de antropogene (door de mens veroorzaakte) emissies in de afgelopen eeuw en de veranderingen in de atmosferische methaanconcentratie zullen besproken worden. Om methaanconcentraties van langer geleden te bepalen zijn deze concentraties gemeten in lucht die ingesloten was in ijskernen. Voor methaan blijken deze gekoppeld te zijn aan temperatuursveranderingen, hoewel er ook uitzonderingen zijn. Methaan draagt ruwweg 20 procent bij aan de extra stralingsforcering als gevolg van broeikasgassen sinds 1750, en daarom zijn de classificatie en de kwantificatie van

de bronnen en afbraakprocessen van belang in de context van de recente klimaatverandering. Isotoopmetingen kunnen een belangrijke rol spelen in het bepalen van de grootte van de individuele bronnen en afbraakprocessen. Daartoe wordt de huidige status van onderzoek naar isotoopverhoudingen gepresenteerd. Tot slot wordt de geschiedenis van het aerobe methaanonderzoek geïntroduceerd.

De belangrijkste meettechnieken worden beschreven in het tweede hoofdstuk. De meest voorkomende methode gebruikt een gaschromatograaf om componenten te scheiden, gekoppeld aan een vlamionisatiedetector voor een robuuste analyse met hoge precisie en nauwkeurigheid. De ontwikkeling van lasertechnologieën gebaseerd op absorptiespectra van moleculen gaat tegenwoordig zeer snel. Na speciale aandacht voor CO_2 en H_2O, is er de laatste jaren veel aandacht voor methaan. De nieuwe instrumenten hebben een zeer hoge precisie, kunnen continu meten en snelle en robuuste metingen zijn mogelijk. Voor de bepaling van de stabiele isotoopverhouding in methaan, $^{13}C/^{12}C$ en D/H respectievelijk voor koolstof en waterstof, is de massaspectrometrie de nauwkeurigste en meest gebruikte techniek. Een overzicht van de basisconcepten van massaspectrometrie voor stabiele isotoopmetingen zal worden gegeven.
In hoofdstuk 3 wordt toegelicht hoe methaan kan worden gevormd wanneer plantenresten met UV-licht worden bestraald en wanneer de temperatuur verhoogd wordt. Verscheidene tests zijn gedaan op verschillende soorten droge en losse bladeren met als resultaat een grote diversiteit in de emissiesnelheden. De reactie vindt snel plaats, wat suggereert dat methaan geproduceerd wordt als gevolg van een snelle fotochemische reactie. In het geval van UV-licht verdwijnen de emissies over het algemeen bij temperaturen rond 0°C. Zonder UV licht is de methaanproductie moeilijk te meten met de gebruikelijke meettechnieken, maar wij hebben zelfs uiterst kleine emissies van methaan bij kamertemperatuur en zonder licht kunnen meten door gebruik te maken van speciale instrumentele isotooptechnieken. Een zeer sterke stijging van de methaanproductie wordt waargenomen bij temperaturen boven 70°C. Deze experimentele studie bevestigt zonder twijfel het bestaan van aerobe productie van methaan uit organisch plantenmateriaal.
De isotoopverhoudingen van methaan worden vaak gebruikt om het mondiale methaanbudget te begrijpen, en de verschillende methaanbronnen en –afbraanprocessen te kwantificeren. Het is bekend dat de koolstof- en waterstofisotoopverhouding, respectievelijk $^{13}C/^{12}C$ en D/H, van bron tot bron verschilt afhankelijk van het productieproces. Gewoonlijk bevatten methaan van geologische oorsprong en methaan dat is gevormd bij de verbranding van biomassa zwaardere isotopen, terwijl methaan uit de biologische bronnen relatief veel lichte isotopen bevat. De aerobe vorming van methaan met UV-licht is een nieuw proces en de doelstelling van hoofdstuk 4 is het identificeren van de karakteristieke koolstof- en waterstofisotoopverhoudingen. Dit wort gedaan worden door droge bladeren van verschillende plantensoorten te bestralen met UV-licht. Voor iedere plantensoort is de karakteristieke isotoopverhouding bepaald met behulp van Keelingplot analyse. Plantensoorten met C3-, C4- en CAM-fotosynthese–werden geanalyseerd en het geproduceerde methaan laat verschillende karakteristieke isotoopverhoudingen zien voor elke categorie. C4- en CAM-planten zijn meer verrijkt in zware isotopen, wat te verwachten was aangezien eerdere biochemische isotoopstudies zulke verschillen al aangetoond hebben voor andere organische stoffen. Niet alleen werden de isotoopnanalyses van methaan hier gemeten, ook de koolstof en waterstofisotoopverhouding van het bulkmateriaal en van de methoxylgroepen (–

OCH_3), het belangrijkste substraat van aeroob methaan, werden bepaald. In feite kon uit de correlaties tussen CH_4 en de andere isotoopanalyses afgeleid worden dat methoxylgroepen betrokken zijn bij de productie, maar zoals in hoofdstuk 6 beschreven wordt, kan dit niet de enige bron zijn. Het is van belang om op te merken dat de berekende emissiesnelheden hoger zijn voor C3-planten in vergelijking met C4- en CAM-planten, en de redenen hiervoor worden kwalitatief verklaard.

De enige bron van waterstof in planten is water en de isotoopbalans van bio-organische verbindingen is sterk gerelateerd aan de isotoopsamenstelling van het water dat de plant gebruikt. Hoofdstuk 5 is een studie gericht op het bepalen van de relatie tussen de waterstofisotopen in het methaan dat uitgestoten wordt door de planten en het water dat ze opnemen. Wij kweekten een aantal planten met water met een verschillend deuteriumgehalte om hun isotoopverhouding te veranderen, en vervolgens verzamelden we de bladeren. De bladeren werden geanalyseerd zoals eerder beschreven. De karakteristieke waterstofisotoopverhoudingen van het uitgestoten methaan zijn verassend goed gerelateerd aan die van het toegediende water volgens een 1:1 relatie. Andere waterstofisotoopanalyses zijn uitgevoerd op het bulkmateriaal en de methoxylgroepen, en vanuit de correlaties tussen methaan en deze groepen bevestigen wij de rol van methoxylgroepen als potentieel substraat voor ruwweg de helft van de productie van CH_4. De bevindingen van deze studie zijn in overeenstemming met eerdere studies van methaan uit micro-organismen waar de isotoopafhankelijkheid van het omringende water ook werd aangetoond. Wij zullen ook de rol van mondiale patronen in het deuteriumgehalte van neerslag op het deuteriumgehalte van methaan bespreken.

In Hoofdstukken 6 en 7 worden twee studies gepresenteerd waarbij ik zeer betrokken was bij de opzet en de experimentele uitvoering van het onderzoeksproject, maar niet de eerste auteur van de publicatie werd. De eerste studie is gebaseerd op laboratoriumexperimenten, waar een reeks isotoopmarkeringsstudies gedaan werd om de chemische voorlopers/substraten die bij het proces van aerobe aerobe methaanvorming een rol spelen, te identificeren. Al in de eerste studie van Keppler et al. werden methoxylgroepen (–OCH_3) geopperd als potentiële kandidaten. In feite heeft men vastgesteld dat ongeveer 50% van het methaan uit deze groepen wordt gevormd, terwijl de rest gevormd zou moeten worden uit nog niet opgehelderde en gekwantificeerde reservoirs.

De tweede studie (hoofdstuk 7) betrof een veldexperiment in een bos, waarbij de veldmetingen zijn uitgevoerd met de eddy-covariantie-techniek. Deze techniek is geschikt voor de bepaling van CH_4-, CO_2- en H_2O-fluxen in het veld over redelijk grote gebieden. Deze micrometeorologische technieken zijn reeds lang gevestigd en worden sinds jaar en dag gebruikt voor het bepalen van CO_2- and H_2O-fluxen in diverse ecosystemen. De verbeteringen in de laserspectroscopie hebben hoge-frequentiemetingen van de concentratie van CH_4 mogelijk gemaakt. Met behulp van de eddy-covariantie-theorie kan de verticale flux berekentd worden wanneer windsnelheid en richting bekend zijn met dezelfde frequentie als de metingen. De studie werd uitgevoerd in het Blodgett bos, met veel bomen van de soort *Pinus ponderosa* dat in bezit is van de Universiteit van Berkeley en is gelegen op de bergrug van de Sierra Nevada, 100 km ten oosten van Sacramento (Californië, V.S.). De meting werden gedaan tijdens de 2^e en 3^e week van augustus 2007, in uiterst droge omstandigheden. Dit was de eerste meting van methaanfluxen in een dergelijk droog ecosysteem. Het oorspronkelijke idee was dat bij hoge temperaturen en relatief hoge UV-niveaus het misschien mogelijk was om aerobe methaanproductie in het veld te

meten. Het resultaat is echter in tegenspraak met de hypothese, aangezien wij slechts negatieve fluxen voor CH_4 waarnamen.
Deze hoge opname wordt veroorzaakt door de hoge methaanconsumptie van de grond in dat gebied. De aerobe methaanemissie moet een kleinere omvang hebben, waardoor het niet mogelijk is om deze van sterke opname te scheiden met micrometeorologische methodes.

Summary

The research presented in this thesis aims to characterize the aerobic methane production from organic material by laboratory experiments using a number of experimental approaches.

Methane, together with H_2O, CO_2 and N_2O, is an important greenhouse gas in the Earth's atmosphere playing a key role in the radiative budget. It has been known for decades that the production of the reduced compound CH_4 is possible almost exclusively in anoxic environments "*per opera"* of one of the most important class of microorganisms which form the *Archaea* reign. Methane can be produced also from incomplete combustion of organic material. The generation of CH_4 in an oxygenated environment under near-ambient conditions is a new discovery made in 2006 by Keppler et al. where surprisingly they measured emissions of this greenhouse gas from plants incubated in chambers with air containing 20% of oxygen. Although the estimates on a global scale are still object of an intensive debate, the results presented in this thesis clearly show the existence of methane production under oxic conditions for non living plant material. Temperature and UV light are key factors that drive the generation of CH_4 from plant matter in a well oxygenated environment. Living plant measurements are not part of dissertation.

Here, several important discoveries have been made thanks to advanced measurement techniques:

1. Validation of the finding that aerobic processes lead the methane production from plant biomass
2. These processes are non-microbial
3. UV radiation and temperature are key parameters determining the strength of the emissions
4. Even in the dark and at room temperature very small amounts of CH_4 are emitted
5. Determination of the isotopic fingerprint for the aerobic methane
6. Determination of a key role of water in driving the deuterium isotope balance in the plant compounds and in the methane emitted

In the first chapter the role of methane in the atmosphere is presented. First the role of methane as greenhouse gas is explained and changes in atmospheric methane concentrations in the last century and the rapid increase due mainly to anthropogenic inputs are discussed. Millennial scale variability has been recorded in ice cores and methane changes are closely coupled to temperature changes, although with exceptions. Methane is contributing roughly 20 % to the radiative forcing due to greenhouse gases since 1750, consequently the classification and quantification of the sources and sinks are of importance in the context of the recent climate change. Isotope measurements can play an important role in examining the individual source and sink strengths, and the present knowledge of isotope signatures is presented. Finally, an introduction to the history of the aerobic methane research is presented.

The main measurement techniques are described in the second chapter. The most common method employs gas chromatographic (GC) separation coupled to a flame ionization detector (FID), which allows robust analyses with good precision and

accuracy. The development of laser technologies, based on the absorption spectrum characteristic of every molecule, nowadays is increasing in science and, after CO_2 and H_2O, special attention has been given to CH_4 in the last years. The new instruments have a very high precision, can measure continuously and fast measurement, the system is robust as well.
For the determination of the stable isotope content in CH_4, $^{13}C/^{12}C$ and D/H respectively for carbon and hydrogen, mass spectrometry is the most precise and most widely used technique. An overview of the basic concepts in mass spectrometry for stable isotope measurements will be given.

The chapter 3 elucidates the topic on how methane can be formed when the plant material is irradiated with UV light and when the temperature increases. Several tests have been made on different dry and detached leaves which interestingly showed diverse emission rates. The evolution of the reaction is fast suggesting that the methane generation follows a rapid photochemical pathway. Under UV light, for temperatures around 0°C the emissions tend to disappear. Without light the methane production is hard to detect with common measurement techniques, but we have been able to measure even tiny emissions of methane at room temperature and without light using special isotope instrumental approaches. A very sharp increase of production is noted when temperatures rise above 70°C. This experimental study confirms without doubt the existence of aerobic production of methane from organic plant matter.

Isotope signatures of methane have been widely used to constrain the global methane budget and to define the different methane sources. It is well known that the carbon and hydrogen isotope ratio, $^{13}C/^{12}C$ and D/H respectively, changes from source to source depending on the formation process. Usually geological CH_4 and methane from biomass burning contain more heavy isotopes while biological sources are more depleted. The aerobic formation of methane with UV light is a new process and the scope of chapter 4 is to identify its carbon and deuterium isotope fingerprint. The objective is achieved with several measurements on dry leaves of different species irradiated with UV light. For each plant species the isotope signature was determined using Keeling plot analysis. Plant species belonging to C3, C4 and CAM metabolic pathways were analyzed and the methane produced reveal distinct isotope signature for each category. C4 and CAM plants are more enriched in heavy isotopes than C3 plants, as expected since earlier isotope biochemical studies already reported such isotope differences for some organic compounds. Not only isotope analyses of methane were performed here but we also determined the carbon and hydrogen isotope ratio for the bulk material and for the methoxyl groups ($-OCH_3$) which are the major substrate of aerobic methane. In fact from the correlations between CH_4 and the other isotopic analyses it has been possible to confirm that effectively $-OCH_3$ are involved in the production but as it will be described in chapter 6, they cannot be the only source. It is of interest to note that the emission rates calculated are higher for C3 plants compared to C4-CAM plants and the reasons for that will be qualitatively explained.

The only source of hydrogen in plants is water and the isotope balance of the biocompounds is strongly related to the isotopic composition of water that the plant uses. Chapter 5 presents a study aimed to define a hydrogen isotope relation between the methane emitted from the plant matter and the source water. We grew some plant species with water of different deuterium content in order to change their isotope

content and successively we collected the leaves which were analyzed like in the previous study. The deuterium signatures of the methane emitted are surprising well related to the source water with a 1:1 relation. Other hydrogen isotopic analyses have been performed on bulk and methoxyl groups, and from the correlations between CH_4 and these moieties we confirm the role of methoxyl groups as potential substrate for roughly 50% of the CH_4 production. The findings of this study are in general agreement with previous studies on methane from microorganisms in which the isotope dependence with the surrounding water was also presented. We will discuss also the role of global isotope precipitation patterns on the deuterium content of the methane emitted from plants.

Chapter 6 and 7 presents two studies, in which I was strongly involved in the setup and experimental work of the projects, but not first author of the publications.
The chapter 6 is reporting a series of isotope labelling studies which were made in order to find out the chemical precursors/substrates participating in the aerobic methane formation. Already the first study of Keppler et al. suggested methoxyl groups ($-OCH_3$) as potentially candidates. In fact it has been established that about 50% of the methane is formed from such chemical moieties, while the rest should derive from other not yet quantified and individuated reservoirs.
Chapter 7 presents the results of a field measurement campaign which was performed by employing Eddy Covariance techniques. They are suitable for the determination of CH_4, CO_2 and H_2O fluxes in the field over reasonably large areas. These micrometeorological techniques are well established and have been utilized for years for assessing fluxes of CO_2 and H_2O in various ecosystems. The improvements in laser spectroscopy detection made similar applications for high frequency measurements of CH_4 concentration possible. From the theory of Eddy Covariance, knowing the vertical wind speed at the same frequency of the measurements, allows the calculations of the vertical fluxes. The study was performed, at Blodgett forest, an afforested area with *Ponderosa* owned by the University of Berkeley and situated on the Sierra Nevada ridge, 100 km east of Sacramento (Ca, U.S.A.). The period of measurement was during the 2^{nd} and 3^{rd} week of august 2007, characterized by extremely dry conditions. These were the first measurement of methane fluxes made in such a dry ecosystem. The original idea was that with warm temperatures and relatively elevated UV levels we may be able to detect aerobic methane production in the field. The result contradicts the hypothesis since we observed only negative fluxes of CH_4. The strong uptake measured is due to soil consumption in that area, and the aerobic methane emission must have a smaller magnitude and it is not possible to separate it from the strong uptake with micrometeorological methods.

Sommario (in Italian)

La ricerca presentata in questa tesi ha avuto come scopo quello di caratterizzare la produzione aerobica di metano dalla materia organica impiegando esperimenti di laboratorio e differenti techniche di misura.

Il metano assieme a H_2O, CO_2 e N_2O, é un importante gas serra presente in atmosfera e gioca un ruolo determinante nel bilancio radiativo atmosferico. É la piu' semplice forma ridotta di idrocarburi e per decenni si é pensato che la sua formazione avvenisse solo in condizioni anossiche per opera di una delle piú importanti classi di microorganismi conosciuta come il regno degli *Archaea*. Il metano puó essere prodotto anche da combustione incompleta di materiale organico; la generazione di CH_4 in atmosfera ossigenata in condizioni naturali é una nuova scoperta fatta nel 2006 da Keppler et al., dove sorprendentemente hanno misurato emissioni di questo gas serra da piante vive incubate in comune aria contenente il 20% di ossigeno. Sebbene le precedenti stime globali sono ancora oggetto di intensi dibattiti, i risultai presentati in questa dissertazione dimostrano chiaramente l'esistenza di produzione di CH_4 da materiale organico non vivente in condizioni ossiche. Temperatura e radiazione ultravioletta sono i fattori chiave che ne dirigono la generazione in ambiente ossigenato. Misure di emissioni da piante vive non sono incluse nella presente.
Importanti scoperte scientifiche sono state effettuate grazie all'utilizzo di tecniche di misura avanzate:

1. Validazione del processo di formazione aerobica del metano da materiale organico
2. Valutazione della abioticitá del processo
3. Temperature e radiazione ultravioletta sono i parametri chiave che determinano l'efficenza di produzione
4. L'emissione di CH_4 avviene anche a temperatura ambiente e senza luce
5. Determinazione delle relative firme isotopiche
6. Determinazione dell ruolo chiave dell H_2O nel guidare il bilancio isotopico del deuterio nei composti biochimici delle piante e conseguenmtemente nel metano rilasciato.

Il primo capitolo descrive il ruolo del metano in atmosfera come gas serra; si descrivono i cambiamenti di concentrazioni avvenuti nell'ultimo secolo e l'incremento avvenuto principalmente per cause antropogeniche. Cambiamenti su scala millenaria sono stati registrati in carote di ghiaccio polari ed i cambiamenti di concentrazioni di metano sono altamente correlati con quelli delle temperature sebbene con eccezioni tuttora non chiaramente spiegabili. Il metano contribuisce per circa il 20% dell effetto serra degli ultimi due secoli, di conseguenza la classificazione e la quantificazione delle emissioni e dei processi che ne determinano la degradazione sono di importanza nel contesto dei recenti cambiamenti climatici. Le misurazioni isotopiche sono un sistema indinspensabile per esaminare le emissioni da varie fonti ed i processi di trasformazione, per questo la conoscenza delle firme isotopiche sará dettagliatamente discussa, cosi come la storia della ricerca effettuata in questo settore.

Le fondamentali tecniche di misura sono descritte nel secondo capitolo. Il metodo piú comune utilizza la tecnica gas cromatografica con rilevatore a fiamma ionizzante (FID). Recentemente si sono sviluppate tecnologie ottiche laser di alta precisione basate sullo spettro di assorbimento caratteristico di ogni molecola e nelle scienze atmosferiche perticolare attenzione é stata data per i costituenti dei gas serra come CO_2 H_2O e ultimamente CH_4.

Per la determinazione del contenuto isotopico nel CH_4, $^{13}C/^{12}C$ e D/H, rispettivamente per carbonio e idrogeno, la spettrometria di massa é la tecnica piú precisa e piú largamente utilizzata. Verranno illustrati i concetti basilari usati in spettrometria di massa per isotopi stabili.

Le cosidette firme isotopiche del metano sono state largamente usate per la determinazione del budget globale in atmosfera e per caratterizzare le diverse fonti. É ben noto che il rapporto isotopico del carbonio e dell idrogeno, $^{13}C/^{12}C$ e D/H rispettivamente, cambiano, dipendentemente dal tipo di processo di formazione. Solitamente le fonti geologiche ed il metano generato da combutione di biomasse é arricchito di isotopi pesanti mentre le sorgenti biologiche rilasciano metano contenente gli isotopi piú leggeri. La formazione aerobica di metano con radiazione UV é un nuovo processo e lo scopo del quarto capitolo é quello di identificarne la firma isotopica rispetto al carbonio e all'idrogeno. L'obbiettivo é stato raggiunto attraverso misurazioni eseguite su foglie, preventivamente essicate, di diverse piante irradiate con luce ultravioletta. Per ogni specie ne é stata determinata la firma isotopica utilizzando l'analisi di Keeling. Le piante appartenenti ai gruppi metabolici C3, C4 e CAM, sono state analizzate e il metano emesso rivela distinte firme isotopiche; C4 e CAM emettono CH_4 piú arricchito di isotopi pesanti rispetto alle C3, come daltronde, simili differenze isotopiche sono giá state riportate da altri studi su composti biochimici. Oltre al CH_4 sono state effettuate analisi isotopiche del totale organico e dei gruppi metossilici ($-OCH_3$) che sono uno dei maggiori substrati di formazione come verrá descritto nel sesto capitolo. E' di interesse notare come le emissioni derivate siano maggiori per le piante C3 rispetto alle piante C4-CAM per ragioni che verranno qualitativamente spiegate.

La sola sorgente di idrogeno nelle piante é l'acqua e il bilancio isotopico delle biomolecole é fortemente influenzato dalla composizione isotopica dell'acqua che la pianta transpira. Il capitolo 5 definisce relazioni isotopiche tra il CH_4 emesso dalla materia vegetale e l'acqua utilizzata per la crescita della pianta. Abbiamo coltivato diverse specie di piante con acqua a diverso contenuto isotopico in deuterio e successivamente abbiamo effettuato analisi isotopiche sulle foglie come precedentemente descritto. La firma isotopica del CH_4 rispetto al deuterio ($\delta D\text{-}CH_4$) é sorprendemente ben relazionata con quella dell'acqua ($\delta D\text{-}H_2O$) per un fattore 1:1. Anche in questo caso sono state effettuate analisi del contenuto isotopico in deuterio (δD) per il totale organico e per i gruppi metossilici, dove si conferma che essi sono effettivamente coinvolti per c.a. il 50% del metano prodotto. Queste scoperte concordano generalmente con studi giá effettuati su microorganismi metanogeni e le loro relazioni isotopiche con l'acqua. Verrá discusso anche il possibile ruolo delle precipitazioni globali nel modulare il contenuto in deuterio del metano atmosferico.

I capitoli 6 e 7 presentano due ricerche in cui, pur non essendo il primo autore delle pubblicazioni, ne sono stato coinvolto per quanto riguarda la coordinazione e la messa in opera degli strumenti.

Il sesto capitolo tratta una serie di studi isotopici atti a identificare i potenziali precursori chimici coinvolti nella produzione aerobica del metano. Siccome Keppler et al. suggerirono i gruppi metossilici come possibili candidati, dalle nostre valutazioni abbiamo stabilito che c.a. il 50% del metano é formato da queste parti esteree, mentre il resto dovrebbe derivare da altri composti non ancora identificati.

Il settimo capitolo e' uno studio di campagna di misura effettuata con le techniche di Eddy Covariance. Sono metodiche di micrometeorologia per la determinazione di flussi di CH_4, CO_2 e H_2O. Conoscendo le componenti vettoriali del vento e le variazioni di concentrazione del gas monitorato é possibile misurare ad alta frequenza questi valori e calcolare la componente verticale del flusso. Questo studio é la prima misurazione di flussi di metano negli Stati Uniti effettuata in foresta (Sierra Nevada, California, U.S.A.) c.a. 100km ad est di Sacramento durante la seconda e la terza settimana di agosto 2007, periodo caratterizzato da condizioni secche estreme L'idea principale fú quella di monitorare i flussi di metano in un ecosistema naturale durante una stagione calda e sotto l'influezza di radiazioni ultraviolette. Di fatto non fú possibile misurare emissioni significative di metano come previsto dalle nostre ipotesi, ma furono osservati flussi negativi diretti verso il suolo ed associati con le ore piú calde delle giornate. Questo é di fatto un segnale tipico dovuto alla presenza di microorganismi metanotrofi nel terreno e la produzione aerobica di CH_4 dovuta alle alte temperature e agli UV, é probabilmente di piccola entitá per essere identificata con le techniche meteorologiche convenzionali.

Chapter 1

About methane & climate

This dissertation is reporting research studies conducted at the Institute of Marine and Atmospheric Research in Utrecht (IMAU), faculty of Physics, Utrecht University.

The project was established to follow and to understand different scientific topics of not defined knowledge, and most of the results reported here were obtained working in the isotope-lab of my supervisor Prof. T.Röckmann.

The subject treated here is the role of methane (CH_4) in the biosphere and its aerobic formation from plant matter.

The most intriguing finding is that the generation of such reduced compound can happen in a non reduced environment as it was always thought in the past for the microbial fermentation.

Studies reported here and published in international scientific journals demonstrated the physical and chemical interactions behind the CH_4 generation, opening a new scenario not investigated in the past. This research also has been possible thanks to new instrumental and advanced measurement techniques.

After on the importance of methane in the atmosphere, we will present a detailed description of the main research activities.

Finally the conclusions will give a general overview and future perspectives in the context of climate change.

.

1.1 Tropospheric methane

Methane (CH_4) is the most abundant and the simplest reduced organic gas in the atmosphere. Its mixing ratio at present is approximately 1.8 ppm (parts per million). Methane is one of the strong greenhouse gases, together with water (H_2O), carbon dioxide (CO_2) and nitrous oxide (N_2O) [*Badr et al.*, 1991; *Collins et al.*, 2006; *Forster et al.*, 2007; *IPCC*, 2007].

Atmospheric CH_4 concentrations have increased by about 150% (1,060 ppb) since 1750 due mainly to human activity [*IPCC*, 2007]. Therefore this gas has been intensively monitored all around the globe for several decades. A slowing down of the increasing mixing ratio has been observed since 1990 and the atmospheric mixing ratio actually stabilized after 2000 [*Bousquet et al.*, 2006; *Dlugokencky et al.*, 1998; *Dlugokencky et al.*, 2001; *Dlugokencky et al.*, 2003; *Khalil and Rasmussen*, 1983; 1985; 1987; *Lelieveld et al.*, 1998; *Rasmussen and Khalil*, 1981; 1984; 1986; *Whiticar*, 1993], but has started to increase again since 2007 (Fig. 1.1, Dlugokencky, 2009).

For more the 800,000 years and until the start of the industrial period, its concentration remained below 800ppb (Fig. 1.2) with fluctuations driven by natural factors [*Loulergue et al.*, 2008] which are still object of intensive studies.

More ancient methane scenarios (2.4-2.7 Gyr) have been investigated trough the use of indirect proxies, like fluctuations in concentrations of Nickel in ultramafic rocks. Nickel is a key metal cofactor in several enzymes of methanogens and its decline would have stifled their activity in the ancient oceans and disrupted the supply of biogenic methane during the so called "*Great Oxidation Event*" [*Konhauser et al.*, 2009].

The CH_4 average mixing ratio is higher in the Northern Hemisphere than in the Southern Hemisphere (Fig. 1.3), as the emissions principally occur in the developed countries located in the Northern Hemisphere [*Mayer et al.*, 1982; *Rasmussen and Khalil*, 1984]. The Northern hemisphere also holds two thirds of the land surface including the majority of the wetlands, known as one of the most prominent CH_4 sources [*Matthews and Fung*, 1987; *Fischer et al.*, 2008; *Frankenberg et al.*, 2008]. The seasonal cycle in methane concentrations at a given location (Fig. 1.3) is determined by its removal reaction, oxidation by OH.

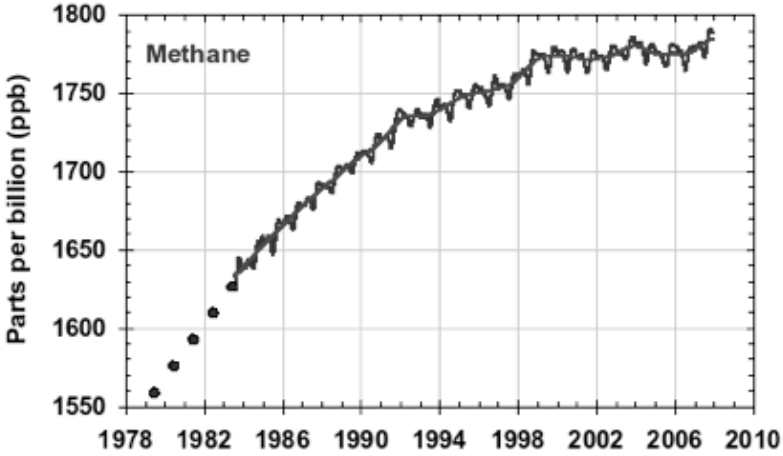

Fig. 1.1 Global average tropospheric methane concentrations (http://www.esrl.noaa.gov/gmd/aggi)

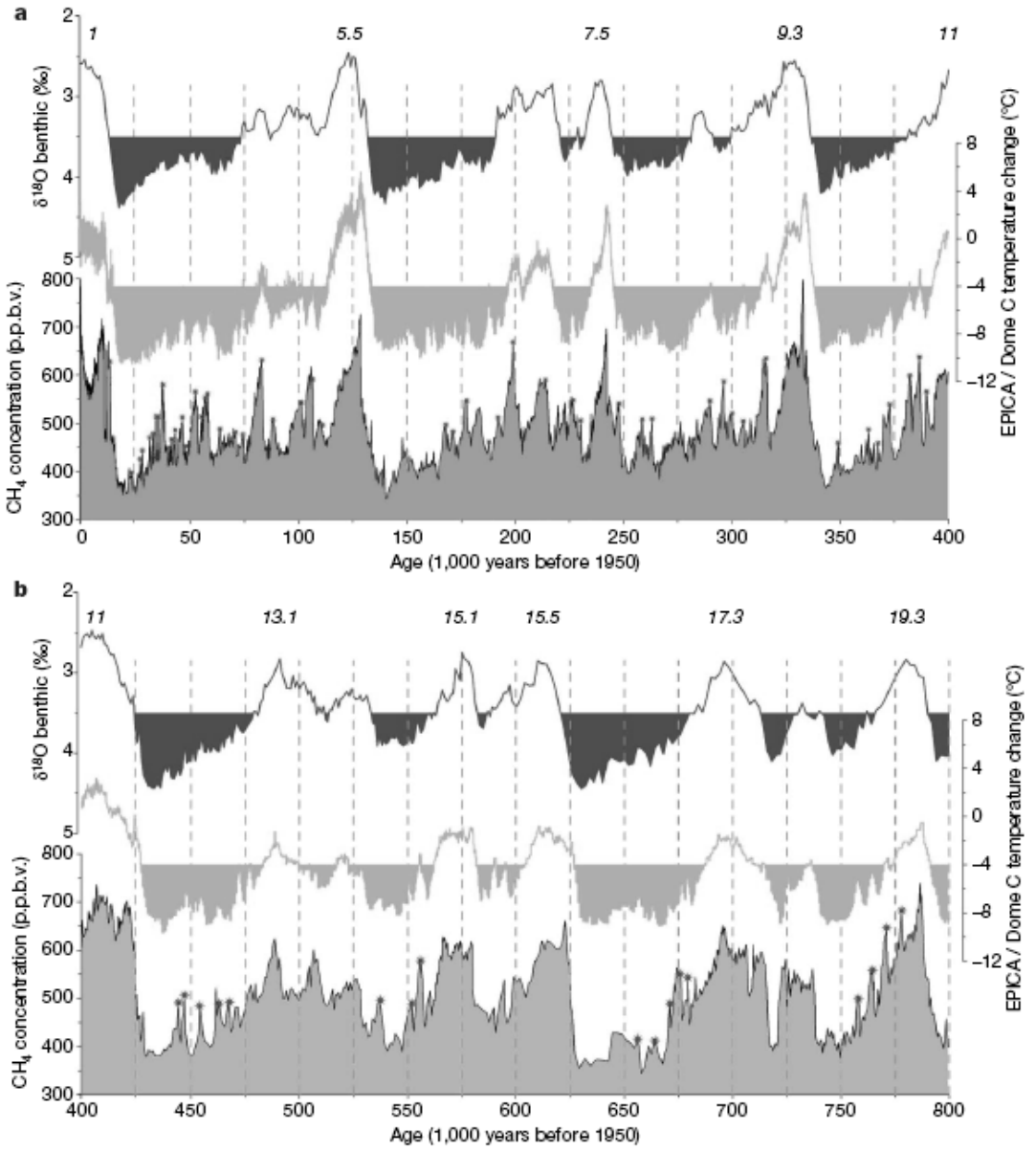

Fig. 1.2 Each panel (a, 0–400 kyr; b, 400–800 kyr) from bottom to top, shows time series of methane (grey shaded curve) with 74 identified millennial changes (stars, mean time between occurrences 6.2 kyr), based on a threshold amplitude of approx50 ppbv and a correspondence (occurrence and peak-to-peak synchroneity) with an Antarctic isotope maximum. Glacial periods (middle shaded) are defined by EPICA/Dome C temperature being at least 4 °C below late Holocene values. Time periods of occurrence of millennial variability (upper shaded area) are defined by a threshold value of 3.5 ‰ in the North Atlantic $\delta^{18}O$ benthic record. The benthic stack is used to compare with the full CH_4 record over 800 kyr (from Loulergue et al. 2008). Warm periods are usually associated with increase of CH_4 concentrations, although there are T independent changes which are still intensive object of studies.

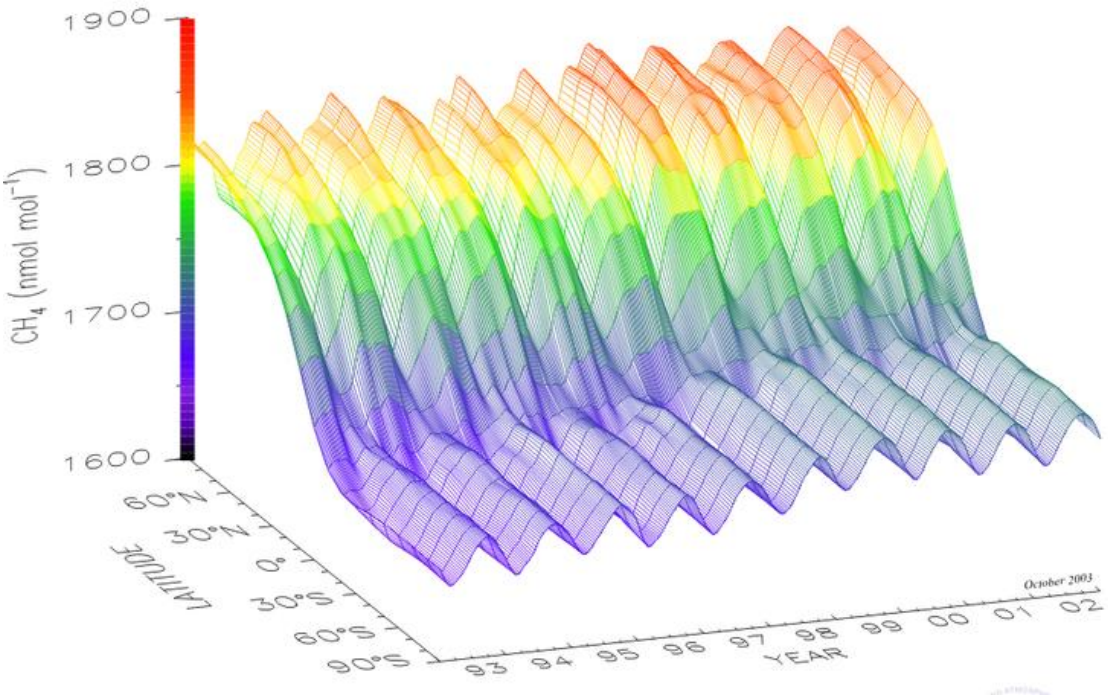

Figure 1.3 Three dimensional representation of the latitudinal distribution of atmospheric methane in the marine boundary layer. Data from the NOAA CMDL cooperative air sampling network were used. The surface represents data smoothed in time and latitude. Principal investigator: Dr. Ed Dlugokencky. NOAA CMDL (ed.dlugokencky@noaa.gov, http://www.cmdl.noaa.gov/ccgg).

1.3 The greenhouse effect

The increased level of methane has important implications for the energy balance and composition of the atmosphere. Known for decades [*Herzberg*, 1972], the radiative effects of methane depend on the physical-chemical properties of the molecule itself.

The interaction between radiation (photons) and matter is a function of wavelength, and compounds in a gaseous phase are able to emit and adsorb defined and characteristic wavelengths. In fact the energy of photons at these wavelengths correspond to energy differences between different vibrational, rotational, and for large photon energies also electronic states of a molecule.

Once a molecule has absorbed a photon, it is moved to an excited state at higher energy. The process is reversible when a photon is re-emitted. Alternatively the energy can be transferred by collision to other molecules.

The Earth-Atmosphere system continuously absorbs radiation from the Sun and emits infrared radiation to space. Radiation from the Sun drives the Earth's Climate and largely determines its temperature distribution.

Most of the solar radiation is in the ultraviolet and visible range (short wave radiation), whereas terrestrial radiation is mainly in the infrared range (long wave). To better understand the role of methane and other greenhouse gases in the climate system, the physical basis and the large scale consequences of the greenhouse effect are briefly described in the following.

1.3.1 Black body radiation

A *black body* is a hypothetical object whose emission spectrum depends only on its temperature. By definition, such an object absorbs all incident radiation; in other words, it is *black.* The *Planck's law* (Eq.1) gives the monochromatic irradiance emitted by a blackbody at temperature T.

Eq.1 $E_\lambda = \frac{c_1}{\lambda^5[\exp(c_2/\lambda T)-1]}$; $(Wm^{-2}\mu m^{-1})$

The wavelength λ_m of the maximum irradiance can be derived from the above equation by determining $\frac{\partial E^*_\lambda}{\partial \lambda} = 0$, which is giving the *Wien's law,*

Eq.2 $\lambda_m = 2898 / T$; (μm)

Integrating *Planck's law* , Eq.1 over all wavelengths gives the total irradiance E^* of a black body at temperature T, and it is called the *Stefan-Boltzman law*:

Eq.3 $E^* = \sigma T^4$; (Wm^{-2})
With $\sigma = 5.67 * 10^{-8}\ Wm^{-2}K^{-4}$

The Sun and the Earth's surface also behave like black bodies at their radiating temperatures. The equivalent blackbody temperature of the sun is about 6000ºK, and consequently λ_m = 502nm which is in the visible part of the spectrum (Fig. 1.4). However, the spectrum of solar radiation at the Earth's surface is slightly different from a blackbody because atmospheric constituents absorb and scatter some wavelengths more than others. In particular most of the ultraviolet radiation is adsorbed by ozone and oxygen in the upper part of the Atmosphere and only UVA and UVB radiation reach the surface. Taking a typical value of the Earth's surface radiating temperature of 288ºK, the maximum wavelength is λ_m = 9700 nm and the radiation is mainly in the infrared. Thus, the wavelength of solar and terrestrial radiation essentially do not overlap.

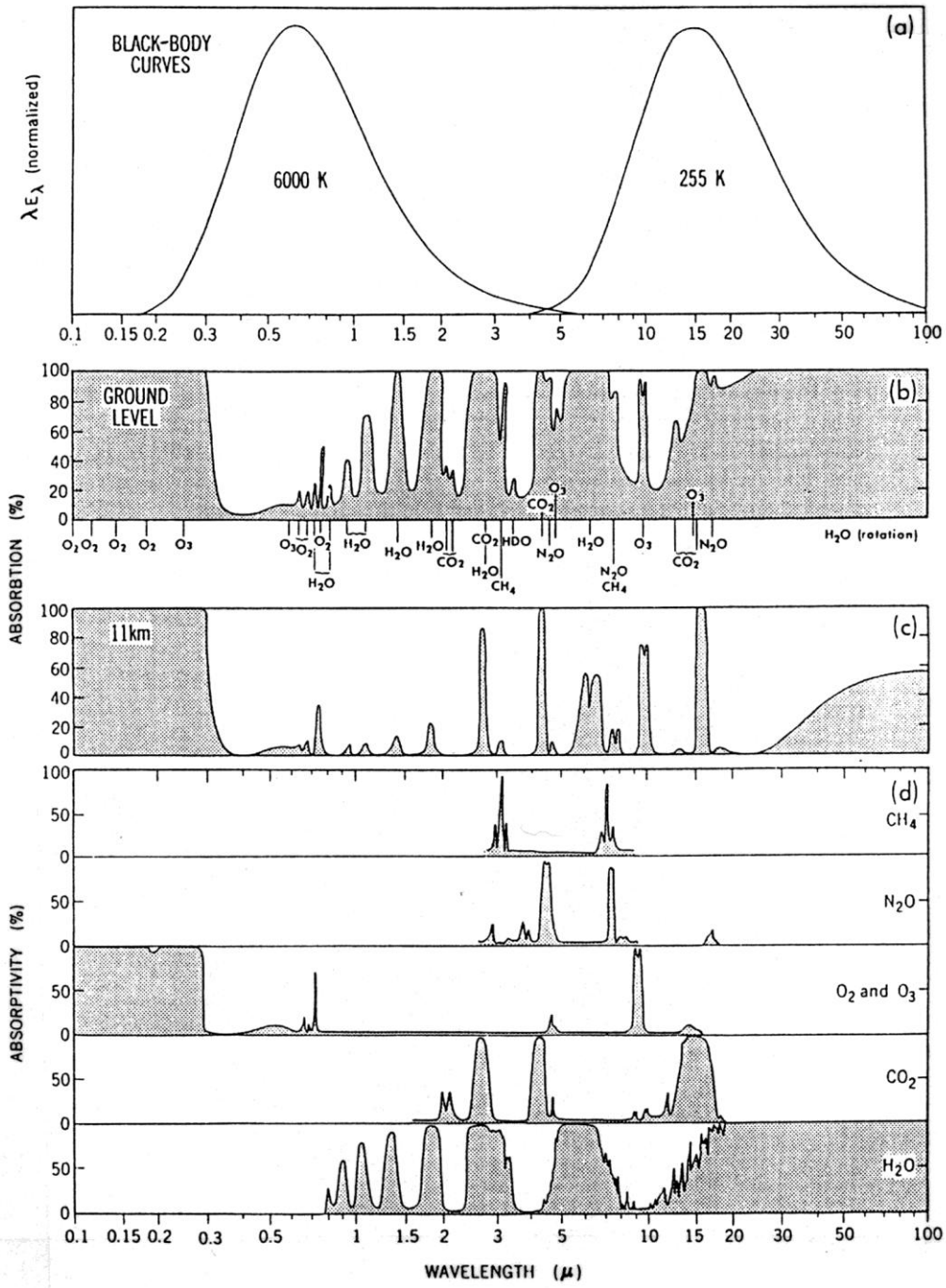

Figure 1.4 Solar and terrestrial radiation spectrum and spectral absorption of the main radiatively active gases. Methane absorbs radiation at approximately 3.3 and 8.6 μm wavelength [*Pickering*, 1996].

1.3.2 The Earth without atmosphere: role of the greenhouse gases

In equilibrium, the solar radiation absorbed by the Earth is equal to the emitted terrestrial radiation, and for this equilibrium we can derive an equilibrium temperature using the Stefan-Boltzmann law. S = 1380 Wm^{-2} is the incoming energy, the so called solar constant, that hits the Earth's cross sectional area of πR_E^2 (R_E is the earth radius). A fraction of this incoming radiation is reflected by clouds and by the surface itself, the so-called albedo, $\alpha = 0.31$. The difference, i.e. the absorbed energy, can be equated to the emitted terrestrial radiation all over its surface, $4\pi R^2_E \sigma T^4_E$.

Eq.4 $(1-\alpha) S\pi R^2_E = 4\pi R^2_E \sigma T^4_E$;

The above equation can be solved for the mean radiative equilibrium temperature of 255ºK without taking into account the radiative effects of the atmosphere. This temperature is more than 30º below the real value and the difference is due to the radiative effect of the greenhouse gases. We can understand now the crucial role of such gases in maintaining conditions under which life as we know it on earth is possible.

Most gases in the atmosphere are transparent to short-wave radiation. An exception is ozone which adsorbs ultraviolet radiation. Especially below 280 nm, the incoming radiation is completely absorbed by ozone and oxygen in the upper atmosphere and partially scattered by clouds in the troposphere.

This amount is about 23% of the solar irradiance, in addition, molecules and particles in the air and water droplets in clouds scatter solar radiation, diffusing it in all directions (Fig. 1.5), so that some is returned to space (8%) and some reaches the Earth's surface as diffuse solar radiation (22%).

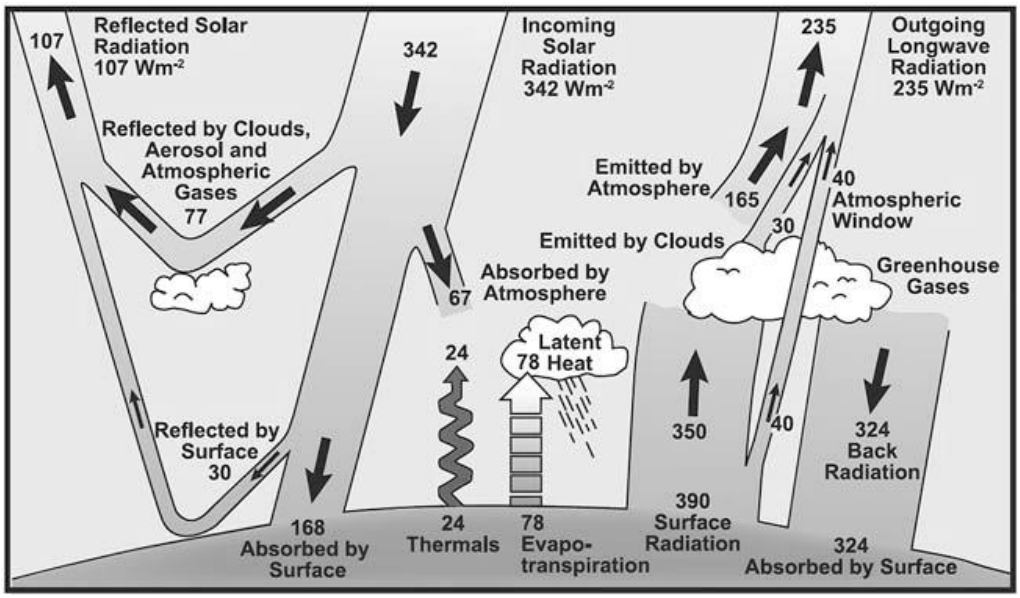

Figure 1.5 Earth Energy Balance

Although there is relatively little absorption of solar radiation in the atmosphere, some minor constituents, particularly water vapour, carbon dioxide, methane and nitrous oxide, are very efficient long-wave absorbers. These, so called greenhouse

gases, emit radiation upwards and downwards to the Earth's surface which is as a result much warmer than the radiative equilibrium temperature previously calculated.

In other words the Earth's surface is warmer because long-wave radiation is reflected back to the surface by the greenhouse gases. This is the "greenhouse effect".

1.3.3 Methane as a greenhouse gas

The radiative forcing

In climate science, radiative forcing is (loosely) defined as the change in net irradiance at the tropopause. "Net irradiance" is the difference between the incoming radiation energy and the outgoing radiation energy in a given climate system and is thus measured in Watts per square meter. The change is computed relative to "unperturbed" values, as defined by the Intergovernmental Panel on Climate Change [*IPCC*] as the measured difference relative to the year 1750, the defined starting point of the industrial era. A positive forcing (more incoming energy) tends to warm the system, while a negative forcing (more outgoing energy) tends to cool it.

The radiative forcing due to all well-mixed greenhouse gases since pre-industrial times was estimated to be 2.45 Wm^{-2} [*IPCC*, 2007; *Myhre et al.*, 1998] and the contribution of methane is about 0.48 Wm^{-2} with 15% of uncertainty. Calculations on how the radiative forcing are made have not been included here. For a detailed description the 1990 IPCC report and studies of Hansen et al. are the main guidelines [*Hansen et al.*, 1997].

Methane is contributing roughly 20% to the forcing of all greenhouse gases, and this estimate is only counting for direct effects (Fig. 1.6). There are also indirect effects involving more complex chemistry reactions with other compounds [*Lelieveld and Crutzen*, 1992]. Tropospheric ozone (O_3) is also a greenhouse gas and in fact increasing methane concentrations yield increasing concentration of ozone thus constituting an indirect radiative forcing.

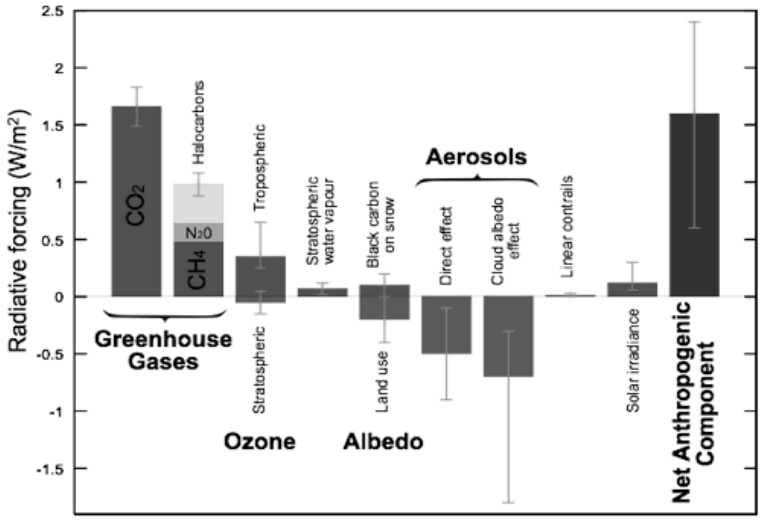

Figure 1.6 Radiative forcing components (IPCC2007)

1.4 Methane sources and sinks

The production of methane can happen following different abiotic or biotic processes which can be natural or anthropogenic. It is very well known from the literature how methane is produced by Archea under anaerobic conditions [*Stadtman*, 1967] in wet environments like rice paddies [*Bachelet and Neue*, 1993; *Bosse and Frenzel*, 1998], marshes, flooded terrains located in tropical regions or in Tundra-Taiga Biomes in spring-summer times [*Aselmann and Crutzen*, 1989; *Bartlett and Harriss*, 1993; *Devol et al.*, 1988; *Matthews and Fung*, 1987]. Methanogenic Archea are present in ruminant stomachs and animal sources have been seriously monitored since growing cattle farms in the recent years [*Johnson and Ward*, 1996; *Steudler et al.*, 1996]. Those microorganisms have been found in termite guts, adding a new potential source [*Rasmussen and Khalil*, 1983; *Zimmerman et al.*, 1982; *Zimmerman and Greenberg*, 1983]. A stock, which is not included in global budget estimates, is the input not only from termites but from the whole *filum* of the arthropods. Emission rates per unit are very small but if we consider the huge biomass of the insects, this could be an important part of the global budget not yet considered [*Hackstein and Stumm*, 1994]. Fossil carbon sources such as coal mining, industrial losses, automobile exhaust, mantle and volcanic emissions are estimated to be 20% of the global budget [*Etiope et al.*, 2008; *IPCC*, 2007; *Piccot et al.*, 1996; *Schoell*, 1988]. The strength of the natural Earth degasification process is not very well monitored and it should be much better quantified since it can be more than 10% of the actual global budget for CH_4.

In the last years the role of dams for hydropower has been under discussion. Published estimations define a source of 100Tg/yr, where the major contribution is from barrier lakes located in tropical regions. The source strength seems overestimated since this is an estimate of the potential reservoir and not a study based on the effective release to the atmosphere [*Lima et al.*, 2008; *Ramos et al.*, 2009].

Biomass burning emissions strongly depend on how humans manage the forests and on socio-economical factors [*Delmas*, 1994; *Hao and Ward*, 1993; *Steudler et al.*, 1996; *Yamada et al.*, 2006]. Clathrates, known as methane hydrate is a pseudo form of ice-water with trapped molecules of methane, can exist only at high pressure environments like at the bottom of the ocean, in sediments. The reservoirs of clathrates have been declared large and of profit for future exploitations but the actual release to the atmosphere is presently considered to be very small. Predictions of future increase of the temperatures, with consequently warming of the oceans, implicate a possible massive release of this methane also from permafrost, with strong feedback effects [*Sowers*, 2006]. In Figure 1.7, present estimates of the magnitude of the different sources of the actual global methane budget are presented.

An unexpected source has been recently discovered [*Keppler et al.*, 2006] and it is the main subject of the research here reported. The main findings will be described in the next chapters; it is the aerobic methane production from plants. Recent experiments demonstrate how the production of methane occurs under aerobic conditions by the effect of UV radiation and temperature [*McLeod et al.*, 2008; *Messenger et al.*, 2009; *Vigano et al.*, 2008]. Its strength is still object of debates, with some a priori estimations which define a contribute less the 5% [*Bergamaschi et al.*, 2006a; *Butenhoff and Khalil*, 2007; *Dueck et al.*, 2007; *Houweling*, 2006; *Nisbet et*

al., 2008]. Plants are also known as mediators of gas transport from the rizosphere (soil) into air [*Bazhin*, 2004; *Nisbet et al.*, 2008; *Nouchi et al.*, 1990]; effects quit studied for rice plants or mangroves [*Ramachandran Purvaja*, 2004] but still unknown for other plants. Satellite observations of the averaged column methane mixing ratio asset two third of the global budget in tropical regions [*Bergamaschi et al.*, 2007b; *Frankenberg et al.*, 2008; *Melack et al.*, 2004], where the tropical forest and landfills are surely one of the natural components [*Crill et al.*, 1987; *Devol et al.*, 1988; *do Carmo*, 2006; *Miller et al.*, 2007b] with variable human input like biomass burning and pasture [*Avissar et al.*, 2002; *Davidson and Artaxo*, 2004; *Steudler et al.*, 1996; *Verchot et al.*, 2000].

The combined strength of all CH_4 sources is estimated at 525-625 $Tg(CH_4)\ yr^{-1}$ (Tg= teragrams or 10^{12}g) [*Breas et al.*, 2002; *Frankenberg et al.*, 2005; *Khalil and Rasmussen*, 1983; *Sheppard et al.*, 1981; *Steele et al.*, 1987; *Vogels*, 1979; *Wahlen*, 1993], as constrained largely from the main removal reaction, oxidation by OH.

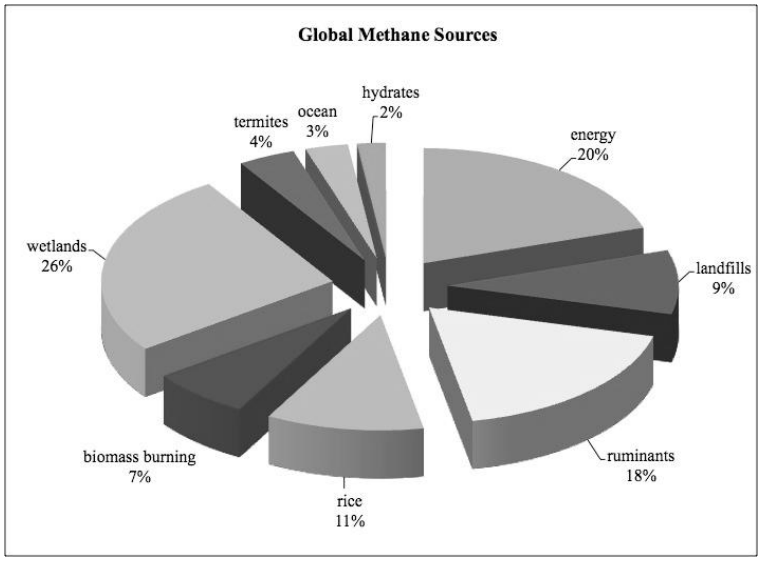

Figure 1.7 Fraction of the methane sources in the global budget (IPCC, 2007)

Methane removal is a consequence principally of tropospheric oxiation with the hydroxyl radical OH• which is the main "cleansing agent" of the atmosphere The primary source the OH radical is a photolysis reaction chain involving UV radiation, ozone, and water vapour (R.1/R.5).. For this reason the mixing ratio of methane can influence the removal rates of other compounds that react with OH, e.g. CO in the troposphere (R.6/R.19) [*Abrajano et al.*, 1988; *Badr et al.*, 1992a; *Brenninkmeijer et al.*, 2003; *Cantrell et al.*, 1990; *Cicerone and Oremland*, 1988; *Tyler et al.*, 2007; *Vaghjiani and Ravishankara*, 1991]. The photochemical reactions with OH, $O(^1D)$ and Cl are responsible for more than 90% of the CH_4 removal, and a small contribution comes from soil consumption which especially occurs in deserts or dry ecosystems [*Dueñas et al.*, 1994; *Dutaur and L.V*, 2007; *Le Mer and Roger*, 2001; *Potter et al.*, 1996; *Striegl and McConnaughey*, 1992; Chapter 7 of this thesis]. The magnitude of soil sink strongly depends on the local meteorology and seasonality as well as human managements and land exploitations [*Ishizuka et al.*, 2005; *Potter et al.*, 1996; *Steudler et al.*, 1996; *Thurlow et al.*, 1995; *Verchot et al.*, 2000].

Hydroxyl radical production

R.1 $O_3 + h\nu \rightarrow O(^1D) + O_2$ ($h\nu$ <310nm);
R.2 $O_3 + h\nu \rightarrow O(^3P) + O_2$ ($h\nu$ <1180nm);
R.3 $O(^1D) + M \rightarrow O(^3P) + M$ (M = N_2,O_2)
R.4 $O(^3P) + O^2 + M \rightarrow O^3 + M$
R.5 $O(^1D) + H_2O \rightarrow 2\ OH\bullet$

The photolysis of ozone generates oxygen in two excited forms ($E_{O(1D)} > E_{O(3P)}$) depending on the wavelength of the radiation. In the free clean troposphere, above the mixing layer, roughly 70% of OH• is removed by reaction with carbon monoxide and the rest with methane [*Jacob et al.*, 1990].

In the propagation process of the hydroxyl radical the inter-conversion between nitrogen monoxide and nitrogen dioxide plays an important role, which depends on solar radiation and local sources.

Carbon monoxide Photochemistry

R.6 $CO + OH\bullet \rightarrow CO_2 + H\bullet$
R.7 $H\bullet + O_2 + M \rightarrow HO_2\bullet + M$
In the presence of NO_x
R.8 $HO_2\bullet + NO \rightarrow OH\bullet + NO_2$
R.9 $NO_2 + h\nu \rightarrow NO + O(^3P)$ ($h\nu$ <410nm)
R.10 $O(^3P) + O_2 + M \rightarrow O_3 + M$

The sum of the above reactions gives:
R.11 $CO + 2O_2 \rightarrow CO_2 + O3$

Methane Photochemistry

R.12 $CH_4 + OH\bullet \rightarrow CH_3\bullet + H_2O$
R.13 $CH_3\bullet + O_2 + M \rightarrow CH_3O_2\bullet$
In the presence of NO_x
R.14 $CH_3O_2\bullet + NO \rightarrow CH_3O\bullet + NO_2$
R.15 $CH_3O\bullet + O_2 \rightarrow HCHO + HO_2\bullet$
R.16 $HO_2\bullet + NO \rightarrow OH\bullet + NO_2$
R.17 $NO_2 + h\nu \rightarrow NO + O(^3P)$
R.18 $O(^3P) + O^2 + M \rightarrow O_3 + M$

The sum of the above reactions gives:
R.19 $CH_4 + 4O_2 \rightarrow HCHO + H_2O + 2O_3$

In polluted areas where high levels of NO_x and CO prevail, the consumption of methane and CO leads to ozone production, while in remote clean areas the ozone is removed by reaction with HO_2 radical.

1.5 History of aerobic methane research

The fact that living plants were found to be a substantial source of the greenhouse gas methane (Keppler et al. [2006] estimate up to 30% of the global budget) created a lot of controversy in the scientific community. In particular the potential role of this source climate change was heavily debated [*Bergamaschi et al.*, 2006a; *Feil*, 2006; *Lelieveld*, 2006; *Lowe*, 2006; *Schiermeier*, 2006a; b].

When the study was published, it was closely linked to the first global scale methane data retrieved from the SCIAMACHY satellite instrument. Frankenberg et al [2005] detected unexpectedly high methane concentrations over tropical rainforests. Keppler et al. associated these findings with the potential source from plants in those regions and they suggested that the recent decrease of methane concentrations [*Bousquet et al.*, 2006; *Dlugokencky et al.*, 1998] maybe linked to anthropogenic deforestation [*FAO*, 2000].

A first reply came few months later from Kirschbaum et al. [2006] suggesting that the extrapolation used by Keppler et al. was not appropriate. They revised the global strength of plant emissions based on physiological parameters [*Kirschbaum et al.*, 2006] which lead to an upper limit of 10%. Another upscaling was done by Parsons et al., giving estimates around 3-4% of the global budget [*Parsons et al.*, 2006]. In general, the biology community was sceptical on the first findings and on the global extrapolation used.

At the same time Sanhueza and Crutzen reevaluated measurements in tropical savannah and forest vegetation finding significant releases of methane from these ecosystems [*P. J. Crutzen*, 2006; *Sanhueza and Donoso*, 2006]. Atmospheric constrains on global emission of plants were derived by Houweling et al. [*Houweling*, 2006] from analyses of preindustrial CH_4, leading to an upper limit of 85Tg/yr or less than 15% of the actual global budget.

In 2007 a new experimental study on living plant emissions was made by Dueck et al., finding no substantial aerobic release of methane from ^{13}C labelled plants. By growing pure ^{13}C species they could not find a significant production of $^{13}CH_4$. The experiment was carried out in closed chambers under controlled conditions [*Dueck et al.*, 2007].

Interesting experimental research was performed by Kitaoka et al., a Japanese group from the Hokkaido University. They found evidence of methane emission from leaves of different species under elevated CO_2 concentrations [*Kitaoka et al.*, 2007].

Sharpaty [2006] was the first to introduce a possible photo-induced mechanism of methane formation from radical reactions in cellulose. Sanhueza et al. [2006] found again evidence of methane emissions from tropical savannah and Sinha et al. [2007] from boreal and tropical ecosystems.

In 2007 Kirschbaum et al. were debating the importance of the methane emission from plants, where they concluded that the aerobic methane production is small compared to other sources and not of significant impact in the context of climate change. Butenhoff et al. [2007] performed global estimates based on the previously measurements of Keppler et al [2006], where they assessed a magnitude of 20-65 Tg/yr by using different parameterisation approaches fro the global upscale.

In 2008 Beerling et al. came out with an accurate study on leaves emissions. They could not find aerobic methane formation when the leaves are irradiated with the common photosynthetic active radiation (400 nm – 700 nm), but they could not exclude that such emission could be linked to a non enzymatic process laying outside the wavelength range for photosynthesis.

At this time when we investigated the role of UV radiation on the production of methane from plant biomass [*Vigano et al.*, 2008], of which a detailed discussion will be given in chapter 3. Another important study with similar conclusions was made by McLeod et al. [2008] studying the effect of UV radiation with respect to methane emission from pectin, a structural plant compound suspected to be the major substrate for methane formation.

To prove that the methane formed from UV radiation is coming from plant compounds, Keppler et al. [2008] demonstrated that CH_4 is really formed from methoxyl groups in pectin by a still not completely understood reaction. In particularly by using galacturonic acid, a de-methoxylated form of pectin (see Chapter 6) it was possible to add deuterium labelled methoxylgroups ($-OCD_3$) to the compound. Experiments were carried out by heating the material or exposing the samples to UV light and thereafter δD of the produced CH_4 was analyzed by mass spectrometry. Results demonstrated that the deuterium content in CH_4 is associated with the deuterium content of the labelled compound and that the pectin is responsible for more than 50% of the methane production [*Keppler et al.*, 2008].

After the studies of Vigano et al., Keppler et al. and McLeod et al. in 2008, the interest in this topic was pushed towards a better clarification. Kirschbaum et al. [2008] investigated the effects of adsorption and desorption of methane in plant tissues when a porous compartment is exposed to high CH_4 concentrations and then to low CH_4 concentrations. The results indicated that such mechanism is of negligible impact [*Kirschbaum and Walcroft*, 2008].

Dueck et al. [2008] commented the possible causes of emissions from plants, where UV light and high temperatures could be indeed the driving factors. Nisbet et al. [2009] did not find genes associated with methane production in plants and performed experiments demonstrating that methane cannot be produced via a biochemical pathway but only trough a degradation process like the UV-Temperature effect. They also discussed the possibility that plants can transfer significant amounts of CH_4 from the soil to the atmosphere as previously studies had shown already [*Bazhin*, 2004; *Garnet et al.*, 2005; *Nouchi et al.*, 1990; *Ramachandran Purvaja*, 2004].

Cao et al. [2008] and Wang et al. [2008] measured anomalous methane concentrations from alpine plants collected on the Tibetan plateau and from plants in the inner Mongolian steppe. The emission rates derived were similar to the previous results of Keppler et al. [2006] but a surprising finding was that some species were emitting and others not. Here it seems not clear how plants can emit methane; this is due probably to either natural factors and also to the rudimental measurement techniques employed.

Frankenberg et al. revised their previously estimates of tropical methane emissions due to a retrieval error in the spectral resolution of the water vapour parameters, which overestimated the column averaged mixing ratio of methane in the previous study [*Frankenberg et al.*, 2008]. Nevertheless the tropical source is still asserted to be two third of the global methane budget.

Another important finding was the discovery of aerobic methane production in the sea, coming from an imbalance of certain nutrients and reactions involving nitrogen fixing organisms [*Karl et al.*, 2008].

[*Smeets et al.*, 2009] carried out eddy flux measurements during a field campaign in summer 2007 at Blodgett forest, California, United States. The main goal was to possibly identify methane fluxes over a dry ecosystem directly [*Smeets et al.*, 2009]. The results showed CH_4 fluxes consistently directed downward and with a diurnal pattern (see Chapter 7). It appears that direct emissions could not be detected, but they may be masked by the larger deposition flux. The properties of an ecosystem and seasonal meteorological effects play a key role in modulating the methane formation or consumption processes [*Ehhalt and Schmidt*, 1978; *Ishizuka et al.*, 2005; *Matthews and Fung*, 1987; *Verchot et al.*, 2000].

Another similar study has been done by Bowling et al. [2009]. They showed also a marked negative flux of CH_4 over a subalpine forest under elevated UV irradiation. In that case the possible methane formation from the UV process is also masked by the strong soil uptake [*Bowling et al.*, 2009].

Messenger et al. published a study on reactive oxygen species associated with methane generation from pectin [*Messenger et al.*, 2009] and chapter 4 of this thesis shows the isotope signature of methane emitted from plant matter under UV radiation [*Vigano et al.*, 2009a].

Surprising findings were recently reported by Qaderi et al. [2009] who declared that stressed crops could emit substantial amounts of methane into the atmosphere. Their values are in agreement with the ones previously reported by Keppler et al. [2006], but do not agree in terms of size of the emissions with the other studies. Both experimental approaches use static chambers flushed with synthetic air, which may lead to problems with quantification of the fluxes [*Ortega and Helmig*, 2008; *Ortega et al.*, 2008].

Our most recent investigation was on a relation between the δD of CH_4 and the δD of H_2O that is used to grow the plants [*Vigano et al.*, 2009b]. In fact we were able to describe how the deuterium content in the methane emitted from plant matter under UV light is linked to the δD of the source water. A similar property has been reported in the past from field studies and lab experiments which showed that the deuterium content of the water is affecting the CH_4 emitted from bacterial communities [*Schoell*, 1988; *Schoell et al.*, 1988; *Waldron et al.*, 1999].

1.6 The stable isotope composition of atmospheric CH_4

Stable Isotopes of methane

Stable isotopes are non-radioactive atoms of the same chemical element having different atomic mass. The nuclei have the same number of protons but different numbers of neutrons.

Methane can be present in nature with 10 different isotopologues, differing in stable isotopes of carbon ($^{13}C/^{12}C$) and hydrogen (H/D) : $^{12}CH_4$, $^{12}CH_3D$, $^{12}CH_2D_2$, $^{12}CHD_3$, $^{12}CD_4$, $^{13}CH_4$, $^{13}CH_3D$, $^{13}CH_2D_2$, $^{13}CHD_3$, $^{13}CD_4$. Because of the low abundance, only the singly substituted isotopologues can be measured precisely and they are of interest in atmospheric science ($^{12}CH_4$, $^{12}CH_3D$, $^{13}CH_4$) the others are usually neglected.

Element	Isotope	Abundance (%)
Hydrogen	H	99.985
	D	0.015
Carbon	^{12}C	98.99
	^{13}C	1.11

For practical reasons, the atomic ratio r of the mixing ratio of the heavier ^{n+1}X to lighter isotope ^{n}X is used instead of abundances. This ratio is defined as:

Eq.5 $$r = \frac{[^{n+i}X]}{[^{n}X]};$$

The superscripts n+i and n are the mass numbers of the isotope.

In most cases, the magnitude of isotope fractionation from kinetic and equilibrium fractionation processes is small; for this reason, enrichments are typically reported in "per mil" (‰, parts per thousand). The delta notation (δ) quantifies the relative difference of the heavy-to-light isotope ratio in the sample (r_{smp}) from the same ratio of a standard (r_{Ref}).

Eq.6 $$\delta X_{\mathrm{Re}f}(Smp) = \left(\frac{r_{Smp}}{r_{\mathrm{Re}f}} - 1\right) \times 1000‰;$$

In order to compare results from different laboratories, the International Atomic Energy Agency has defined for every isotope standard materials, which define the zero point of the delta scale.

For the H/D ratio the VSMOW (Vienna Standard Mean Ocean Water) standard was created in 1967 by distilling oceanic water collected all around the globe ($r_{D/H}$=0.000015575). VSMOW is a recalibration of the original SMOW definition that was created in 1960 from average ocean water and melted snow used as reference points [*Craig*, 1961].

For Carbon a new reference material is actually used; the so called the NBS 19 [*Irving et al.*, 1982]. The reference material NBS 19 (in literature also referred to as TS-Limestone) was obtained from a single slab of white marble of an unknown origin. The reference material NBS 19 is intended for $^{13}C/^{12}C$ and $^{18}O/^{16}O$ isotope-ratio analysis of carbonates and is used to define the VPDB scale [*Hut*, 1987]. Therefore these δ-values bear no associated uncertainty. In 2006 new guidelines were published for $\delta^{13}C$ calibration, and recommend additionally the use of an assigned $\delta^{13}C$ value for LSVEC reference material to obtain an improved two-point calibration [*Toman et al.*, 2006].

The PDB (Pee Dee Belemnite) is a Cretaceous marine fossil, Belemnitella americana from the PeeDee Formation in South Carolina. This material has a higher $^{13}C/^{12}C$ ratio than nearly all other natural carbon-based substances ($r_{13C/12C}$=0.0111802) and was used to define the so called VPDB scale.

Atmospheric methane has characteristic δ values of ~-90‰ for deuterium and ~-47‰ for ^{13}C, largely determined by isotopic fingerprints of the sources and by kinetic

fractionations in the removal reactions [*Barker and Fritz*, 1981; *Quay et al.*, 1999; *Saueressig et al.*, 1996].

We already discussed that methane can be formed via 3 main processes: microbial, anthropogenic and from incomplete combustion of biomass [*Schoell*, 1988]. Differences in the formation processes for the different sources [*Games et al.*, 1978], lead to different isotopic signature of the methane emitted from these sources. Coal and gas emissions can be separated in two categories: from energy consumption and from geological sources respectively [*Etiope et al.*, 2008]. Table 1.1 reports the strength of the various sources with their characteristic isotopic signatures.

Source	Strength (Tg CH_4/yr)	$\delta^{13}C$-CH_4 (‰)*	δD-CH_4 (‰)*
Coal	33±5[a]	-36	-140
Gas	70±14[a]	-43	-185
Gas hydrates	10[b]	-60	-200
Biomass burning	30[c]	-24	-228
Waste	40±8[a]	-52	-300
Tropical wetlands	200±50[d]	-58	-330
Ruminants	58[e]	-60	-300
Rice	69±12[b]	-63	-320
Boreal Wetlands	100±30[g]	-65	-330
Plants	5÷25[f]	-58	-275
UV-plants	2÷5[h]	-59	-334

* Values reported by Vigano et al. 2009
[a] Values from Quay et al. 1999
[b] Values from IPCC report 2007
[c] Values from Hao et al. 1993
[d] Values from Houweling et al. 2000 and from Bergamaschi et al. 2007.
[e] Values from Johnson 1996
[f] Values from Parsons et al. 2008
[g] Values from Matthews and Fung 1987
[h] Values calculated from leaf area index [*Scurlock et al.*, 2001] considering 0.3 W/cm^2 of incoming radiation (subtropical) and 5ng/gDWcm^2 as average value from unpublished experiments

Little is known about how the methane source inventory and sinks have evolved over recent centuries. Detailed records of the stable isotopic composition of CH_4 ($^{12}CH_4$, $^{13}CH_4$) from analyses of air trapped in polar ice and firn have been investigated for the last 2000 years (Fig. 1.8) [*Ferretti et al.*, 2005], where large $\delta^{13}CH_4$ variations indicate that the methane budget changed unexpectedly during the late preindustrial Holocene (circa 0 to 1700 A.D.). During the first thousand years (0 to 1000 A.D.), $\delta^{13}CH_4$ was at least 2 ‰ enriched compared to expected values, and during the following 700 years, a 2 ‰ depletion occurred. The reasons of these changes are still subject of intensive studies although a theory is assessing the relative enrichment in ^{13}C due to large biomass burning events [*Houweling et al.*, 2008]. The period 1700-

1900 A.D. is characterized by ^{13}C depletion associated perhaps to increases of the light wetland emissions. In the last century the ^{13}C enrichment from fossil fuel combustion dominates. This finding clearly follows also from the study of Lassey et al. [2007] which employs the Emission Database for Global Atmospheric Research (EDGAR).

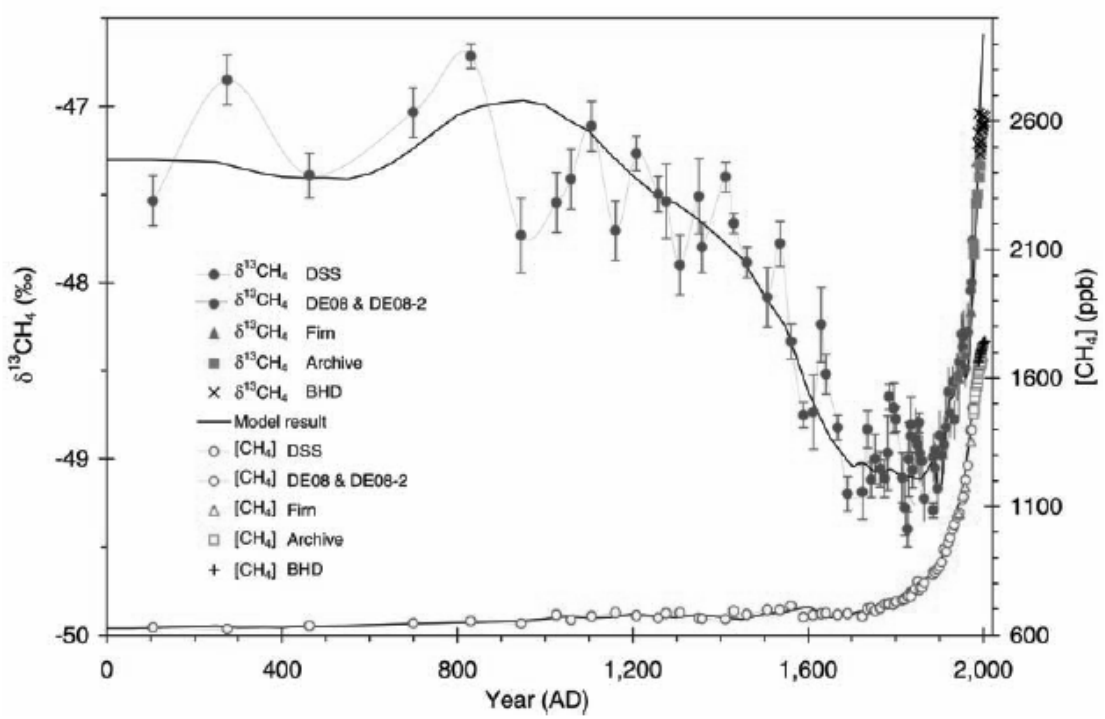

Figure 1.8 The 2000-year Law Dome records of $\delta^{13}CH_4$ (full circles) and $[CH_4]$ (open circles). Air samples are from ice cores (DSS, DE08, and DE08-2), firn, archives (Cape Grim, Australia), and Baring Head, New Zealand (BHD) (11). $\delta^{13}CH_4$ errors represent both measurement and diffusion correction uncertainties. $[CH_4]$ and dating errors are smaller than plotted symbols (from Ferretti et al., [2005]).

1.7 Research aims and thesis outline

Following a discovery by Keppler et al. [2006] who postulated that plants are a substantial source of atmospheric methane, this thesis has as central goal the verification and characterization of aerobic methane production, in particular from the interaction of UV radiation with plant matter. Experiments were performed on dry matter or fresh detached leaves, but not on the whole living organism. A second goal was to further understand the chemical and physical processes driving this aerobic methane production.

The work involved the use of novel and highly sensitive techniques for methane detection, in particular real-time fast CH_4 monitoring using integrated cavity output spectroscopy and high precision isotope ratio mass spectrometry. These techniques, as well as the experimental setup for the experiments, will be described in chapter 2.

The measurements presented in chapter 3 are the first experimental prove that methane is definitely released under aerobic conditions by the effect of UV irradiation and temperature.

The kinetics of the reaction is fast and rules out any biological activity. At high UV irradiation, CH_4 production continues for more than a month with constant emission rates, indicating that the reservoir for methane formation via this physical-chemical degradation process is very large. By using special lamps with different spectral distributions it has been possible to give first information on the action spectra involved in the CH_4 aerobic production and it is clearly demonstrated that UVB radiation is much more effective than UVA radiation and visible light. A further important factor in aerobic CH_4 production is temperature. Changes in temperature affect strongly the emission under UV irradiation, with almost no emission when the temperature is around 0°C. An isotope labelling experiment shows that even without light the methane emission is still present although not detectable with the common techniques. The isotope changes in experiments with ^{13}C labelled plant leaves nevertheless allowed to quantify the emission rate, which is by far the lowest limit ever detected.

Chapter 4 is mainly focused on isotope studies and is the first study reporting the isotope signatures of the methane emitted from plant matter under UV irradiation. Different sources emit methane with different isotope signatures as described in section 1.6 with values of $\delta^{13}C$ and δD spread over a wide range. The signatures derived from the UV interaction are surprisingly depleted in both heavy isotopes, similar to methane from wetlands, suggesting that they cannot really be distinguished in the environment. The values proposed in previous studies for the living plants are slightly more enriched compared to the results found here but in the previous studies the process may have been different (no UV light was used). In this isotope study, we did not only determine the isotope signatures of methane, but also performed isotope analyses of bulk organic matter and methoxyl groups in order to investigate the relations between those chemical moieties and the methane emitted. In fact, the isotopic relations suggest that the methoxyl groups are not the only reservoir involved in the methane generation, but there should be other chemical components involved which have not been identified to date.

In chapter 5 the origin and production process of aerobic methane is further investigated by studying the influence of the isotopic composition of water used to grow plants on the deuterium isotope fractionation in plant bulk biomass, methoxyl groups, and the methane emitted. Plants were grown with water of different deuterium content, and successively the leaves were collected and the isotopic composition of the methane emitted upon irradiation with UV light was determined. Isotope analyses of the bulk and of the methoxyl groups were performed as well in order to further explain the origin of the methane formed. Bulk biomass, methoxyl groups and methane are successively depleted in D compared to the source water. The variation of the deuterium content in the water is well mirrored in the methane emitted, but to a much smaller degree in the bulk and in the methoxyl groups. The different compounds allow to characterize the amount of hydrogen incorporated into the plant at different stages. Again it is shown that other reservoirs than methoxyl groups contribute to CH_4 formation, but the exact process has not been elucidated and will require further work.

The following two chapters present two further publications where I am not the first author, but contributed significantly to the research.

Chapter 6 is an experimental study on the precursors of aerobic methane, where specific deuterium labelling experiments on methoxyl groups of plant pectin reveal how these compounds are indeed involved for more than 50% in the methane formation.

Chapter 7 is a field measurement where methane fluxes at a Ponderosa pine plantation in California have been investigated with eddy covariance technique. It is reported for the first time a continuous flux measurement of methane over an afforested area is reported during the dry season characterized by a strong diurnal methane uptake.

Chapter 8 summarizes the whole research reported in this dissertation and provides further suggestions on how to proceed. The study on CH_4 plant emissions should adress the complete reaction pathway leading the methane formation from plant compounds, since 50% of the precursors are still unknown. Particular emphasis should be given to the global role of this aerobic methane emission, although its magnitude is smaller compared to anthropogenic emission which are the main cause for the increase of all greenhouse gases.

Chapter 2

The measurement systems

2.1 How we can measure atmospheric methane

Methane can be determined with several instruments that have different precision.

Here we want to describe all the methods used in our laboratory, which differ theoretically by the physical measurement principle.

The most commonly used technique is gas-chromatography combined with a *Flame Ionization Detector (GC-FID)* which will be described in section 2.4. This system is quite sturdy, easy to set up, and still the most used for calibration purposes. In the last years a lot of progress has been made in the field of high-precision methane detection by laser spectroscopy. It is basically based on the Lambert-Beer Law. In short a light-beam of a certain intensity and wavelength is absorbed by the molecules and it is measured afterward. In our case we worked with Cavity Ring Down Spectroscopy (LOS GATOS® inc.). This commercial instrument is very robust and has impressive stability.

For the isotopic composition of $\delta^{13}C\text{-}CH_4$ and $\delta D\text{-}CH_4$ we used the CF-IRMS technique [*Miller et al.*, 2002; *Rice et al.*, 2001] coupled to a Thermo Delta^{+}XL isotope ratio mass spectrometer. The system used in the IMAU lab was developed by M.Braß and T.Röckmann. The system is completely automated, and allows high precision isotope measurements on only 40 ml of air. In addition it returns data for the methane mixing ratio which are comparable in precision to standard gas chromatography techniques.

In principle, isotopes can be determined also with spectroscopy techniques and applications, for example for the oil industry, are well established, but the sensibility is still too low for atmospheric research, since we are dealing with concentrations of hundreds of ppb to 2 ppm in the case of methane.

Details for each method will be given in the following sections.

2.2 Cavity ring-down laser absorption spectroscopy (CRLAS)

Cavity Ring-Down Spectroscopy or CRDS (Fig 2.1), was developed by Anthony O'Keefe and David Deacon in the mid-1980's [*O'Keefe and Deacon*, 1988] as a means of measuring very weak molecular absorption signals using a pulsed light source. The technique is founded upon several earlier schemes used to characterize ultra-high reflectivity mirror coatings [*Anderson et al.*, 1984; *Herbelin et al.*, 1980]. In CRDS, the intensity decay rate of light trapped in an optical cavity is used to obtain the associated total intra-cavity losses (per pass) as a function of the optical wavelength. When the cavity loss is dominated by cavity mirror scatter and transmission, the frequency resolved "loss" curve maps out the mirror reflectivity function. When a narrow band absorbing species is present, absolute atomic or molecular absorption intensities can be inferred by subtracting the baseline (non-resonant) loss of the cavity, which is determined while the laser is tuned off-resonance with the transitions. The great utility of the CRDS method lies as much in the extremely high sensitivity as in the simplicity of the technique. Absolute concentrations are easily inferred from the absorption data that CRDS provides. CRDS concentration detection limits for many species have been demonstrated to be in the part-per-billion to part-per-trillion range [*von Lerber and Sigrist*, 2002].

Absorption measurements of CH_4 in ambient are obtained by tuning a diode laser over three overlapping CH_4 transitions near 1653.723 nm at a 600-Hz rate for a 1-s integration time. At this wavelength, the measured cavity decay time (~7μs) yield an effective optical path of approximatively 2100 m [*Baer et al.*, 2002].

The CRDS ICOS instrument for methane has a detection limit of 1 part-per-billion when operating with dry air.

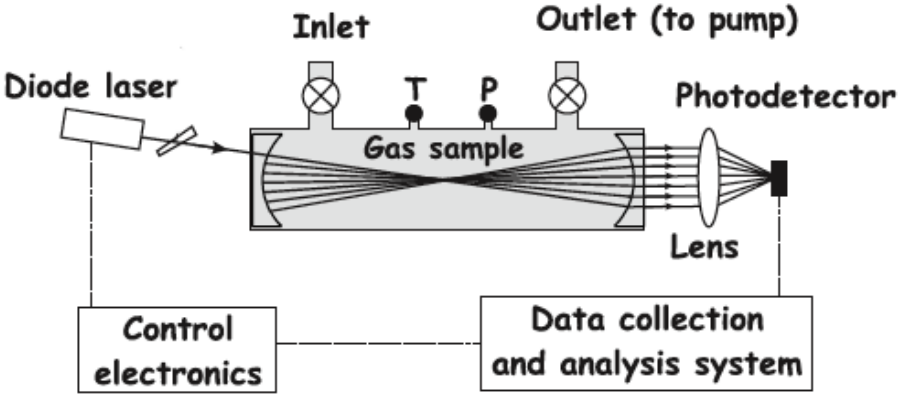

Figure 2.1 Schematic diagram of the instrument based on off-axis ICOS (D.Baer 2002) for high-sensitivity absorption measurements in the near-infrared region. The measurement cell is comprised of a cylindrical tube sealed by a pair of high reflectivity mirrors. T & P are the temperature and pressure sensors respectively.

The effect of moisture in the plant chambers on trace gas concentrations

When measuring plant samples, water is usually transpired and mixes with the air in the chamber. Even if the concentrations of gases are not changed, this additional water dilutes the mixing ratio of the gases that exit the plant chamber compared to the incoming (in our case dry) gas flow, which will result in artificially decreased mixing ratios. To avoid this dilution artifact, I always used a Nafion® dryer type MD-110-48S which gives a dew point of -5ºC at 100ml/min. Dry compressed air (~2000ppb CH_4) or dry synthetic air (<10 ppb CH_4) were provided as drying counter-flow depending on the experiment running.

Lamberts-Beer'Law & Maintenance of stable conditions

First of all the CRDS should measure under stable conditions of temperature and pressure and these parameters are kept constant by the internal software running under LINUX and made by LOS GATOS® inc. The effects of pressure and temperature on methane absorption are already well known and studied [*McMahon et al.*, 1972].

Here we introduce (Eq.7) the main concept behind every system based on absorption measurement, the so-called the Lambert-Beer Law:

Eq.7 $T(v) = exp\ (-k(v)x)c;$

$k(v)$ is the absorption cross section of the molecule at frequency v, x = pX, p being the pressure, X the geometrical path length, and c is the mixing ratio of the gas, in our case CH_4. This law may break down at large intensities because of saturation effects.

For combined Doppler and collision broadening, it is well known that $k(v)$ is given by the Voigt function:

$$\textbf{Eq.8}\quad k(v) = \frac{S(\ln 2)\alpha_0 p}{\Delta v_D{}^2 \pi^{3/2}} \int_{-\infty}^{\infty} \frac{\exp(-x^2)}{\left(\frac{\alpha_0 p}{\Delta v_D}\right)^2 \ln 2 + \left[\frac{(v - v_0)(\ln 2)^{0.5}}{\Delta v_D} - x\right]^2};$$

Here S is the line strength, α_0 is the half width due to pressure broadening at 1 atmosphere pressure, p is again the pressure, and Δv_D is the Doppler half-width.

The Doppler effect is pressure and temperature affected, so that is why those optical devices have to operate under stable conditions.

2.2.1 Fast methane analyzer CRD type RMT-200

In 2006-2007 we purchased two Fast Methane Analyzers (FMA) CRD type RMT-200 (Racket Model) from the LOS GATOS® research centre (Ca, USA).

The first model arrived in summer 2006 showing an reproducibility of 10-15 ppb and a detection limit of ~400 ppb, so I was not able to measure at really low

concentrations and with good precision. From spring 2007 we had continuously running both instruments in the lab or in the field, and both showed similar performance in terms of precision and stability, making those Fast Methane Analyzers very useful tools to easily get high frequency and high precision data.

The figure 2.2 below shows a typical snapshot of 5000s measurements at 1 Hz of sampling on air with stable ambient methane concentrations. The precision is around +-5ppbv with minor drift due to small changes in temperature (+-0.5ºC).

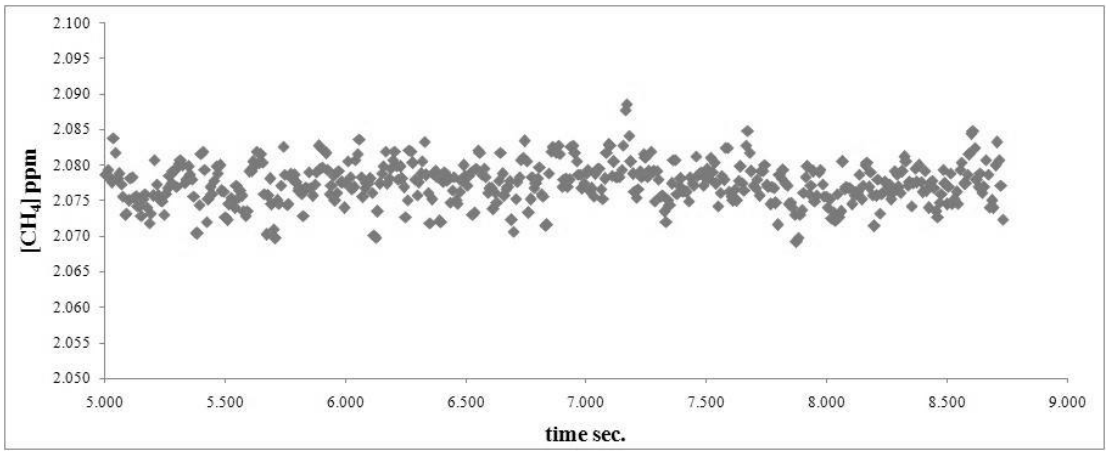

Figure 2.2 Continuous measurement of compressed air showing the excellent stability

Technical Overview

These FMAs have an evacuated cell of 408 cc volume, operated at ~142 Torr provided by means of an internal two Head Diaphragm Pump, which is the core of the CRDS.

Gas from the instrument inlet flows through one or both of the inlet paths shown in Figure 2.3, depending on whether the instrument is in normal flow mode or fast flow (flux) mode. In normal flow mode, the high flow solenoid valve is closed, and all gas flows through the electronic pressure controller. This controller throttles the flow to maintain the cell at its target pressure under potentially variable ambient inlet pressures and variations in the pumping speed. In fast flow mode, the high flow solenoid valve opens, and the inlet gas flows through both of the inlet paths. The high flow throttle valve provides coarse manual control of the flow to adjust for various external inlet configurations, and the electronic pressure control provides trim control to again maintain the target cell pressure under variable conditions.

The cell "flush" time (cell volume/flowrate) is approximately 7.4 seconds while operating with the internal pump, and approximately 0.042 seconds while operating with an external BOC Edwards XDS-35i scroll pump (Fig. 2.3).

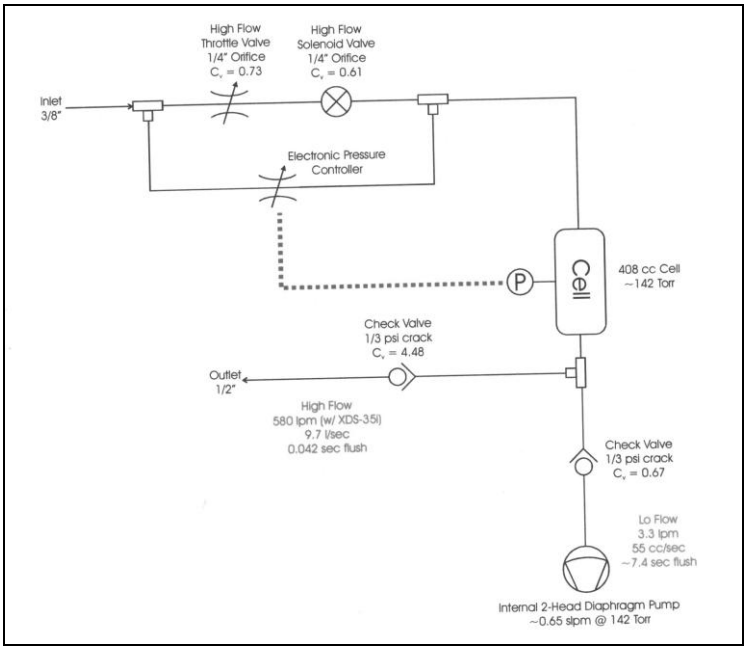

Figure 2.3 Operating scheme of the CRD (D.Baer, Los Gatos inc.)

2.2.2 Measuring emission rates (ER) in dynamic systems

The CRD, when operating with the internal pump, is flushed with a flow rate of 650 ml/min and this means that the same flow rate is needed to flush the reactor or plant-chamber. In dynamic systems, the flow rate is a critical factor, since it affects the detection limit of the system. A constant emission is added to a certain flow rate, and if this flow rate is lower, than the resulting steady state increase in mixing ratio is larger. If a certain concentration increase Δc (*ppbv*) can be detected with the analytical device the minimum emission rate ER that can be detected depends on the flow rate *f (ml/min).* The formula given below (Eq.9) is used to calculate the Emission Rate of a gas-source in a dynamic open system.

$$\textbf{Eq.9} \quad ER = \frac{f \cdot \Delta c \cdot M_{CH_4}}{M_{air} \cdot DW}; \ (ng_{CH4}/gDWh)$$

M_{CH4} and M_{air} are the molar mass of air in one litre of air (24,04 l_{air}/mol_{air}) and the molar mass of methane (16 g/mol) , at constant temperature (20ºC), respectively and DW is the dry-weight of our material.
Whereas a low flow rate leads to a lower detection limit, it also lowers the response time of the system, i.e. the time one has to wait until a steady state concentration elevation Δc has been reached.

If now we consider the measurements of Keppler et al. [2006], the emissions of methane from plants and other materials ranged widely from 0.13 ng CH_4/gDWh (pectin 30ºC darkness) up to 873 ng CH_4/gDWh (living Sweet Vernal Grass under sunlight). For example, considering a fixed amount of 5gr of DW and with our flow-rate of 650ml/min, the CRD should give differentiable concentrations ranging from 0.025 ppbv to 168 ppbv. The sensitivity of the CRD is in the best cases of 1ppbv and consequently to measure low emission rates it has to be increased the final differential

concentration Δc (Eq.9) has to be increased just by reducing the incoming flow. The internal methane source of the system, in this way, reaches a new steady-state at larger magnitude.

The plot below shows of the expected differential concentrations (Δc in ppbv) from the CRD running with a flow-rate of 100ml/min.

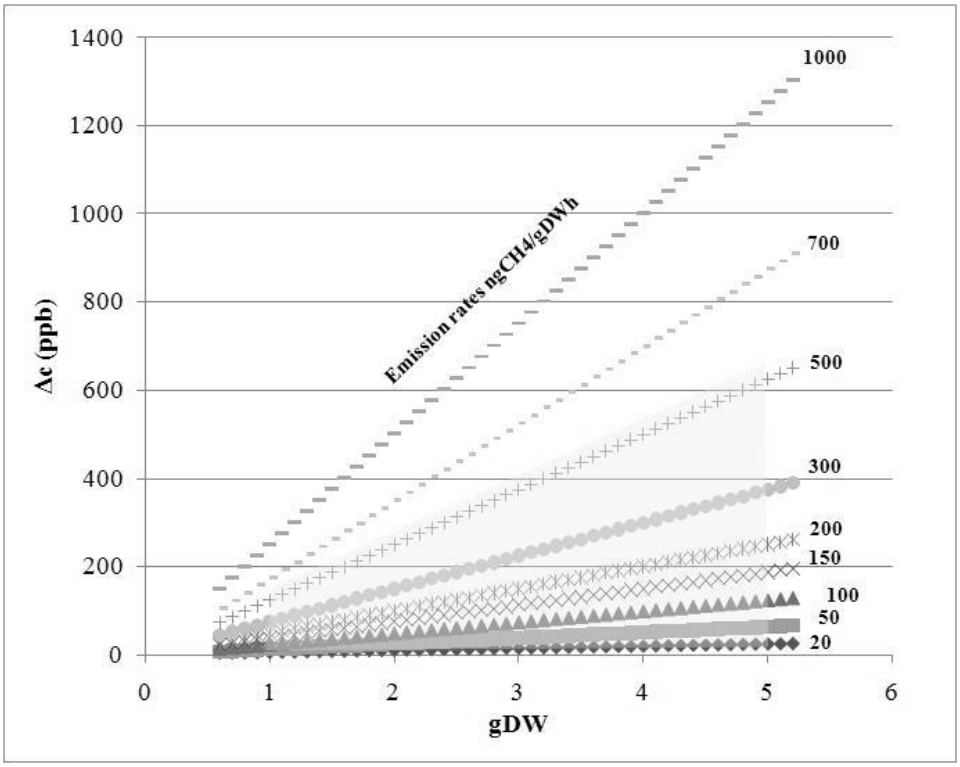

Figure 2.4 Detectable emission rates (ER) depending on the amount of material used (gDW, gram of dry weight) and on the flow rate. A detection limit of ΔC=1ppb has been used for the CRD system. This means that with 5 g material and at a flow rate of 100 ml/min it is possible to detect emission rates of 1 ngCH_4/gDWh. The detection limit can then be lowered by either increasing the amount of material, or lowering the flow rate. If emissions are sufficiently high, the flow rate can be increased in order to investigate, for example, the response time of the system. The shaded area represents the range of the Keppler et al. [2006] values of emission rates.

Personal internal modifications

At the beginning we faced the problem on how to modify the flow rate of the CRD without compromising the stability of the instrument. We found the solution by inserting a Bellows Sealed Metering Valve (NUPRO® SS-4BMC) between the internal pump and the cell. In this way you can reduce the flow-rate into the cell and consequently trough the reactor or plant chamber. The internal software, via feedback to the Electronic Pressure Controller, maintains the cell automatically at ~142Torr.
Considering the Keppler et al. [2006] results, the flow can be adjusted at typical values of 10-500 ml/min, although working with flow rates below 50 ml increase drastically the waiting time in order to reach the steady state in the reactor and also increase the flushing time into the cell of the CRD.

2.3 The GC-IRMS system: measurement system for $\delta^{13}C$ and δD of CH_4 (BRETT)

Brett is the name of the automated experimental setup used in our lab (Fig. 2.4), based on continuous flow isotope ratio mass spectrometry (CF-IRMS). The system is similar to others already used to measure isotopes of methane [*Miller et al.*, 2002; *Rice et al.*, 2001]. The system is fully automated and allows continuous measurements of multiple samples via remote process control. The control unit is called V25 and made at the Max Planck Institute for Chemistry in Mainz. The analytical system was built and programmed by M.Braß, at the MPI für Kernphysik in Heidelberg.

The combination of cryogenic and gas chromatographic purification of atmospheric methane with isotope ratio mass spectrometry, allows measurement of the different isotopologu after chemical conversion of the methane into carbon dioxide for $\delta^{13}C$ or hydrogen for δD. The reasons why methane is converted and not analyzed itself is because methane has same molecular mass like O^+, O_2^{++} for mass 16 or OH• for mass17, and thus water and oxygen interfere in the measurements. Furthermore, CH_4 has rather low ionization efficiency. The most important point, when both heavy isotopes need to be analyzed, is that both ^{13}C and D lead to ions with m/z=17 and can thus not be distinguished.

Through combustion to CO_2 (~900ºC), it is possible to determine the ratio of carbon avoiding isotope molecular interferences. In order to measure the ratio H/D, methane is pyrolysed at high temperatures (~1270ºC) to H_2 and residual carbon which is covering, with a thin layer, the inside of the ceramic tube of the oven, and it can also be partially converted to CO_2 via oxygen transfer from the silica (SiO_2). A more detailed description of lab isotope analyses will be given in the next section.

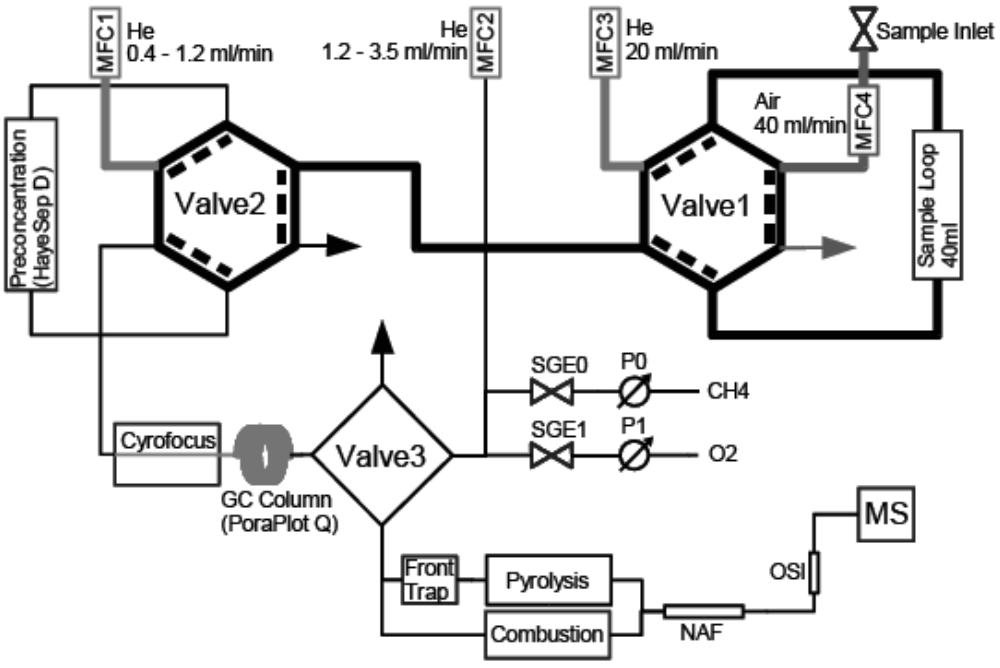

Figure 2.4 Operational scheme of the measurement system for methane isotopes (M.Braß, 2004)

Operative principle (Fig.2.4)

In continuous flow setups (CF-IRMS), the system is permanently purged with a Helium flow (purity at least 99.999%) from an external gas cylinder that in addition has an extra Helium purifier (Supelco, catalogue nº2-3801) mounted before the measurement device. In our system, there He flows are needed and the flow rates are regulated via three mass flow controllers (MFC1, MFC2, MFC3; MKS®. Three valves direct the flows through the system (Valve 1, Valve 2, Valve 3; VALCO®).

In default position (dotted lines Fig.2.4) Valve 1 is set to "inject" and He from MFC2 purges constantly the sample loop of 40ml. When Valve1 is switched to the load position, the sample can be admitted to the loop either from a multiport valve MULTI1 (VALCO) via MFC4 (in case of high pressure flasks) or manually in case of low pressure samples like the plant samples I was measuring for my experiments. For high pressure samples, when Valve 1 is switched to "load", the sample flushes the loop at 40 mL/min via MFC4. After 90 seconds Valve 1 is switched back to position "inject' and the air sample is transferred to the preconcentration unit by He from MFC3 at 20mL/min. The preconcentration unit is a 1/16" stainless steel tube filled with HayeSep D (HSD, 80/100 mesh), which connected in a loop at valve 2. Hayesep D is able to trap methane at ~-120ºC, while N_2 and O_2 are flushed out from this unit. When the bulk air has been flushed out, the temperature is increased to -30ºC to release the trapped methane and the Valve2 is switched to "inject" shortly before methane is actually released. The sample then enters the cryofocus unit where the methane is concentrated at ~-158ºC. MFC1 provides the He carrier gas at 1.2 mL/min which transports methane from the preconcentration unit to the cryofocus unit, where the low temperatures do not allow molecular dispersion of the gases and this is critical in order to get a sharp peak.

In the last step Valve 3 is switched to "inject", MFC1 adjusts the flow rate of He to 0.5 or 0.8, depending on the analyses (δD or $\delta^{13}C$), and the cryofocus is quickly heated up to -75ºC in order to release all the methane trapped and to avoid broadening of the final peak. Initially, the sample was further purified on a GC column, but in fact the cryogenic separation described above is so selective that the GC was later removed.

Successively methane is combusted or pyrolysed depending on the kind of analysis, and thereafter is injected into an open split interface (OSI, GasBench II ThermoFinnigan), which is connected to the mass spectrometer (ThermoFinnigan MAT Delta^{plus}XL).

The sequence which controls the switching time of the valves and the temperatures of the two cryo-units is very critical and has to be fine-tuned, and regularly re-tuned to achieve the best performance.

Some adjustments to the original setup were made during the course of the thesis. A new Cryofocus was made out of a 0.45mm o.d. PoraPlot GC column of 15cm length, and the original 25m Poraplot GC column was disconnected. The original cryofocus was working with a different stainless steel case which had problems with the temperature control. The new cooling setup for the cryofocus is similar to the Preconcentration unit, permitting faster analyses with excellent precision (0.05 ‰ for δ13C and 2‰ for δD).

In addition, a "front trap", which is a piece of capillary immersed in liquid nitrogen, has been added in some experiments before the combustion oven. The front trap was sometimes useful to eliminate unstable baselines before the methane peak in

the IRMS with the old Cryofocus unit when measuring δD. With the new structural developments and the better temperature control the front trap is no longer necessary.

The combustion is made inside a ceramic tube (1.5mm external diameter, 1.0 mm internal diameter, t~900ºC) where three pure 0.25mm Nickel 99,9% wires are placed. The external surface of the wires is oxidised to NiO or NiO_2, and methane is converted in CO_2 trough the following reactions:

R.20 $4NiO + CH_4 \rightarrow 4Ni + CO_2 + 2H_2O$
R.21 $2NiO_2 + CH_4 \rightarrow 2Ni + CO_2 + 2H_2O$

The oxidative capacity of the Nickel decreases every time that methane is combusted and in order to have always quantitative conversion, a single injection of pure O_2 is made before every run. Under stable temperature, the amount of oxygen is a critical factor to get a stable conversion, run after run, but it turns out that even when the CO_2 yield, indicated by the peak area, varies, this does not compromise the isotopic values at the end.

Pyrolysis is the crackdown of the methane molecule into molecular hydrogen and carbon [*Christophe Gueret*, 1997] and in CF-IRMS systems it occurs in a ceramic tube (1.5mm external diameter, 0.5mm internal diameter) without a special catalyst like Nickel used for the combustion.

Measuring the δ difference

The sample gas (partially diluted with the carrier gas, Helium) enters the MS ion source, were the molecules are ionised by electron impact. The ion beam is then accelerated, guided trough a magnetic field and collected at the detectors, which are so called Faraday cups (Fig. 2.5).

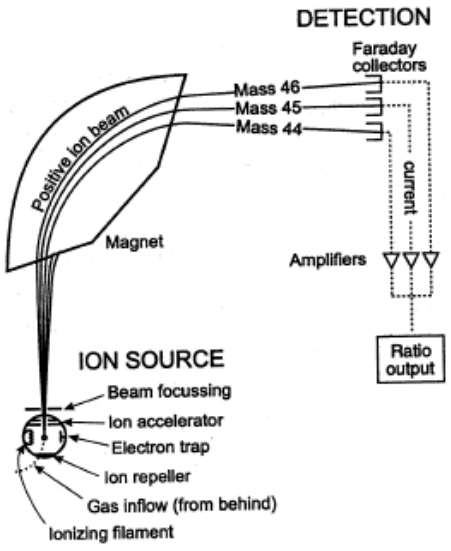

Figure 2.5 Operational scheme of a general mass spectrometer

The magnetic field separates the ions, in our case the different isotopologues of CO_2 or H_2, according to their mass to charge ratio, in base of the Lorentz force (Eq.10) and the Newton's second law (Eq.11)

Eq.10 $F = q(E + v \times B);\quad (N)$

Eq.11 $F = ma;\quad (N)$

Where F is the force in *newtons* (*N),* E is the electric field in *Volts per metre (V/m),* B is the magnetic field in *teslas (T)* , q is the electric ion charge in *coulombs (C),* v is the instantaneous velocity in *metres per second (m/s),* m the mass of the ion (*Kg*), a the acceleration (m/s^2). Equating, the above expressions yields:

Eq.12 $(m/q)a = E + v \times B;$

The signal is a voltage proportional to the ion current registered into the collectors. The signal is then stored in a raw file which can be read and evaluated via the ThermoFinnigan software ISODAT NT 2.0.

The software is used to calculate the δ values directly from the measurements and it applies necessary ion corrections, like the H_3 factor [*Sessions et al.*, 2000] for hydrogen or the ^{17}O correction [*Kaiser*, 2008] for carbon dioxide. It gives also the values of the peak area that is used to derive the concentration.

The mass spectrometer ThermoFinnigan MAT Delta^{plus}XL in our lab has the capacity of 8 Faraday collectors and it can measure simultaneously the signals from 3 cups; by default, cup2, cup3 and cup 4 are used to measure CO_2 on masses 44, 45, 46 respectively, while cup1 and cup 8 are used for hydrogen and deuterium respectively.

As already mentioned the sample ratio r_{smp} is compared to a reference with known ratio r_{ref}, the ISODAT software calculate at the end the δ_{ref}(smp): the delta value of the sample (in our case H_2 or CO_2 derived from CH_4 conversion), compared to a reference of known δ value, that is injected into the MS before and after the "methane" peak.

In most continuous flow applications the reference peak is injected via an open split system right in front of the ion source and therefore has a typical square shape while the sample peak is Gaussian (Fig. 2.6a/b).

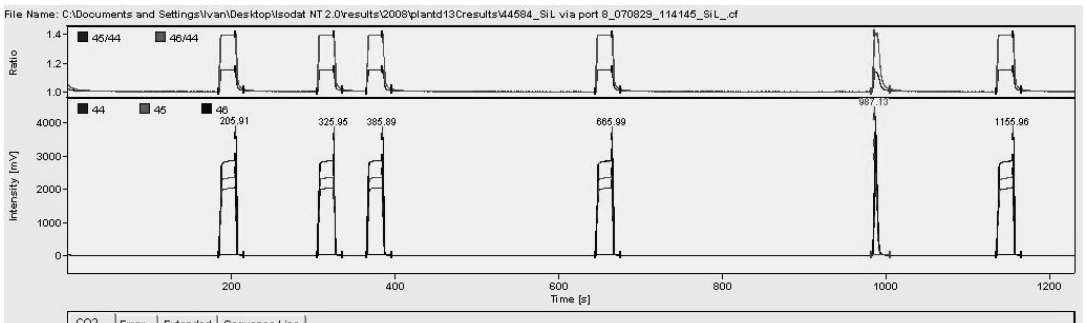

CO2 | Error | Extended | Sequence Line

Filename	Peak Nr.	Rt [s]	Width [s]	Ampl. 44 [mV]	BGD 44 [mV]	BGD 45 [mV]	BGD 46 [mV]	Area All [Vs]	rd 45CO2/44CO2 [per mil] vs. CO2_UT1	d 45CO2/44CO2 [per mil] vs. VPDB	rd 46CO2/44CO [per mil] vs.	d 46CO2/44C [per mil] vs. VPDB	d 13C/12C [per mil] vs.	AT% 13C/12C [%]	d 18O/16O [per mil] vs. VSMOW
44584_SiL via port 8_070829_1141	1	205.9	31.0	2543	0.6	0.7	0.4	40.609	-0.065	-26.410	-0.210	19.933	-28.878	1.074072	20.014
44584_SiL via port 8_070829_1141	2	326.0	30.7	2525	0.9	1.0	0.8	40.680	-0.095	-26.440	-0.153	19.991	-28.911	1.074036	20.073
44584_SiL via port 8_070829_1141	3	385.9	30.9	2522	1.8	2.1	2.2	40.856	-0.207	-26.549	-0.046	20.100	-29.031	1.073904	20.182
44584_SiL via port 8_070829_1141	4*	666.0	30.6	2514	0.6	0.6	0.3	40.574	0.000	-26.347	0.000	20.148	-28.818	1.074138	20.229
44584_SiL via port 8_070829_1141	5	987.1	22.8	2948	0.5	0.6	0.4	10.725	-13.855	-39.837	9.864	30.211	-43.562	1.058004	30.334
44584_SiL via port 8_070829_1141	6	1156.0	30.7	2513	0.5	0.5	0.3	40.463	0.054	-26.294	-0.136	20.008	-28.757	1.074205	20.090

a

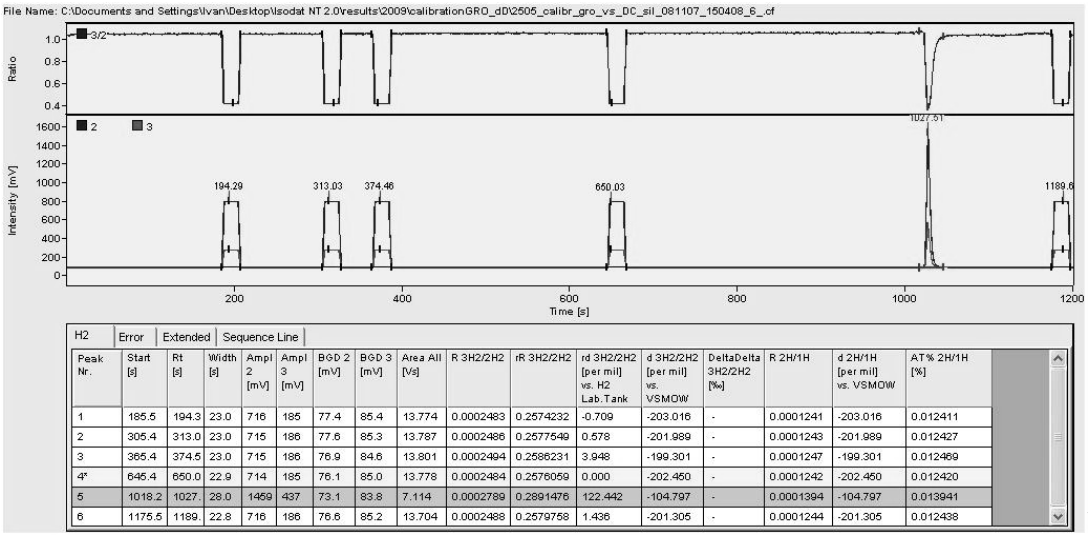

Peak Nr.	Start [s]	Rt [s]	Width [s]	Ampl 2 [mV]	Ampl 3 [mV]	BGD 2 [mV]	BGD 3 [mV]	Area All [Vs]	R 3H2/2H2	rR 3H2/2H2	rd 3H2/2H2 [per mil] vs. H2 Lab.Tank	d 3H2/2H2 [per mil] vs. VSMOW	DeltaDelta 3H2/2H2 [‰]	R 2H/1H	d 2H/1H [per mil] vs. VSMOW	AT% 2H/1H [%]
1	185.5	194.3	23.0	716	185	77.4	85.4	13.774	0.0002483	0.2574232	-0.709	-203.016	-	0.0001241	-203.016	0.012411
2	305.4	313.0	23.0	715	186	77.6	85.3	13.787	0.0002486	0.2577549	0.578	-201.989	-	0.0001243	-201.989	0.012427
3	365.4	374.5	23.0	715	186	76.9	84.6	13.801	0.0002494	0.2586231	3.948	-199.301	-	0.0001247	-199.301	0.012469
4*	645.4	650.0	22.9	714	185	76.1	85.0	13.778	0.0002484	0.2576059	0.000	-202.450	-	0.0001242	-202.450	0.012420
5	1018.2	1027.	28.0	1459	437	73.1	83.8	7.114	0.0002789	0.2891476	122.442	-104.797	-	0.0001394	-104.797	0.013941
6	1175.5	1189.	22.8	716	186	76.6	85.2	13.704	0.0002488	0.2579758	1.436	-201.305	-	0.0001244	-201.305	0.012438

b

Figure 2.6 The typical ISODAT "chromatogram" for $\delta^{13}C$ (a) and δD (b) of CH_4. Square peaks are reference injections of pure standard gas (CO_2 for $\delta^{13}C$, H_2 for δD), while the Gaussian peak is the sample coming from the BRETT system. The isotope ratio is calculated from the ratio of the areas of the different isotopologues detected at the Faraday cups. The value of the δ_{Smp} in ISODAT is calculated automatically by comparing the isotope ratio of the sample with the isotope ratio of the references.

The final δ value returned by the software is not correct, and we need to compare the sample peak with a calibrated standard gas which is processed like the sample. This is because the sample may be affected by isotopic fractionations present in the cryo-steps as well as in the conversion, while the pure reference is not affected, since it comes directly into the MS.

In the past, until end 2008 we were using a lab standard coming from Germany, so called *SchauinsLand* ($\delta^{13}C$=-48.02‰; δD=-92.27‰), thereafter it was replaced with air from *Groningen* in The Netherlands ($\delta^{13}C$=-47.54‰; δD=-89.26‰). The equation used to calculate the delta values of a sample relative to the laboratory standard is the following:

$$\textbf{Eq.11} \quad \delta_{STD}(Smp) = \overline{\delta_{\mathrm{Ref}}(Smp)} + \overline{\delta_{STD}(\mathrm{Ref})} + \frac{\overline{\delta_{\mathrm{Re}\,f}(Smp)} \cdot \overline{\delta_{STD}(\mathrm{Ref})}}{1000};$$

The δ_{STD}(Ref) is the value of our reference CO_2 relative the standard cylinder. When the system is running with good stability, the standard is measured after 4 runs of samples (STD-Smp_1-Smp_1-Smp_2-Smp_2-STD). The sample is always measured at least twice and the final values δ_{STD}(Smp) is calculated using the mean values of the two STD measurements (δ_{STD}(Ref)) before and after. An equation similar to Eq. 11 is then used to convert the δ values to international standards.

The concentrations are derived from the peak area and relative to the standard gas which has a known and well-calibrated concentration [CH_4](STD):

$$\textbf{Eq.12} \quad [CH_4](Smp) = [CH_4](STD) \cdot \frac{Area(Smp)}{\overline{Area(STD)}};$$

When both isotope signatures, $\delta^{13}C$ and δD are measured, two values are derived for the concentration. Typically there is an offset probably due to a not complete conversion in the pyrolysis. At the end the mean value of the two analyses is taken.

Calibration, Linearity tests and special measurements

The calibrated value of a single standard gas is a necessary but not sufficient condition for providing calibrated values in case of samples with a wide range of delta values. In order to have a calibration curve that covers the most common range of isotopic values we should have calibrated gases at different isotopic composition. In our lab we use cylinders filled with firn air sampled at Dome Concordia in Antarctica, supplied from the MPI in Mainz [*Braunlich et al.,* 2001], covering a range of of 3‰ for $\delta^{13}C$ and 10‰ for δD (values in Table 1, see Appendix). Additional artificial calibration gases are available from earlier developments of a laser based method for δD measurements at the MPI in Mainz . These samples have particularly enriched and depleted values of $\delta D\text{-}CH_4$, ~+21.1‰ and -167‰ respectively, and these samples were used to fix the scale of the system. The same gas cylinders are used also to calibrate the concentration scale (Fig. 2.7).

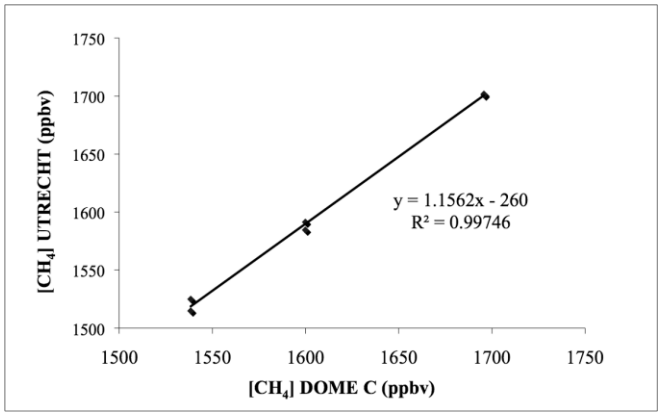

b

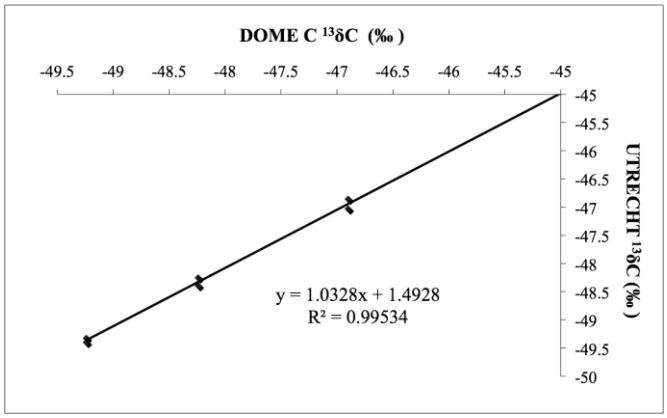

a

Figure 2.7 Calibration measurements for concentrations (a) and for $\delta^{13}C\text{-}CH_4$ (b) of the DOME C reference firn air samples. The values on the x-axis are from Bräunlich et al [2001].

Chemical-physical processes in the measuring device itself can also lead to changes in the isotopic values, and such changes often depend on the amount of sample analyzed. This leads to a dependency of the δ values on the peak area, i.e., the concentration of the sample, which is called non-linear behaviour. The non-linearity can be considerable and has to be carefully calibrated.

Usually for tropospheric-stratospheric samples at high pressure an automatic linearity test is done before the analysis. The test is performed by partially filling the sample-loop of BRETT; this is realized by varying the fill time for the sample loop between 10 and 90 seconds. The resulting calibration curve then covers the range of samples measured.

Typically there is a change of 1‰ for $\delta^{13}C$ analyses when the area is of half size and the linearity correction is of importance especially for stratospheric samples where the low concentrations (<1.5ppm) need to be calibrated against troposheric air at ~1.9 ppm.

Special calibration procedure has been developed for low pressure samples, where the isotopic values depend on the initial pressure and the reference is measured at the same pressure of the samples. Here comparing only the peak size it is not sufficient since the low pressure measurements are processed differently along the separation steps of BRETT with other isotope fractionations.

2.4 The GC-FID system

Gas chromatography has proven to be one of the most powerful tools available for the determination of trace amounts of organic substances in air. The instrument used in the lab for measuring methane concentrations is a GC8000^{top} from CEinstruments®.

In gas chromatography, a carrier gas, usually Helium, is flushing the sample trough a stationary phase in a capillary column. The most commonly used stationary phase is Carboxen-1000 particles with a mean pore diameter of 70Å, a surface area of more than 1200 $m^2\ g^{-1}$ and a distribution of macro, meso, and micro-pores optimized to provide effective kinetics for GC analyses and high efficiency (SIGMA-ALDRICH).

The limited separation of nitrogen/air from methane requires low starting temperatures (about 40ºC), but this increases analysis time and may affect the accuracy of the analysis. In our lab we mainly used ramps of oven temperature increasing to values of up to 240ºC.

A multiple port valve with a sample loop of 1 ml introduces the gas sample into the column of 3 m length and 2.1 mm internal diameter stainless steel column packed with 60/80 mesh Carboxen^{TM}–1000. In our system, the carrier gas flow rate is 30mL/min provided by 100kPa head pressure.

While passing the column, methane is separated from other gaseous components. After the column, the gas enters a detector chamber where a signal is produced proportionally to the quantity of the sample.

The most commonly used detector for methane at atmospheric concentrations is the flame ionization detector (Fig. 2.8) where the sample eluted is mixed with a hydrogen stream and air from cylinders and burned in a special quartz chamber. The collector of the burner is standing between two electrodes supporting 300V. The active part of the detector is a small flame of few mm^3. The FID measures perturbations in the differential voltage due to ions produced in the flame when

methane is burned. A signal in mV is usually given and integrated over the time producing the peak of methane in the classic chromatogram.

A standard gas from a certified cylinder was used to make a calibration curve by injecting diluted quantities for deriving a regression equation.

Our method allows determinations of atmospheric methane concentrations with a precision of ± 20ppb [*Vigano et al.*, 2008].

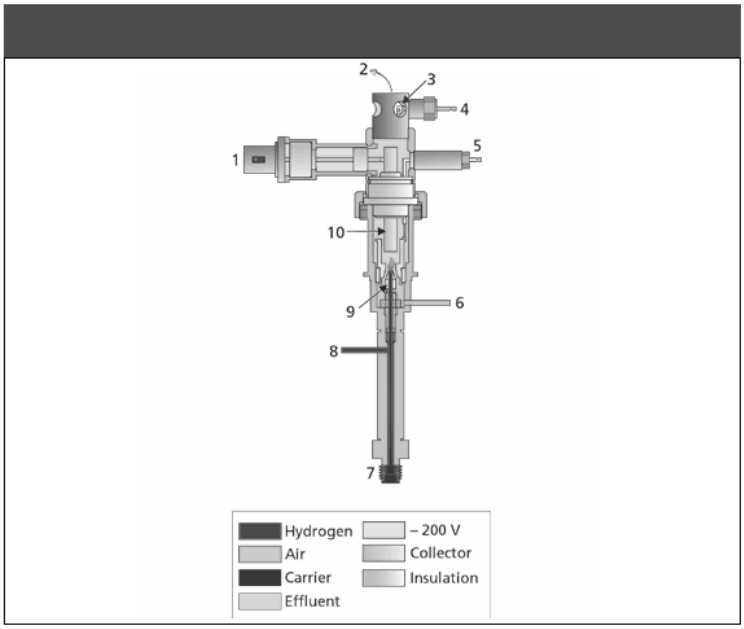

Figure 2.8 Flame ionization detector cross-section. 1 electrometer connection, 2 = effluent exit, 3 = igniter coil, 4 = igniter power connection, 5 = polarizing voltage supply connection, 6 = air input, 7 = column connection, 8 = hydrogen input, 9 = flame jet, 10 = collector electrode. (Derived from a figure courtesy of PerkinElmer Instruments, Shelton, Connecticut).

Chapter 3

Effect of UV radiation and temperature on the emission of methane from plant biomass and structural components

The recently reported finding that plant matter and living plants produce significant amounts of the important greenhouse gas methane under aerobic conditions has led to an intense scientific and public controversy. Whereas some studies question the up-scaling method that was used to estimate the global source strength, others have suggested that experimental artifacts could have caused the reported signals, and two studies, one based on isotope labeling, have recently reported the absence of CH_4 emissions from plants. Here we show – using several independent experimental analysis techniques – that dry and detached fresh plant matter, as well as several structural plant components, emit significant amounts of methane upon irradiation with UV light and/or heating. Emissions from UV irradiation are almost instantaneous, indicating a direct photochemical process. Long-time irradiation experiments demonstrate that the size of the CH_4 producing reservoir is large, exceeding potential interferences from degassing or desorption processes by several orders of magnitude. A dry leaf of a pure ^{13}C plant produces $^{13}CH_4$ at a similar rate as dry leaves of non-labeled plants produce non-labeled methane.

Published in *Biogeosciensces*, (2008), 5(3), 937-947, Ivan Vigano[1], Huib van Weelden[2], Rupert Holzinger[1], Frank Keppler[3], Andy McLeod[4] and Thomas Röckmann[1]

[1]Institute for Marine and Atmospheric research Utrecht (IMAU), Princetonplein 5, 3584ED Utrecht, The Netherlands
[2]Department of Dermatology and Allergology Utrecht University Medical Center Utrecht, Heidelberglaan 100, 3584CX Utrecht, The Netherlands
[3]Max-Planck-Institute for Chemistry, Joh.-Joachim-Becher-Weg 2, 55128 Mainz, Germany
[4]School of GeoSciences, University of Edinburgh, Crew Building, The King's Buildings, West Scotland, UK;

3.1 Introduction

Methane (CH_4) is the second most important anthropogenic greenhouse gas after CO_2 [*Forster et al.*, 2007] and the most abundant reduced organic compound in the atmosphere, which makes it an important participant in atmospheric chemistry. According to established knowledge, it is produced primarily by anaerobic bacterial activity in wetlands, rice fields, landfills and the gastrointestinal tract of ruminants, with non-bacterial emissions occurring from fossil fuel usage and biomass burning. The main tropospheric sink of CH_4 is chemical removal by the hydroxyl (OH) radical. Microbial uptake in soils and loss to the stratosphere are small sinks. Recently, Keppler et al. [2006] published results from laboratory experiments indicating that living plants, plant litter and the structural plant component pectin emit methane to the atmosphere under aerobic conditions. These findings are heavily debated, since they have far-reaching implications, mainly for two reasons: 1) It is generally believed that the reduced compound CH_4 can only be produced naturally from organic matter in the absence of oxygen, or at high temperatures, e.g. in biomass burning, and in fact no mechanism for an "aerobic" production process has been identified at the molecular level. 2) The first extrapolations from the laboratory measurements to the global scale indicated that these emissions could constitute a large fraction of the total global emissions of CH_4.

After publication of the paper, in particular the second point and the underlying extrapolation procedure were criticized, and other up-scaling calculations were performed, which would result in a lower – but potentially still important – source strength [*Bergamaschi et al.*, 2006b; *Butenhoff and Khalil*, 2007a; *Ferretti et al.*, 2006; *Houweling et al.*, 2006; *Kirschbaum et al.*, 2006; 2007]. It should be kept in mind, however, that without further insight into the nature of the production process, any up-scaling approach bears considerable uncertainties. For example, it is not known yet which parts of plants (e.g. leaves, roots, and stems) emit how much CH_4 and how this depends on environmental parameters. This uncertainty was acknowledged by Keppler et al. [2006], who presented their result as a first estimate. On the other hand, if an aerobic CH_4 production mechanism exists, then there are independent indications that it could be indeed a large source. For example, satellite and recent aircraft observations suggest a strong CH_4 source in the tropical forest region [*Frankenberg et al.*, 2005; *Frankenberg et al.*, 2006; *Miller et al.*, 2007] and attempts to combine the satellite observations with the existing ground network require significantly higher CH_4 emissions in the tropics [*Bergamaschi et al.*, 2007]. In addition, the high ^{13}C content of methane before 1500 a.d. as recovered from ice cores [*Ferretti et al.*, 2005] is hard to reconcile with the standard picture that pre-industrial emissions were dominated by isotopically depleted wetland emissions. The initial hypothesis that pre-industrial anthropogenic biomass burning caused the high ^{13}C levels [*Ferretti et al.*, 2005] is questioned by new data that show an even higher ^{13}C content in the early Holocene [*Schaefer et al.*, 2006]. Thus the high biomass burning levels would have to be natural, but an alternative scenario that involves significant levels of vegetation emissions has also been suggested [*Houweling et al.*, 2006; 2007]. Direct atmospheric measurements [*Crutzen et al.*, 2006; *do Carmo et al.*, 2006; *Sanhueza and Donoso*, 2006b; *Sinha et al.*, 2007] are consistent with CH_4 emissions from plants. The most recent published study reported CH_4 emissions from shrubs in the inner Mongolian steppe, but not from grasses [*Wang et al.*, 2007].

However, here remains considerable doubt about the existence of CH_4 emissions from vegetation.

Therefore, the principle scientific questions are: if, by how much and by what mechanisms is methane emitted from plant matter under normal atmospheric conditions and without bacterial activity? The first follow-up study [*Dueck et al.*, 2007] did not confirm the findings: No $^{13}CH_4$ emissions were found from plants, which were grown in a $^{13}CO_2$ atmosphere and should thus have produced $^{13}CH_4$ only. Beerling et al. [2008] similarly reported no CH_4 emissions from a C3 and a C4 species but suggested a possible role of non-enzymatic processes with an action spectrum outside the photosynthetically-active range. Nevertheless, to the best of our knowledge there is no scenario other than direct emissions from the plant matter that can explain the (natural abundance) isotope signatures observed in the earlier experiments by Keppler et al. [2006].

Facing this important apparent contradiction we designed a series of measurements in order to investigate whether an aerobic CH_4 production mechanism indeed exists. In order to exclude potentially complicating factors from living plants we restricted this project to dry and fresh plant matter, as well as defined structural plant components such as pectin, lignin and cellulose. Therefore, effects related to photosynthesis and respiration do not interfere, for example, it is not necessary to actively stabilize CO_2 concentrations and we eliminate potential problems due to high levels of water vapour from transpiration of living plants. We also avoided possible artifacts that can be associated with static enclosure systems by using dynamic flow reactors.

3.2 Experimental

The study of Keppler et al. [2006] had indicated that the CH_4 emissions from plants and plant matter are light and temperature dependent. Therefore, we irradiated more than 20 types of dry and fresh plant matter (see Table 1, Appendix A), as well as several structural plant compounds, with different light sources covering the wavelength range from visible light to UVC. The experiments were mostly carried out in dynamic UV transparent (Suprasil) flow reactors rather than the static chambers used previously. The substrates were placed in ~50, ~100 or ~300 ml volume glass or Suprasil vials, which were purged with 100 to 500 ml/min of either dry air (normal ambient CH_4 concentration) or dry synthetic air (no methane). The CH_4 production rate was determined from the difference in concentrations of the in- and out-flowing air and the airflow rate. In some experiments we also used humidified air, and in those cases the water content of the reference and sample air was set to a common level using a humidity exchanger (Nafion), in order to avoid artificial mixing ratio changes arising from different humidity. Additional heating experiments were carried out by heating the Suprasil vials with heating tape to temperatures up to 100ºC.

Three different methods were used to quantify CH_4 levels: 1) An off-axis integrated cavity output spectrometer (Los Gatos Inc.) that allows real-time high-precision monitoring of CH_4 mixing ratios at a frequency up to 10 Hz and with a precision of ±2 ppb for 5-second averaged data. No cross-sensitivities from other species are known for this instrument, and we verified this for the abundant plant

emission CH_3OH 2) A GC-FID instrument for grab sample analysis (reproducibility ± 10 ppb) for occasional cross-check for the optical technique and for the experiments with small static vials, where the small sample amount does not allow measurements with the optical system. 3) The isotope ratio mass spectrometry (IRMS) technique, also used by Keppler et al. [2006], to measure not only the concentration (reproducibility ± 20 ppb at ambient concentration), but also the ^{13}C and D isotopic composition of the CH_4.

As light sources we used 6 types of lamps: A Philips 400W HPS Na lamp, four UVA and UVB lamps (20W Phillips TL01, TL09, TL12, TUV (15W) and Osram Vitalux (300W), spectra are shown in Figure 1 of the Appendix), and one 5W Radium NTE-220 HG penray UVC lamp (Oriel Instruments) with the typical emission line at 254 nm. The UVC penray lamp was placed inside a Suprasil finger protruding inside the sample vial and was thus at 1-2 cm distance from the sample. This may lead to heating of the material, which was not measured. All other lamps irradiated the sample from the top. In case of the Osram Vitalux lamp, a single lamp was used, whereas for the three Phillips lamp types we used an array of six UV lamps. The UV content (UVA and UVB separately) was determined with a Waldmann UV meter (Waldmann, Schwenningen, Germany) calibrated for each individual UV lamp, except for the UVC lamp. The relative spectral distribution measurements and the calibration of the Waldmann device were performed with a calibrated standard UV-visible spectroradiometer (model 752, Optronic Laboratories Inc, USA).

In the absence of a reliable action spectrum for CH_4 release from biomass upon UV irradiation, the UV strength is reported as the non-weighted integral over the UVA range (400-320 nm), UVB range (320-280 nm) or total UV range (400-280 nm). Except for the Hg lamp, and a very small amount from the TL12 lamps, the lamps do not emit in the UVC range. In most experiments unfiltered light was used, but tests were carried out with a cellulose diacetate filter in order to investigate the influence from short-wave radiation (see below).

Choosing this approach (using unfiltered, non-weighted UV radiation) we neglect a possible wavelength dependence of the biologically effective dose. This has to be kept in mind when comparing the observed emissions to the real atmosphere. For example, when we irradiate the material with an integrated UVB amount similar to the atmosphere, the individual lamps still possess strongly (TL01) or slightly (TL12, VITALUX) more shortwave UVB radiation (loosely defined as wavelengths below 295 nm) than the natural solar spectrum at the surface of the earth, where such wavelengths are virtually absent. The possible effects of higher levels of shortwave radiation will be discussed below, as well as first semi-quantitative information on an action spectrum.

To increase signal to noise ratio, the average non-weighted UVB intensity used in the experiments was 5 times higher than natural UVB levels, in some experiments even >10 times higher, but we also carried out experiments at close to natural total UV levels. Temperatures were mostly determined directly at the leaf surface with a micro-thermocouple attached to the material, in the early experiments the gas temperature was measured.

Blank experiments were carried out by repeating the same experiment under identical conditions but without the organic matter sample. In none of the blank experiments could we detect any CH_4 production.

3.3 Materials

The full list of materials investigated in the irradiation experiments is given in Table 2 of the Appendix. Most of the plant material was obtained from the Botanical garden of Utrecht University; some leaves were collected from regular outside plants or plants grown inside a building. Material was dried by heating the plants in an oven overnight at 80-100ºC. Fresh materials were usually analyzed within 1 hour after detachment from the living plant. The organic compounds used for experiments were obtained from Sigma (apple pectin, purity 95%, CAS number 9000-69-5, cellulose microcrystalline, purity 95%, CAS number 9004-34-6, pectin esterified from citrus fruit, purity 99%, CAS number 37251-70-0, lignin, purity 95%, CAS number 8068-05-1, palmitic acid, Grade II, purity 95%, CAS number 57-10-3). In a typical experiment we used between 0.1 and 5g of dry material.

3.4 Results and discussion

3.4.1 Methane emission from organic matter – the effect of UV light and temperature

Significant amounts of methane were produced from all materials when irradiated with lamps that contain UV radiation (Table 2, Appendix), but the emissions were below the detection limit of the dynamic flow system (~2 ng/g dw/h, improved in the later experiments) when a Na lamp with a cutoff wavelength of ~400 nm, i.e., without UV radiation, was used. To investigate the dependence of the CH_4 emission on wavelength in the UV range, we adjusted the distance to the different lamps such that in 4 similar experiments with the same sample of dry grass (*Lolium perenne*) the sample received the same total UV content (280-400 nm, without filters and unweighted) of 30 W/m^2 from all four UV lamps. To avoid excessive heating, in those experiments the vial was cooled from the outside with a strong ventilator and the temperature did not exceed 28ºC, which is only slightly above the lab temperature of 22ºC.

The results imply that UVB radiation is more efficient than UVA radiation in inducing CH_4 emission, giving first qualitative information about the UV action spectrum (Figure 3.1): the highest emissions are obtained with the broad band and narrow band UVB lamps (Phillips TL01 and TL12), followed by the Osram Vitalux lamp, which has the largest part of its UV content in the UVA region, and the lowest emission are obtained with the UVA lamp (Phillips TL09). Emissions with the UVC penray lamp are still significantly higher than with the UVB lamp, but cannot be directly compared to the other lamps since the irradiation geometry is different.

To further investigate the wavelength dependence of the emission rates, two optical filters were used: a) a cellulose diacetate filter that strong attenuates short-wave UVB radiation (transmission <1% below 291 nm) and b) a sheet of window glass that blocks virtually all UVB radiation (transmission <1% below 323 nm). Those filters reduce the total amount of UV radiation reaching the sample and also the CH_4 emission rates, as shown in Figure 3.1. The cellulose diacetate filter reduces the total UV radiation (unweighted) from the broadband UVB lamp (TL12) by ~20%, and

the CH_4 emission by ~30%. This indicates a slightly, but not extremely increased efficiency in CH_4 production of those wavelengths that are preferentially filtered (λ<290nm). For the other lamps, the changes in emission rate and the reduction of the total UV radiation are not significantly different. A similar conclusion can be drawn from the results of the unfiltered TL01 and TL12 lamps. At the same level of total UV radiation, the emission rates are very similar, although the spectral distribution is strongly different (see Figure 1, Appendix). The fraction of UVB radiation shorter than 295 nm is 13% for the TL12 lamp, but only 0.5% for the TL01. The absence of a strong difference in emission rates and the results with the cellulose diacetate filter indicate that the action spectrum for CH_4 production may not be very steep in the UVB region, in contrast to, e.g., the action spectrum for human erythema or DNA damage.

The window glass reduces the emission rates much more strongly. The reductions are strongest for the UVB rich light sources and are not significant for the UVA lamp, which again highlights the important role of UVB radiation (Figure 3.1).

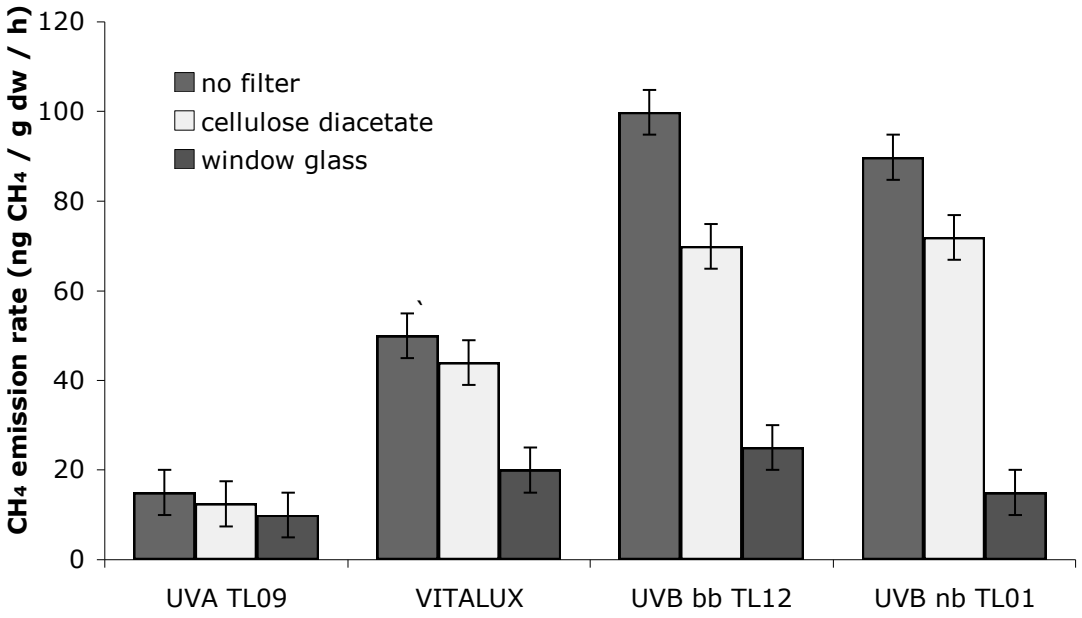

Figure 3.1 Emission rate from a grass sample (*Lolium perenne*) irradiated with different lamps with the same total UV content. The ER increases with increasing relative UVB content. The emission rate decreases when a cellulose diacetate filter or a glass sheet are placed between the vial and the lamp. Error bars are derived from the noise level of the optical instrument.

Several of the lamps used for photolysis are based on a Hg arc, and thus also emit small traces of UVC radiation at 254 nm. The figure 1 in the Appendix indicates that those traces are highest for the TL01 and TL12 lamps. To investigate a possible disproportionate effect from this very small fraction of UVC radiation, a similar lamp that irradiates only the Hg arc (UVC) was used. At a similar total UV level, the UVC lamp produces nine times higher CH_4 emissions than the TL01 lamp. This again implies a wavelength dependence, but excludes a disproportionate effect from the UVC wavelengths. These experiments provide important first semi-quantitative

information about the action spectrum, as called for in [*Kirschbaum et al.*, 2006], but a full deconvolution is beyond the scope of this work.

Typical ambient (non-weighted) summer UVB irradiances near the Earth surface range from 2 W/m^2 at mid latitudes to 4 W/m^2 in the tropics [*Bernhard et al.*, 1997]. When biomass is irradiated with similar non-weighted levels of total UVB, CH_4 emissions increase linearly with UVB intensity (Figure 3.2).

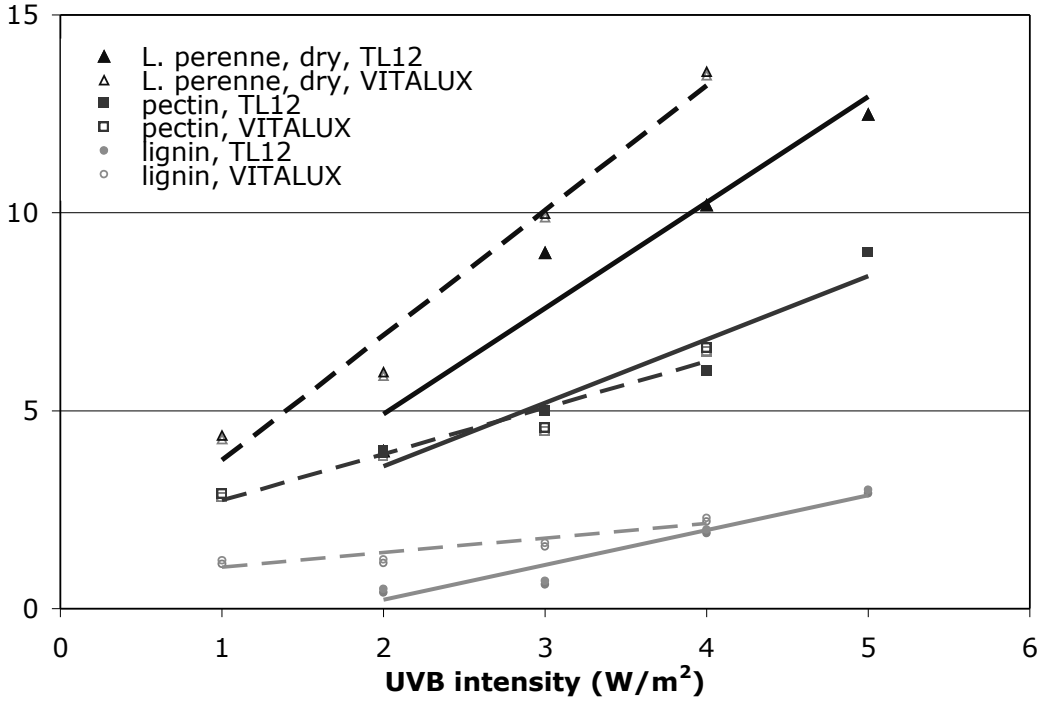

Figure 3.2 Dependence of the CH_4 emission rate from dry grass (*L. perenne*), pectin and lignin on UVB intensity over the naturally occurring UVB range (unweighted) using the TL12 (solid symbols and linear trend lines) and the VITALUX (open symbols and dashed linear trend lines) lamps.

Typical emission rates in the temperature range from 25 to 40ºC are 7 to 50 ng CH_4/g dw/h (g dw = gram dry weight). It should be kept in mind that a full action spectrum is required to compare those emission rates to the atmospheric situation, however, our experiments with different light sources and filters indicate that the slope of the action spectrum may be rather low. This implies that the CH_4 emissions reported here may not be strongly affected by details in the spectral distribution. The CH_4 emission rates under UV irradiation are significantly higher than reported by Keppler et al. [2006] for their experiments with plant litter, which were carried out without UV irradiation, but lower than their emissions from living plants, even without light. Emissions of methane increase linearly with the amount of material irradiated, so that it is adequate to report the emission rates per amount of material (units ng CH_4/g dw/h). The linear dependence of CH_4 emission rate on light intensity provides the link to the results in the following part of the paper, where we used UV intensities up to 10 times higher than typical tropical surface values in order to increase signal to noise level of the analytical system. As mentioned above, blank experiments without an organic matter sample showed no detectable CH_4 production.

In addition to UV light, heating also leads to CH_4 emissions, as was already shown by Keppler et al. [2006]. However, irradiation with UV strongly changes the temperature dependence. (Figure 3.3).

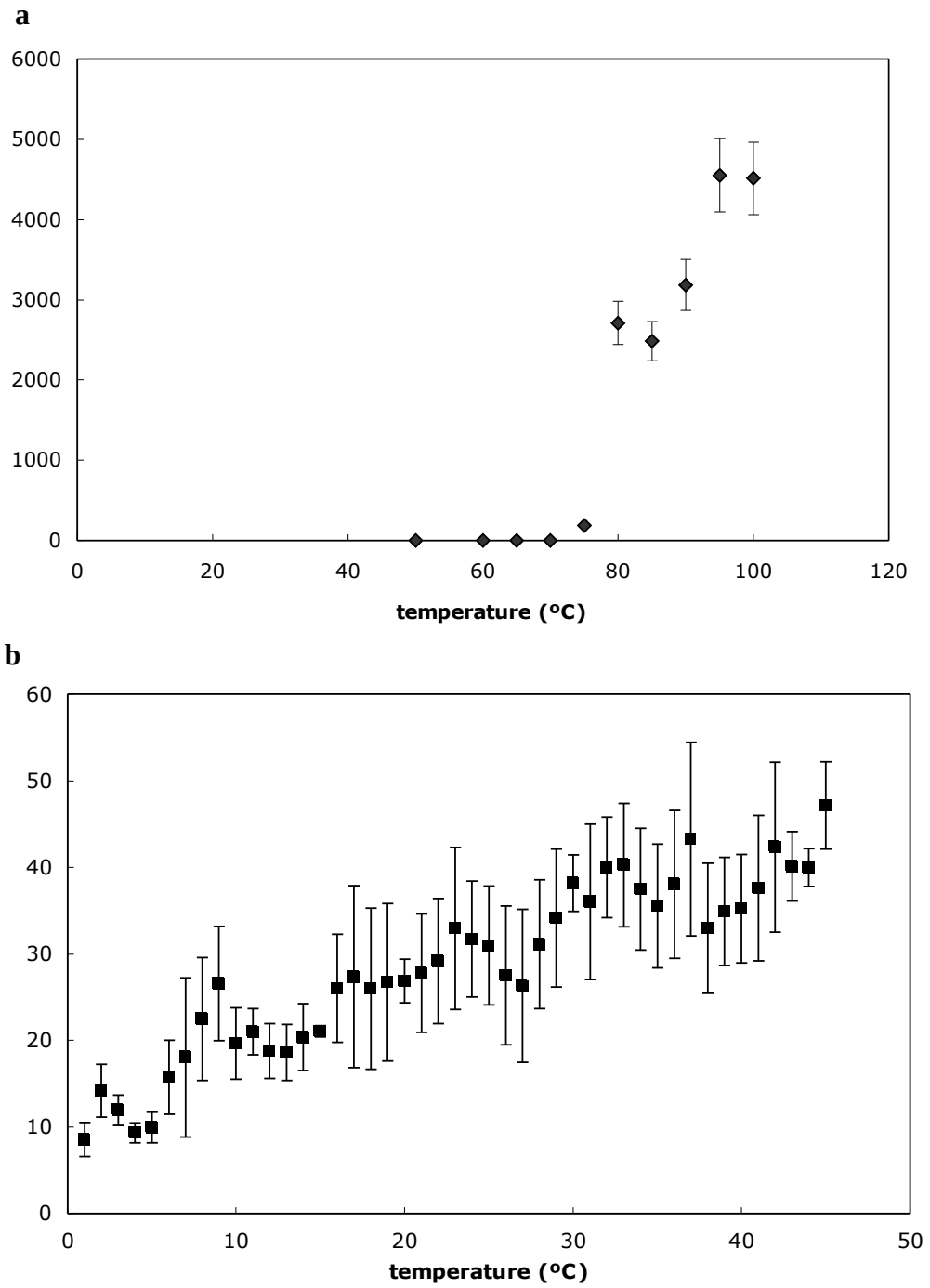

Figure 3.3 Dependence of the emission rate from dry milled grass (*Lolium perenne*) on temperature without UV irradiation (a) and with UV light (5 W/m^2 UVB) from the Philips UVB bb TL12 lamp (b). Error bars in (a) are derived from the uncertainty of the concentration measurements, error bars in (b) denote the average of three similar experiments.

Without UV irradiation, CH_4 production is not detectable in our dynamic system (below 2 ng/g dw/h) until the temperature reaches 70-80ºC, at which the emission rate increases sharply. Under UV irradiation with the broadband UVB lamp TL12 (5 W/m^2 UVB, i.e., similar to typical tropical noon levels, but unweighted), emissions are already significant at room temperature and increase almost linearly with increasing temperature in the ambient temperature range from 0 to 50ºC. This difference in emission behaviour indicates at least two different production mechanisms. The low-temperature UV facilitated emissions are expected to be ubiquitous. Both the linear increase of methane emissions observed during irradiation with UV light as well as the strong emission of methane at elevated temperatures rule out a microbial mediated formation pathway.

Similar experiments were carried out with the structural plant components pectin, lignin, cellulose and palmitic acid. In addition to pectin, which was already studied by Keppler et al. [2006], also lignin and cellulose emit significant amounts of CH_4 upon irradiation with UV light (Figure 3.4). On the other hand emissions of CH_4 from palmitic acid, a component in the cutin layer of plants, are very low, but can be "forced" by using a higher dose of UV light.

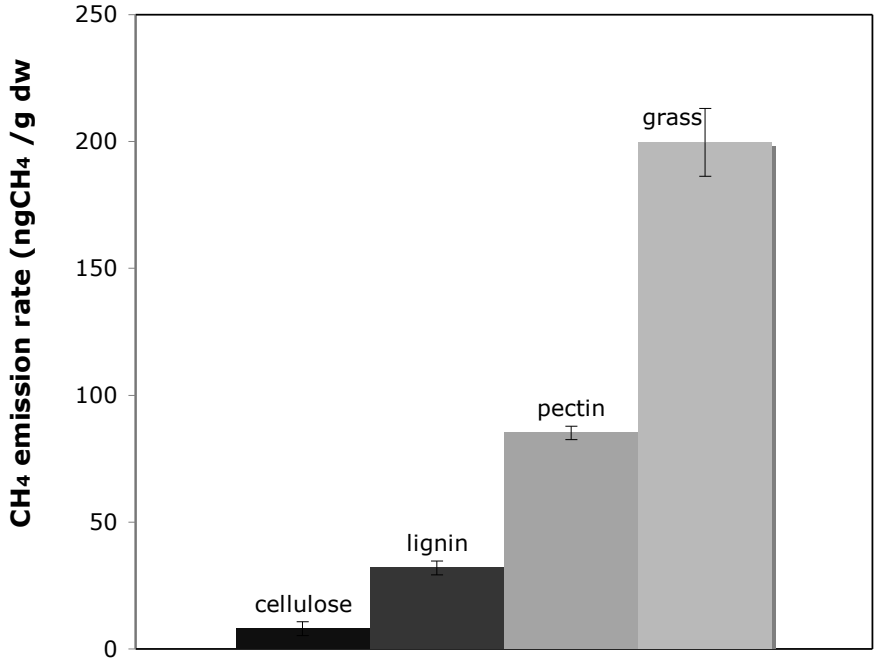

Figure 3.4 Comparison of methane emission rates from dry grass and various plant structural compounds under UV irradiation (Vitalux lamp, UVA 53 W/m^2, UVB 7.4 W/m^2). Error bars are derived from the uncertainty in the concentration measurement.

In particular the emissions from cellulose, the primary structural component of green plants, are noteworthy. Keppler et al. [2006] suggested that esterified methyl groups could be the source substrate for CH_4 production in pectin. In fact new results by Keppler et al. [2007] show isotopic evidence that methyl esterified groups of pectin can act as a precursor for methane formation under aerobic conditions.

Cellulose does not possess such groups, and thus our results imply (if those emissions are not caused by contamination from impurities) that UV irradiation leads to CH_4 production from other carbon moieties of polysaccharides, in addition to the methoxyl groups. Interestingly, a free radical process has recently been suggested for the formation of methane from polysaccharides under the influence of UV light [*Sharpatyi*, 2007]. Figure 3.4 shows that under comparable conditions emission rates of dry plant material are generally higher than from the individual chemical components, with emissions from cellulose being significantly lower than those from pectin and lignin. Similarly, emissions from cotton flower (*Gossypium hirsutum*), which consists primarily of pure cellulose, are much stronger than from the synthetic compound (Table 2, Appendix).

3.4.2 Characterization of the substrate reservoir and the emission process

The experiments described so far were carried out for periods of hours to several days. The emissions provoked by heating usually show a transient emission signal that diminishes after several hours. Two to 16 hour heating cycles between 25ºC and 80-100ºC were carried out over several days. The emission signal is provoked repeatedly in subsequent cycles, but the integrated amounts released per heating cycle decrease in subsequent cycles. This indicates that an available limited reservoir is discharged. We note that we never observed a recharge of such a reservoir when the vial was cooled to room temperature again, which would be easily identified by an uptake of CH_4, i.e., a drop of the CH_4 mixing ratio below that of the incoming air. This suggests that the underlying process involves chemical reactions, since physical storage as suggested by Kirschbaum et al. [2007] should be reversible. Further work is required to investigate these heat-driven CH_4 emissions, which are not well understood. Isotope labeling experiments should allow distinguishing between adsorption/desorption and chemical production mechanisms.

In sharp contrast to the heating experiments, the CH_4 emissions provoked by UV light are continuous and do not drop. Having observed constant emissions in several experiments for up to one week, we attempted to determine the size of the CH_4 forming reservoir and kept 1g of dry grass under UV irradiation for 35 days. The high UV levels and high temperatures employed for this test resulted in an emission rate of 200 ng/g dw/h. This high emission rate was constantly monitored for 10 days, and a typical 24 h snapshot of raw data is shown in Figure 3.5.

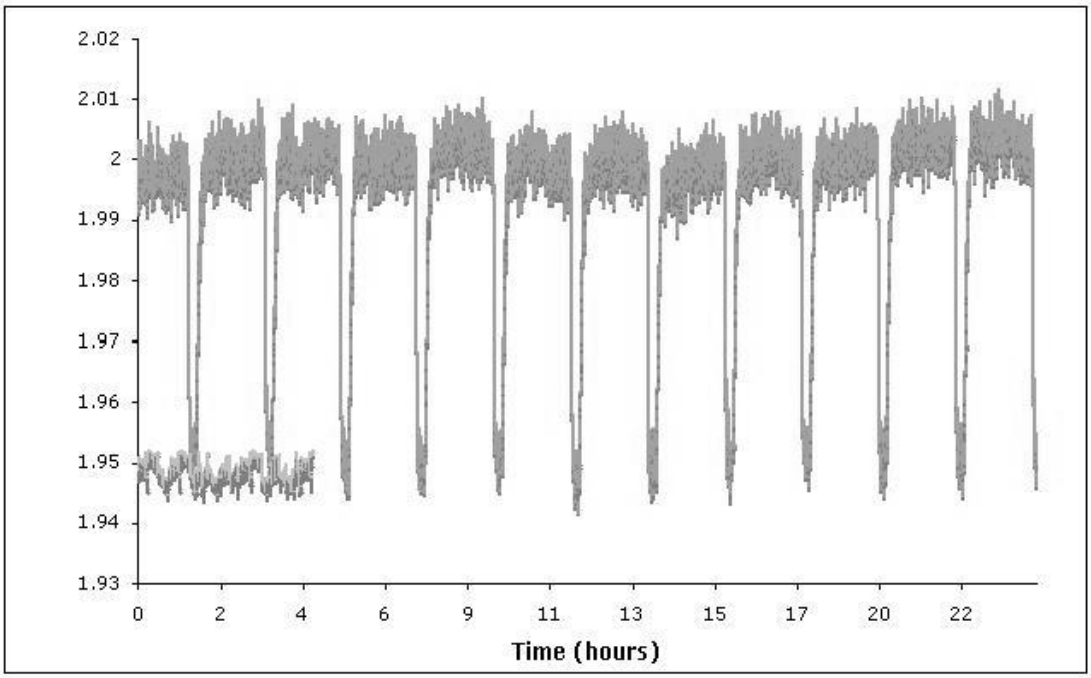

Figure 3.5 Typical 24 hour snapshot of raw CH_4 concentration data from the optical instrument during the long time UV irradiation experiment. During each 2 hour period the UV lamp is switched on for 105 minutes and off for 15 minutes to monitor possible instrument drift and to continuously verify that the CH_4 emission signal is related to UV irradiation. Numerous blank tests without samples were performed and the lower line shows a ~4h blank test using the same bottle of compressed air. UV light was switched on and off respectively for 1h periods and no CH_4 emission is observed without an organic matter sample.

The experiment was continued unobserved for another 20 days and monitored again for 5 days, during which the emission rate was still 200 ng/g dw/h. This means that during those 5 weeks a total of ~0.17mg CH_4 was formed from 1g of dry grass, which by many orders of magnitude rules out any of the potential contamination sources discussed recently [*Kirschbaum et al.*, 2007]. We stress that these experiments were not carried out under typical ambient environmental conditions and we do not suggest that such amounts are produced realistically in the environment. However, the experiment shows the enormous size of the reservoir that is available. We note that the methoxyl carbons of pectin typically constitute approximately 1.4% of the carbon in plant matter, thus this reservoir is still ~2 orders of magnitude larger than the observed total emission of CH_4 over 35 days.

Another test series involved several experiments in synthetic, CH_4-free air. Figure 3.6 shows the results of two subsequent UV irradiation experiments using the same sample of dry grass (*Lolium perenne*), the first carried out in normal air, the second in CH_4-free air after a flushing period of 24h at 80ºC. In both experiments the CH_4 concentration increases upon UV irradiation by ~30 ppb, corresponding to an emission rate of 100 ng CH_4/g dw/h. Thus, the emission does not depend on the presence or absence of CH_4 in the carrier air. This result is evidence against the hypothesis that adsorption-desorption processes could be responsible for the observed emissions.

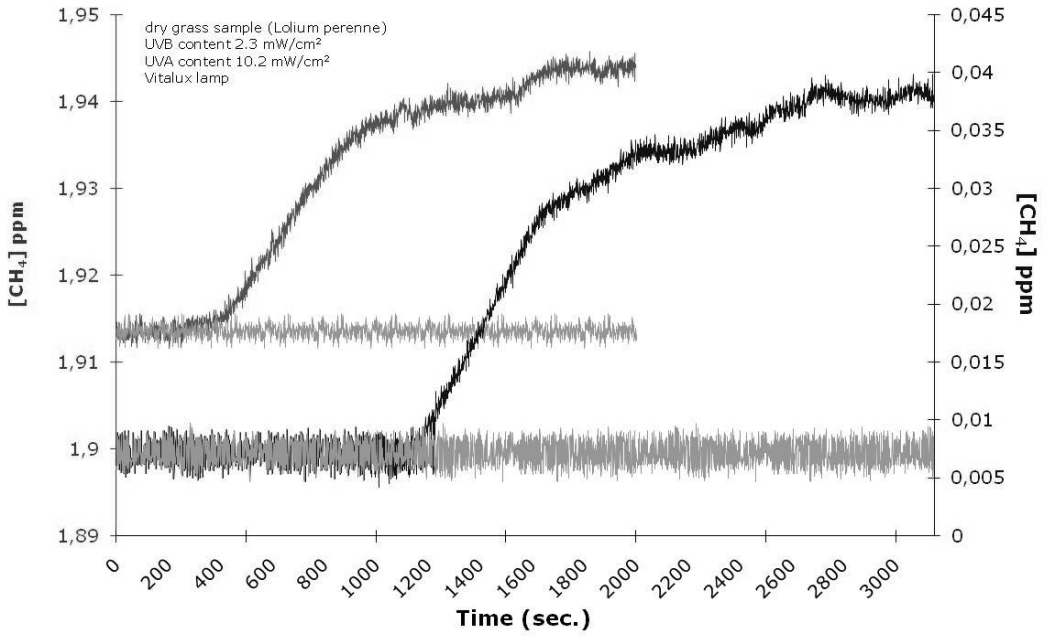

Figure 3.6 CH_4 emission observed from grass under UV irradiation in compressed air (right y-axis) and synthetic, methane-free air (left y-axis). The increase in the mixing ratio is ~30 ppb for both experiments. Blank experiments without samples (lower lines) demonstrate that the emission comes from the grass sample exclusively.

We also investigated the response time of CH_4 emissions to UV irradiation. Figure 3.7 shows the response of a dry grass (*Lolium perenne*) sample to three short and strong UV pulses with the Vitalux lamp (189 W/m^2 UVA and 27 W/m^2 UVB irradiance). When the air transport time from the vial to the detector is taken into account, it is evident that emission is almost instantaneous and also stops immediately after the UV source is turned off. Furthermore, the integrated emissions roughly scale with the period of irradiation. The short response time is a strong indication that a photochemical process is the source of the CH_4 emission. On the other hand, the fact that the increase in concentration has not leveled off after two minutes indicates that, although the emission starts immediately after irradiation, the emission rate still increases with time of irradiation after 1-2 minutes.

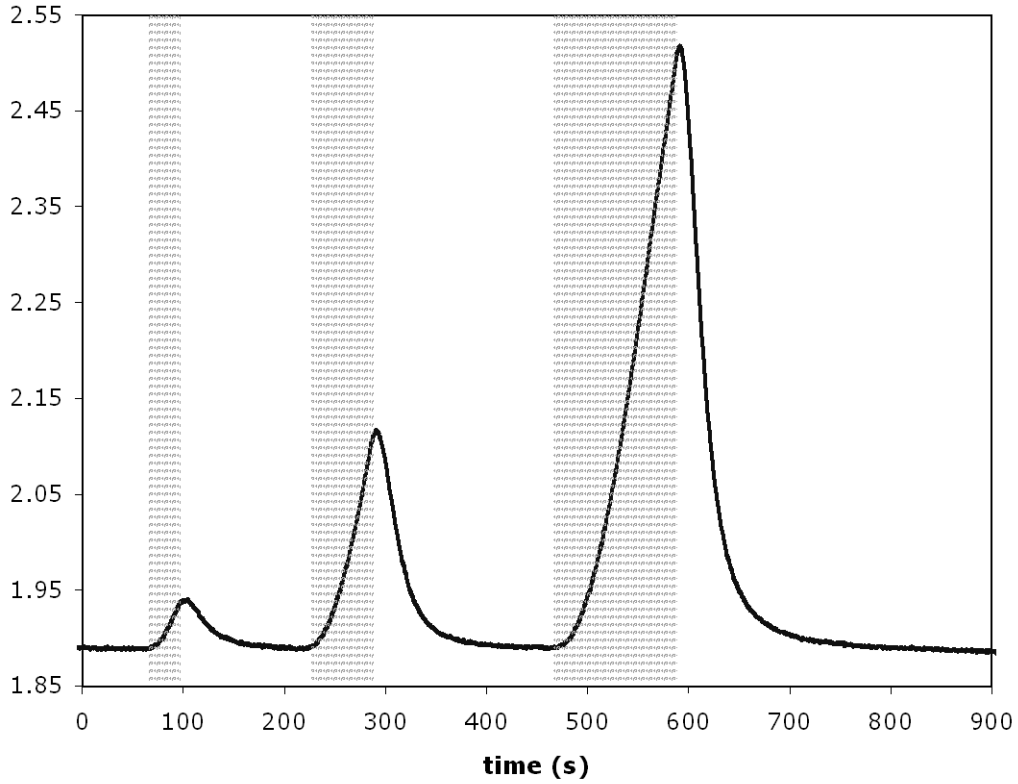

Figure 3.7 Response of a grass sample (*Lolium Perenne*) to UV irradiation (189 W/m^2 UVA and 27 W/m^2 UVB irradiance, Vitalux lamp). The shaded areas mark the times of illumination with the UV light source for 30, 60 and 120 s, corrected for the flushing time of the vial and connecting lines. This flushing time was determined by adding a spike of CH_4 at the inlet. It is about one minute, in agreement with the size of the vial (100 ml) and the flow rate (100 ml/min). Taking this delay into account the response of the plant matter to light is almost instantaneous.

As mentioned above a free-radical mechanism has been suggested for methane formation from polysaccharides [Sharpatyi, 2007].

Dueck et al. [2007] used pure ^{13}C plants (98 atom % ^{13}C) for their study and did not detect $^{13}CH_4$ emissions higher than ~ 0.4 ng/g dw/h. We obtained a fully senesced wheat (Triticum aestivum) leaf (~100 mg; IsoLife BV, the Netherlands) used in their experiments and investigated it with our analytical setup. The emissions from this small leaf were analyzed in a 40 ml volume static vial. Figure 3.8a shows the strong buildup of $^{13}CH_4$ in these experiments. The $\delta^{13}C$ value increases from the typical value of atmospheric methane of -47‰ to ~6000‰ within one hour of UV irradiation. This translates into an emission rate of 32 ng $^{13}CH_4$ / g dw /h, at a UVB content three times higher than typical tropical conditions. Thus, the $^{13}CH_4$ emission rate of this ^{13}C plant is similar to the emission rate of CH_4 of normal plants.

The huge $\delta^{13}C$ signal obtained in the UV irradiation experiments illustrates the sensitivity of the isotope ratio mass spectrometry technique for those labeled experiments and we continued to determine a "dark" emission rate from this ^{13}C wheat leaf. In a ~500 ml vial stored in the laboratory without UV light and at 22ºC, we still clearly observed a steady increase of $^{13}CH_4$ over 6 weeks (Figure 3.8b).

The emission rate of 0.03 ng $^{13}CH_4$ /g dw/h is an order of magnitude below the upper limit value given by Dueck et al. for their experiments, but can be precisely quantified with our equipment.

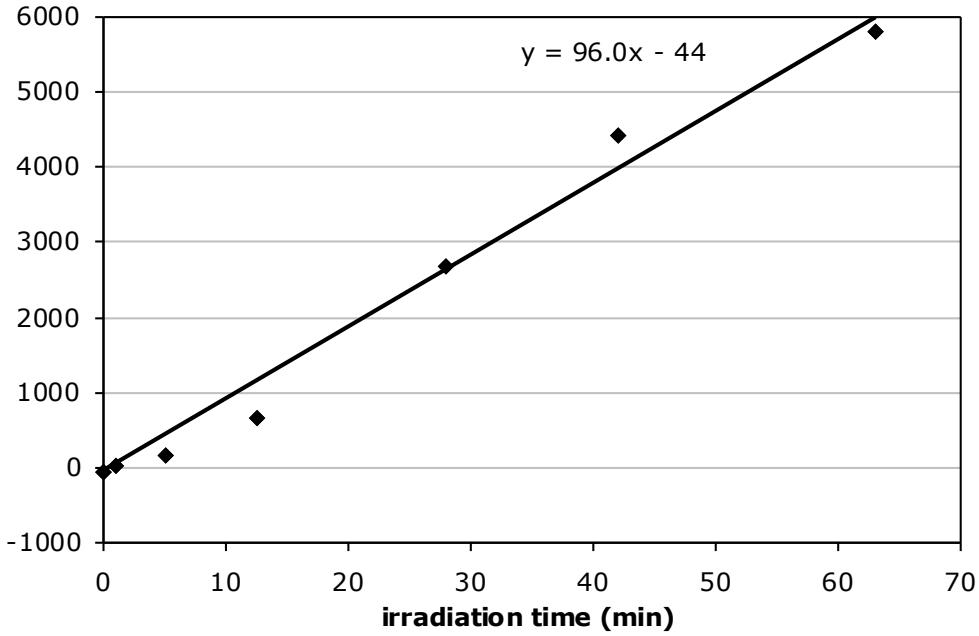

Figure 3.8 $^{13}CH_4$ emission observed from a dry, senesced ^{13}C labeled wheat leaf (*Triticum aestivum*; 98 atom % 13C) under UV irradiation from the VITALUX lamp (~5 W/m^2 UVB) (a) and in the dark without UV (b) in two different static volumes (A, 40 ml; B, 500 ml, see text).

In two additional static dark experiments at 40ºC and 60ºC for 16h the emission rate increased to 0.6 ng $^{13}CH_4$ /g dw / h at 40ºC and 2.8 ng $^{13}CH_4$ / g dw / h at 60ºC. This shows a strong temperature dependence of the emission also without UV light

over the ambient temperature range. Whereas we cannot yet positively rule out that bacterial activity could be responsible for the low temperature dark emissions, the strong increase observed in the dynamic system at even higher temperatures (Figure 3.3) rules out bacterial activity at least for those higher emissions. Furthermore the irradiation experiments above show that UV light increases the emissions by two orders of magnitude, and that these emissions have a non-bacterial, most likely photochemical origin.

3.5 Conclusions and outlook

Methane is produced from fresh and dry organic matter, as well as several structural plant components. UV radiation and temperature are key parameters that control CH_4 formation. Our experiments suggest that UV mediated CH_4 production is a ubiquitous process, that it readily occurs in the presence of oxygen and that it is not mediated by bacteria. Furthermore we can exclude physical adsorption - desorption processes or out-gassing from other reservoirs as a possible explanation for the observed methane emissions in the UV irradiation experiments. The emission rates for dry matter, on a per mass basis, are higher than those reported previously without UV light [*Keppler et al.*, 2006a]. Additional experiments, e.g. isotope labeling studies as performed in [*Keppler et al.*, 2007] are needed to further elucidate the reaction mechanisms.

We have restricted the experiments reported here to dry and detached fresh organic matter and some structural compounds in order to identify the existence of an aerobic CH_4 production process without interference of potentially complicating factors from living plants (including consumption processes). As a next step, we will investigate CH_4 emissions from living plants. If UV is also an important factor there, then it is not surprising that no emissions were found by Dueck et al. [2007], who used metal halide HPI-T lamps and glass chambers for their measurements. We note that the UV and temperature mediated CH_4 emissions presented here can most likely not explain the recent results from Wang et al [2007], who measured CH_4 emissions from stems of woody species of the Mongolian Steppe region, because they carried out dark enclosure experiments in the laboratory. Keppler et al. [2006] found significantly higher emissions from living plants, which further increased when the plants were exposed to direct sunlight. We recently recorded UV transmission spectra for the static plant chambers that were used there and found that the chambers are made of two different kinds of Plexiglas; the side walls of the chamber are transparent to UVA and UVB radiation, but the top plate has a cutoff in the long wave UVA region. So solar UV penetrating through the side walls could indeed have played a role there, but the emission rates from dry and fresh leaves at natural UV levels reported above are lower than those determined by Keppler et al. [2006] from living plants. Furthermore, in that study relatively high emissions were also observed from living plants under normal laboratory conditions and this needs to be further investigated with dedicated experiments.

Acknowledgements

This work was funded by the Dutch NWO project 016.071.605. Special thanks to Ries de Visser (Isolife, Wageningen) for providing a leaf of a ^{13}C labeled wheat plant. We thank S. Houweling, M. Krol, Ü. Niinemets, C.A.M. Brenninkmeijer, M. Kirschbaum, R. de Visser and H. Poorter for useful discussion and/or comments on the manuscript. Thanks also to the people of the Utrecht Botanic Garden for providing many plant species and Cascamificio Vigano for the cotton flowers from Tadzhikistan.

Chapter 4

The stable isotope signature of methane emitted from plant material under UV irradiation

Recent experiments have shown that dry and fresh leaves, other plant matter, as well as several structural plant components, emit methane upon irradiation with UV light. Here we present the source isotope signatures of the methane emitted from a range of dry natural plant leaves and structural compounds. UV-induced methane from organic matter is strongly depleted in both ^{13}C and D compared to the bulk biomass. The isotopic content of plant methoxyl groups, which have been identified as important precursors of aerobic methane formation in plants, falls roughly halfway between the bulk and CH_4 isotopic composition. C3 and C4/CAM plants show the well-established isotope difference in bulk ^{13}C content. Our results show that they also emit CH_4 with different $\delta^{13}C$ value. Furthermore, $\delta^{13}C$ of methoxyl groups in the plant material, and ester methoxyl groups only, show a similar difference between C3 and C4/CAM plants. The correlation between the $\delta^{13}C$ of emitted CH_4 and methoxyl groups implies that methoxyl groups are not the only source substrate of CH_4.

Interestingly, δD values of the emitted CH_4 are also found to be different for C3 and C4 plants, although there is no significant difference in the bulk material. Bulk δD analyses may be compromised by a large reservoir of exchangeable hydrogen, but no significant δD difference is found either for the methoxyl groups, which do not contain exchangeable hydrogen. The δD difference in CH_4 between C3 and C4 plants indicates that at least two different reservoirs are involved in CH_4 emission. One of them is the OCH_3 group, the other one must be significantly depleted, and contribute more to the emissions of C3 plants compared to C4 plants. In qualitative agreement with this hypothesis, CH_4 emission rates are higher for C3 plants than for C4 plants.

Published in *Atmospheric Environment* 43(35) (2009), pp. 5637-5646, Ivan Vigano[1], Thomas Röckmann[1], Rupert Holzinger[1], Arnold van Dijk[2], Frank Keppler[3], Markus Greule[3], Willi A. Brand[4], Heike Geilmann[4] and Huib van Weelden[5].

[1]Institute for Marine and Atmospheric Research, Utrecht University, Utrecht, The Netherlands,
[2]Department of Earth Sciences, Utrecht University, Utrecht, The Netherlands
[3]Max Planck Institute for Chemistry, Mainz, Germany
[4]Max-Plank Institute for Biogeochemistry, Jena, Germany
[5]Department of Dermatology and Allergology, Utrecht University Medical Center, Utrecht, The Netherlands

4.1 Introduction

Greenhouse gases are important for the radiative balance of the earth, and their increase over the past centuries, related to anthropogenic activities, is of concern [*IPCC*, 2007]. Therefore, their global cycles have been studied intensively over the past decades. Neglecting water vapour, methane is the second most important greenhouse gas after CO_2 [*Collins et al.*, 2006] with a radiative forcing of about 0.5 W/m^2 [*IPCC*, 2007]. It is the most simple and most abundant reduced organic compound in the atmosphere and an important component in atmospheric chemistry.

According to established literature, reduced compounds like CH_4 can be formed only in anoxic environments. Major sources include, for example, wetlands, rice paddies and ruminants, where CH_4 is formed by methanogens in the absence of oxygen [*Breas et al.*, 2002; *Houweling et al.*, 2000]. Recently, it was suggested that plants can emit methane under aerobic conditions [*Keppler et al.*, 2006b]. The scientific community has been arguing over the following years on the existence of this source and possible causes and effects [*Beerling et al.*, 2008; *Bergamaschi et al.*, 2006a; *Butenhoff and Khalil*, 2007; *Dueck and van der Werf*, 2008; *Dueck et al.*, 2007a; *Houweling*, 2006; *Kirschbaum et al.*, 2007; *Nisbet et al.*, 2008; *Sharpatyi*, 2007; *Xie et al.*, 2009].

Recent findings clearly demonstrated the important role of UV radiation and temperature in methane production from organic plant matter under atmospheric oxygen concentrations [*McLeod et al.*, 2008; *Vigano et al.*, 2008], and the role of reactive oxygen species involved [*Messenger et al.*, 2009]. Lab experiments under stress conditions have been carried out showing how emissions vary from uncut to cut plants [*Wang et al.*, 2009]. New field studies on the Mongolian and Tibetan plateaus reported measurements of methane emitted from plants, although with uncertainty [*Cao et al.*, 2008; *Wang et al.*, 2008]. Furthermore, boreal and tropical ecosystems were investigated [*Sinha et al.*, 2007].

According to the latest published data, emissions of methane have been observed from living plants even under low light (without UV) conditions by using a stable isotope approach [*Bruggemann et al.*, 2009]. Methane production in oxygenated environments has recently also been reported in sea water [*Ingall*, 2008; *Karl et al.*, 2008]. As an interesting note, experiments of organic matter degradation under high UV levels typically present on Mars showed methane as the most commonly observed reaction product [*Stoker and Bullock*, 1997]

Strong CH_4 emissions from plants were regarded as a possible explanation for elevated methane concentrations detected by satellite observations over tropical forest areas [*Frankenberg et al.*, 2005]. New new spectroscopic data have recently led to a downscaling of these missing methane emissions [*Frankenberg et al.*, 2008]. However, still one third of the global methane source strength is allocated to tropical regions .

Isotope studies are an established useful tool for quantifying the relative emissions of CH_4 from different sources [*Brenninkmeijer et al.*, 2003; *Pataki et al.*, 2003]. In the biosphere, isotopic signatures can be used to characterize a multitude of individual compounds [*Phillips and Gregg*, 2001] and isotope studies have led to a deeper insight into the main photosynthetic pathways described as Calvin Cycle (C3), Slack-Hatch cycle (C4) and Crassulacean acid metabolism (CAM), respectively [*Farquhar et al.*, 1989; *Hobbie and Werner*, 2004; *Smith and Ziegler*, 1990; *Ziegler et al.*, 1976].

Stable isotopes are often used to investigate biogeochemical cycles [*Goldstein and Shaw*, 2003b] where plants are important emitters of trace gases and thus affect atmospheric chemistry [*Lelieveld et al.*, 2008]. Vegetation is a direct emitter of biogenic volatile organic compounds (VOCs) during the plant lifecycle [*Goldstein and Shaw*, 2003a; *Loreto et al.*, 2008] and an indirect emitter, if we consider plant biomass degradation [*Keppler et al.*, 2000].
Strong ^{13}C depletions relative to the bulk biomass have been measured for methoxyl groups (OCH_3) present in pectin and lignin [*Keppler et al.*, 2004]. The fractionation associated with the methoxyl pools is retained and even further enhanced during their conversion to C1 VOCs such as methanol (CH_3OH), chloromethane (CH_3Cl), bromomethane (CH_3Br) and iodomethane (CH_3I) [*Keppler et al.*, 2004]. Methane is the most reduced C_1 plant-derived organic compound and isotopic labelling studies on pectin and polygalacturonic acid (PGA), have recently established that methoxyl groups are important precursors of methane that is emitted from these compounds under UV irradiation and heating [*Keppler et al.*, 2008].

The work of Keppler et al. [2006] already indicated that plants emit methane with a carbon isotope signature that is characteristic for the C3 and C4 photosynthetic pathways, respectively.

We have determined the $\delta^{13}C\text{-}CH_4$ (carbon) and $\delta D\text{-}CH_4$ (deuterium) isotopic signatures of methane emitted from different dry plant materials exposed to UV light. These isotope source signatures will be compared to the isotopic composition of the bulk biomass and methoxyl groups as potential precursors of CH_4.

4.2 Experimental methods

4.2.1 UV irradiation experiments

The study of Vigano et al. [2008] explains in detail the effect of UV radiation and temperature on CH_4 emissions from plant biomass. The experiments presented here follow a similar experimental approach, but a static quartz reactor of 100 ml was used so that sufficiently high CH_4 levels could build up to derive the source isotope signatures by applying different irradiation times as described in 4.1. Several leaves, as well as structural plant compounds, (Table 3, Appendix) were dried at 60ºC overnight (for at least 10 hours) in an oven. Then they were enclosed in the reactor and pre-flushed with 100mL/min of compressed air at ambient methane level (~1.9 ppm, $\delta^{13}C\text{-}CH_4$~-48‰, $\delta D\text{-}CH_4$~-90‰) for at least 15 min. An OSRAM Vitalux lamp (300W) served as UV source. This type of lamp is commonly employed for medical purposes, with a UVA/UVB content comparable to solar radiation if the source is kept at appropriate distance. The total unweighted UVB radiation was determined with a calibrated Waldmann UV meter (Waldmann, Schwenningen, Germany). The relative spectral distribution measurements and the calibration of the Waldmann device were performed with a calibrated standard UV-visible spectro-radiometer (model 752, Optronic Laboratories Inc, Orlando, FL, USA).

The lamp irradiated a leak tight 100ml Suprasil finger (UV transparent) and to increase the amount of methane emitted, the UVB intensity was 5 times higher (20

W/m^2) than typical natural tropical levels (4 W/m^2). For one sample, it was verified that the isotope signature did not depend on UV intensity, i.e., the same isotope signature was derived using 4 W/m^2 and 20 W/m^2.

When the lamp was turned on, the amount of methane increased linearly with irradiation time. Temperature inside the quartz finger was monitored with a micro-thermocouple placed inside the vial and always kept below 30ºC by using a powerful ventilator that was located outside the vial.

4.2.2 Continuous Flow Isotope Ratio Mass Spectrometry for measurements of $\delta^{13}C$ and δD of methane

After irradiation, the gas was sampled by expansion of the air in the Suprasil finger into a 100 ml evacuated glass bottle from which sub-samples were successively injected into a continuous flow-isotope ratio mass spectrometry (CF-IRMS) system for high precision analysis of $\delta^{13}C$-CH_4 (reproducibility ~ 0.1‰) and δD-CH_4 (reproducibility ~ 2‰) [*Keppler et al.*, 2008; *Vigano et al.*, 2008]. The grab samples were taken at different times in order to allow determination of the source isotopic composition using a Keeling plot analysis with at least 3 points (Fig. 4.1a-b).

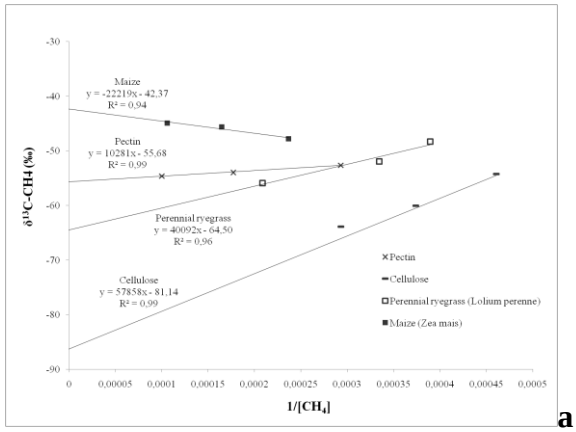

a

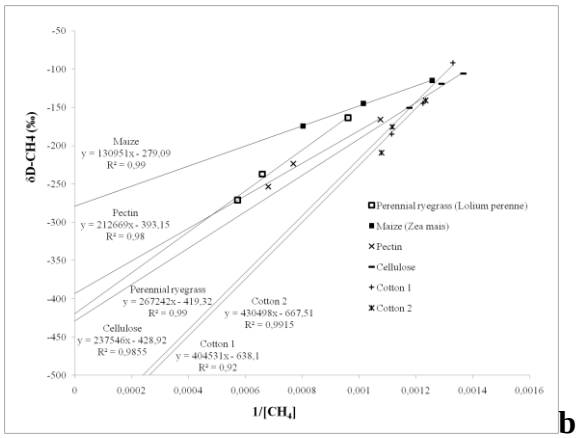

b

Figure 4.1 Examples of keeling plot for different plant material and compounds analyzed. The equations of the regression lines show the intercept at $[CH_4] \rightarrow \infty$. (a) for $\delta^{13}C$ analyses and (b) for δD. Cotton experiment repeated twice for δD.

The CF-IRMS analysis provides isotope values and concentrations derived from the peak areas of the chromatogram. The source signatures were then determined from the y-axis intercept in a Keeling plot (δ value versus inverse peak area). The method allows determining single signatures within 6-8h with an accuracy of ±0.5‰ for $\delta^{13}C$-CH_4 and ±5‰ for δD-CH_4.

$\delta^{13}C$ and δD values are the relative deviations of the $^{13}C/^{12}C$ and D/H ratio in a sample relative to the respective recognized international standards: $\delta^{13}C$ refers to Vienna PeeDee Belemnite (VPDB) and δD refers to Vienna Standard Mean Oceanic Water (VSMOW).

4.2.3 Bulk isotope analysis

Bulk $\delta^{13}C$ analyses were performed at the Earth Sciences Dept. of Utrecht University (The Netherlands) and bulk δD was determined at the Stable Isotope Laboratory of the Max-Plank Institute for Biogeochemistry in Jena (Germany).

Carbon isotopes of the bulk leaves were analysed on a Fisons NA1500NCS Elemental Analyser coupled to a Thermo Delta$^+$XL isotope ratio mass spectrometer. A labstandard (Graphite Quartsite) was used for calibration. That in turn was calibrated with NBS-22 and USGS-24. Stdev of the lab-standards are <0.1‰.

The method for bulk δD analysis using a High Temperature Conversion (HTC) mass spectrometric technique closely follows the procedure described for $\delta^{18}O$ determination in bulk material by Brand et al. [2009]. Samples are weighed into Ag-foil and positioned into an Autosampler (‘Zero-Blank’, Costec, Milan, Italy). Upon actuation, the packets drop into a helium flushed high temperature reactor (HTO, Hekatech, Wegberg, Germany) kept at 1450°C.

The reactor has an outer SiC tube and an inner tube made from glassy carbon with reversed carrier gas flow to ensure that the full helium flux passes through the core of the reactor [*Gehre et al.*, 2004]. In addition, the inner tube is filled with glassy carbon chips up to the highest temperature zone where the reaction to CO, H_2, and carbon plus further unspecified reaction products and residues takes place. From the reactor, the sample gas passes a fine filter containing NaOH on pumice (‘Ascarite’) and $Mg(ClO_4)_2$ before entering a packed column (5-Å) gas chromatograph at 70°C for separating H_2 and CO. An open split interface (‘ConFlo III’, [*Werner et al.*, 1999]) provides the connection to a Delta$^+$XL stable isotope mass spectrometer (both from Thermo-Fisher Scientific, Bremen, Germany). By monitoring the ion currents at m/z 3 and 2, the hydrogen isotopic composition is analyzed. As primary reference for reporting on the VSMOW scale we used NBS22 oil with an assigned value of -118.5‰. Using this material, a local reference material ‘PET-J1’ (polyethylene, ‘Uvasol’, purchased from Merck, Darmstadt, Germany) was calibrated with a δD value of -80.75‰ vs. VSMOW. Aliquots of these materials were interspersed together with the samples and analyzed in the same sequence.

The reported sample results are based on the relative differences to the working reference material results. As a quality control reference we included one sample of IAEA-CH7 polyethylene in the daily sequence of measurements. IAEA-CH7 has an assigned value of -100.3‰ on the VSMOW scale.

4.2.4 Isotope analysis of plant methoxyl groups

The $^{13}C/^{12}C$ and D/H isotope ratios of the plant methoxyl groups were analyzed using a new method, which was recently published by Greule et al., [2008] and Greule et al., [2009]. In brief, methoxyl groups of plant material are cleaved off with hydriodic acid (HI) at 130°C in closed reaction vials. Subsequently, a headspace analysis of the gaseous product methyl iodide (CH_3I) is carried out using gas chromatography pyrolysis/combustion isotope ratio mass spectrometry (GC-C/P-IRMS). This rapid and precise method enables the determination of both $\delta^{13}C$ and δD values of plant methoxyl groups without apparent isotopic discrimination.

Plant methoxyl groups exist in two different types of chemical bondage, ester methoxyl groups (mainly appearing in pectin) and ether methoxyl groups (main sources in nature is lignin). To determine the $\delta^{13}C$ values of pectin methoxl groups (pectin-$\delta^{13}C$-OCH_3) the plant material was treated with a 1-molar sodium hydroxide solution at 50°C to quantitatively hydrolyze ester methoxyl groups to methanol [*Keppler et al.*, 2004]. The methanol containing liquid phase was separated from the residual sample and heated with HI at 130°C. In the following the generated CH_3I was analyzed as described by Greule et al. [2009].

4.2.5 Materials

The full list of materials investigated is given in Table 3 (Appendix). Most of the plant material was obtained from the Botanical Garden of Utrecht University; some leaves were collected during summer (June-August) from regular outside plants or plants grown inside the greenhouse. The same day of the collection they were dried as previously described and stored in a vacuumed exicator in order to keep stable the moisture content. The organic compounds used for experiments were obtained from Sigma® (apple pectin, purity 98%, CAS number 9000-69-5, cellulose microcrystalline, purity 95%, CAS number 9004-34-6, lignin, purity 95%, CAS number 8068-05-1). Typical amounts used in our experiments ranged from 0.1 to 2 *g* of dry material.

4.3 Isotopic composition of CH_4

4.3.1 Determining the source isotopic signatures

During the static experiments the methane mixing ratio increased proportionally with irradiation time and this change in mixing ratio usually leads to a change in the isotopic composition. Typically we irradiated the samples for at least three different time periods (1h, 2h, and 3h). Before and after every run the reactor was flushed for 15 min. with 100ml/min of conventional compressed air (~1.8 ppm CH_4). Keeling plots of isotopic composition versus inverse mixing ratio, $1/[CH_4]$, yield good linear correlations ($R^2 > 0.9$) and the isotope source signatures are derived by extrapolating

to $[CH_4] \Rightarrow \infty$, which corresponds to the y-axis intercept of the linear fit to the δ versus $1/[CH_4]$ data. Figures 4a and 4b show some examples of Keeling plots.

In the following sections the results of isotopic signatures and the median values of isotope discriminations have been discerned for C3 plants and for C4-CAM plants. Notwithstanding the differences in C4 and CAM plants, for simplicity they have been grouped together in the data evaluation based on the fact that they have almost similar isotope values here measured (Table 3, Appendix). Separate discussions on CAM plants have been done for cases where values are rather outliers (especially for δD analyses).

4.3.2 $\delta^{13}C$-CH_4 signatures from plants and structural compounds

More than twenty species from a wide variety of plants were analyzed and for each one a Keeling plot analysis was carried out to determine the $\delta^{13}C$-CH_4 source signature as explained in 5.1. The results in Table 3 (Appendix) and Figure 4.2 show that it is possible to define two main groups of plants with different $\delta^{13}C(CH_4)$ values, which relate to their photosynthetic pathways.

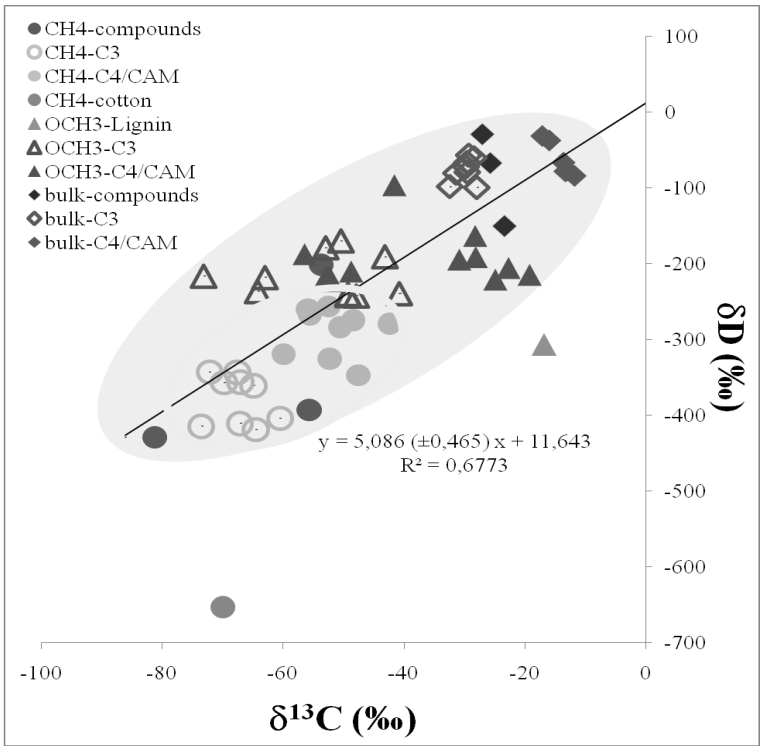

Figure 4.2 General scatter plot of $\delta^{13}C$ vs δD for most of the measurements, showing the relation 1:5 between carbon and hydrogen fractionation in plants. Into the circle are positioned the CH_4 signatures.

The group with more depleted $\delta^{13}C$ values contains the C3 species measured, while more enriched values are observed for the C4 species and CAM plants. A similar difference is well established for the ^{13}C of the bulk biomass (see below). Unexpected outliers were observed for Madagascar dragon tree, banana, bamboo and maize. The Madagascar dragon tree, banana and bamboo leaves that were analyzed produced CH_4

with $\delta^{13}C$-CH_4 values characteristic of the C4 group, although they are C3 plants, while our maize sample was particular enriched within the C4 group (Table 3, Appendix). In order to avoid biases from such outliers, for the following calculations we use median values instead of average values.
Median $\delta^{13}C$-CH_4 values for C3 and C4-CAM are -67.0 (±4.5)‰ and -52.3 (±5.5)‰ respectively. The study of Keppler et al. [2006] reported average $\delta^{13}C$-CH_4 values for C3 and C4 plants of -58.2‰ and -49.5‰, respectively for CH_4 produced from fresh and dried material at 30-40ºC, which is 3-8‰ enriched relative to our signatures obtained with UV light. The general relation, that CH_4 from C3 plants is lighter than from C4 plants, is in good qualitative agreement. The difference may be due to the different experimental setups. Heat and UV irradiation may produce CH_4 with different isotopic composition. A recent study using isotopically labeled pectin has shown that the fraction of CH_4 derived from methoxyl groups of pectin is larger for heating than for UV irradiation and that in the latter there must be a substantial additional reservoir [Keppler et al, 2008]. In this context, Messenger et al. [2009] suggested that acetyl esters (*O*-acetyl groups) are a potential minor CH_4 source and may account for discrepancies in previous labeling experiments of Keppler et al. (2008).

Isotopic signatures of UV induced CH_4 were obtained also from analyses of plant structural compounds; these were purchased from commercial suppliers (Sigma®) and not directly extracted from fresh plant material. Apple pectin and lignin liberate CH_4 with $\delta^{13}C$ values of -55.7‰ and -52.3‰ respectively, which are similar to those found for C4 plants (Table 3, Appendix). In contrast, cellulose produces very depleted CH_4 with $\delta^{13}C$= -81.1‰, the lowest value observed in this study. Earlier irradiation experiments on cellulose had shown non-zero CH_4 emissions, although far less then emissions observed from lignin and pectin [*Vigano et al.*, 2008]. The lower emission rates could in principle be a cause for the stronger fractionation, however, the CH_4 formation pathway for cellulose must be different, as this molecule has no methoxyl groups which are hypothesized to be important (but not the only) precursors for CH_4 emission from lignin and pectin [*Keppler et al.*, 2008]. More specific kinetic studies on the formation mechanism for cellulose may help understand the additional formation pathways for other compounds, too.

4.3.3 δD-CH_4 signatures from plants and structural compounds

δD-CH_4 source signatures were determined from a subset of the same samples with the same approach. δD-values for C3 and C4-CAM plants fall again in two separate groups with median δD values of -360 (±32)‰ and -279 (±32)‰ respectively (Table 3, Appendix and Fig. 4.2). In contrast to ^{13}C, a similar δD difference is not found in the bulk material, and thus the difference indicates a difference in the production pathways of CH_4 from the different plant types.
Our results establish CH_4 liberated from plants under UV irradiation as one of the more depleted CH_4 sources in Nature (Fig. 4.3).

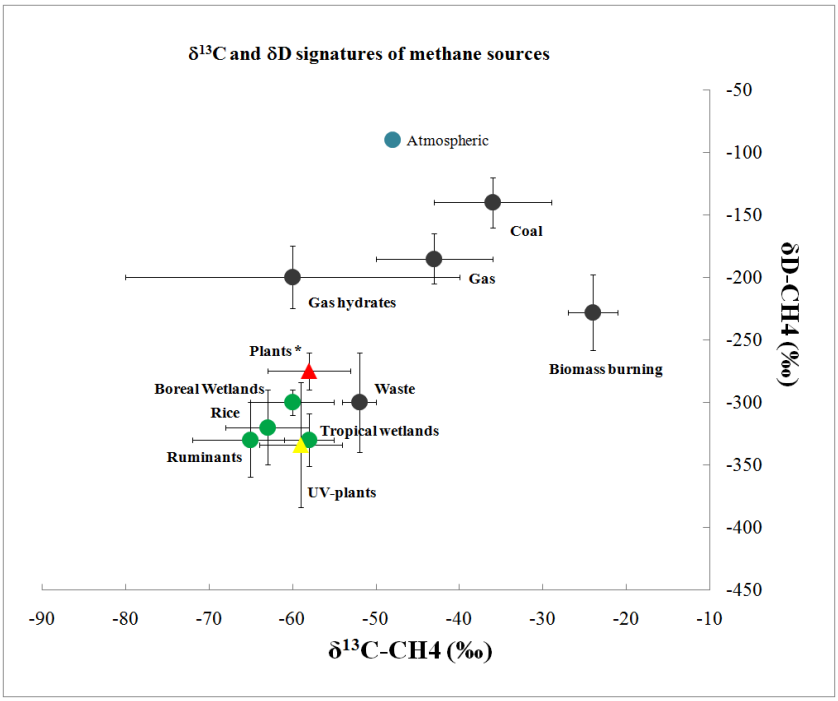

* $\delta^{13}C$ data are from Keppler et al. 2006 while the δD is in the range of the projections made by Whiticar et al.2007 and Fisher et al. 2008.

Figure 4.3 Data are from Quay et al. 1999 and Whiticar M.J. 1993. Mainly non microbial sources are indicated by grey dots, mainly bacterial sources by green dots. Plants signatures are indicated with triangles: red for the old evaluations, yellow for the new UV signatures here described. The error bars indicate the spread of reported values. Actual atmospheric δ values are indicated with a blue dot.

In fact deuterium signatures of methane range from values of ~ -120‰ for methane from coal mining down to ~ -400‰ for methane emitted from termites [*Fischer et al.*, 2008; *Quay et al.*, 1999; *Schaefer and Whiticar*, 2008; *Whiticar*, 1993]. Deuterium-depleted CH_4 is generally viewed as clear signature for microbial production. Our results show that D-depleted CH_4 can also be formed by non-microbial processes. The measured values are slightly (C4 plants) or even much (C3 plants) lower than the value of -260 ‰ that was recently estimated for plant-derived CH_4 in a study targeted at constraining the global methane budget using stable isotopes [*Whiticar and Schaefer*, 2007].

We also measured $\delta D\text{-}CH_4$ values for commercially available plant structural compounds. CH_4 emitted from lignin is significantly enriched in deuterium relative to CH_4 from plant material ($\delta D\text{-}CH_4$ = -201‰). The $\delta D\text{-}CH_4$ value from pectin, on the other hand is in the range of the C3 plants ($\delta D\text{-}CH_4$ = -393‰) and cellulose has a δD value slightly lower than the natural plant samples ($\delta D\text{-}CH_4$ = -429‰). The absolute values of these samples are not conclusive, however, since the D source for those materials is not known and may be different from the plant samples and between the compounds.

Nevertheless, the CH_4 formation from cellulose deserves some further discussion: cellulose is a chain/polymer of D-glucose molecules, which contain hydroxymethyl-groups $–CH_2OH$ that chemically differ from methoxyl-groups

–OCH_3. If CH_4 can also be formed from such functional groups, this has at least two important implications: (i), two hydrogen atoms are added to the CH_2 group instead of one to the CH_3 group; and (ii), the reaction kinetics must be different.

The fact that for all compounds the emitted CH_4 is isotopically so much lighter than the bulk material and the methoxyl groups (see chapter below) implies either strong kinetic isotope effects or a strongly depleted source for the 4th H atom that is incorporated when the CH_4 molecule is formed. The light δD value for cellulose implies that the isotopic composition of the additional D atoms is light. It would be interesting to carry out an isotope labeling study on cellulose to identify the carbon and hydrogen source for CH_4 generated from this molecule.

An unexpected strong depletion was observed for cotton flower (cotton fibers) from two repeated measurements, which showed an average value of δD ~ -653‰ (Table 3, Appendix).

Cotton fibers, also previously investigated under UV irradiation [*Vigano et al.*, 2008], consist mostly of cellulose. As discussed above the δD-CH_4 value of cellulose is the most depleted of all investigated structural compounds (δD ~ -429‰), but still, the strong depletion of δD of methane emitted from cellulose cannot explain the extremely low values observed for cotton flower.

4.4 Relation between ^{13}C and D content of bulk plant material and methoxylgroups

Methoxyl groups are generally depleted in ^{13}C and D versus the bulk biomass (Figure 4.2), and the CH_4 emitted is even further depleted. It is important to note that plant methoxyl groups exist in two different types of chemical bondage; ester methoxyl groups (mainly appearing in pectin) and ether methoxyl groups (main sources in nature is lignin). Recently it has shown that pectin methoxyl groups are an important precursor of CH_4 formation when dried plant matter is exposed to UV light [Keppler et al., 2008; McLeod et al. 2008]. Moreover, it was found that $\delta^{13}C$ values of pectin methoxyl groups differ from $\delta^{13}C$ values measured for the total methoxyl pool (composite of pectin and lignin OCH_3 groups)[Keppler et al. 2004, Greule et al, 2009].

However, this appears not to be the case for δD values of pectin and lignin OCH_3 groups measured in the same plant sample. This is why in this study we measured both $\delta^{13}C$ values of total methoxyl pool (pectin and lignin OCH_3 groups) and the methyl ester pool (pectin-OCH_3 groups). The data in Figure 4.2 show a considerable scatter, but a linear square fit yields a slope ~5, which indicates that the overall fractionation from the bulk biomass to CH_4 is ~5 times stronger for δD than for $\delta^{13}C$.

For a better understanding of isotope fractionation in the formation of CH_4 from plant biomass, we introduce the isotope discrimination between two substances a and b defined as $\Delta_{a-b}=\delta_a-\delta_b$ (Table 4, Appendix), which quantifies the difference in isotopic content between two reservoirs due to kinetic isotope effects [*Criss and Farquhar*, 2008].

4.4.1 $\delta^{13}C$

Figure 4.4a shows a scatter plot of $\delta^{13}C$ of CH_4, total methoxyl pool (OCH_3 groups) and the methyl ester pool (pectin-OCH_3 groups), with the bulk ^{13}C content of the biomass. For all signatures, the average ^{13}C content in the C3 plants is lower than in the C4 and CAM plants. $\delta^{13}C$ of pectin-OCH_3 groups is slightly lower than $\delta^{13}C$ of all OCH_3 groups, and $\delta^{13}C$ of CH_4 is clearly the lowest. The slopes of the linear fits through the data are largely determined by the average $\delta^{13}C$ difference between C3 and C4 plants. The slope of the CH_4-bulk correlation is 1.01±0.15, indicating that the difference in the bulk ^{13}C content is transferred 1:1 to the CH_4 emitted. Surprisingly, the slope of the OCH_3-bulk and ester OCH_3-bulk correlations is >1. Supposedly, similar processes as those leading to the ^{13}C difference in the bulk biomass between the two plant types cause even stronger ^{13}C differences in the OCH_3 groups. Although there is a large scatter in the ^{13}C content measured in these compartments, the difference from slope 1 is significant at the 2σ level. The observed signals are also much larger than the measurement uncertainty (see above). The origin of the large scatter within the two groups is unknown at present.

In Figure 4.4b the same data are presented as isotope discrimination relative to the $\delta^{13}C$ value of the bulk biomass. The discrimination of the produced CH_4 is similar for the two plant categories with levels around -36‰. For both, total OCH_3 and pectin OCH_3 groups, however, isotope discrimination in C3 is stronger than in C4 plants. Again, the origin of this enhanced discrimination, as well as of the scatter within the two groups, is not known at present.

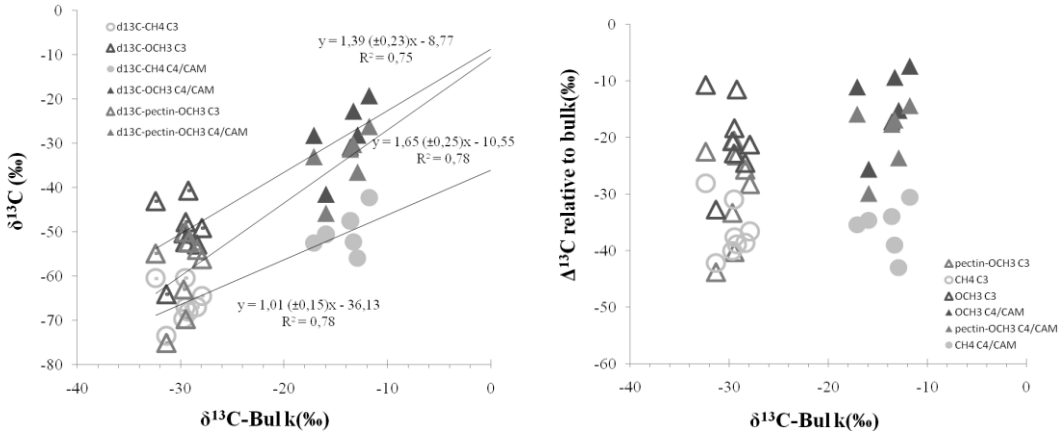

Figure 4.4 Scatter plot between $\delta^{13}C$-bulk and $\delta^{13}C$ of the CH_4 emitted and of the methoxyl-groups (a). Scatter plot of the $\Delta^{13}C$ discriminations for CH_4, OCH_3 groups and pectin-OCH_3 groups (b) relative to bulk $\delta^{13}C$.

In Figure 4.5 we investigate in more detail the relation between $\delta^{13}C$ in the OCH_3 groups and in CH_4. First, as expected, pectin OCH_3 groups correlate well with the total methoxyl pool, and the slope of the linear fit is indistinguishable from 1 at the 1σ level. However, the correlation slope between $\delta^{13}C$ in CH_4 and the pectin OCH_3 groups, which are considered an important source substrate for CH_4 formation, is only 0.5. This directly implies that pectin OCH_3 groups cannot be the only source substrate for CH_4 formation, as already concluded by [*Keppler et al.*, 2008].

The additional C source must be characterized by a ^{13}C difference between C3 and C4/CAM plants that is smaller than the one for the OCH_3 groups in order to explain the smaller slope.

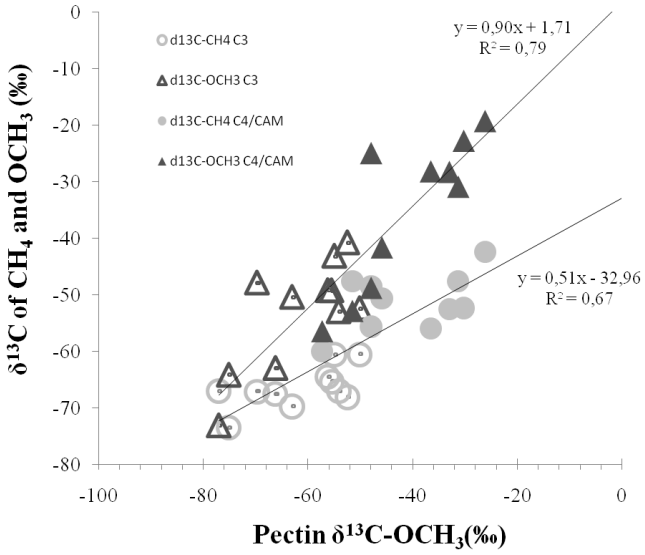

Figure 4.5 Relationship between $\delta^{13}C$ of methoxyl-groups and CH_4

4.4.2 δD

δD-bulk values do not display significant isotopic difference between C3 and C4-CAM plants, with median values for δD-bulk of -80 (±18)‰ and -77 (±19)‰, respectively (Table 5, Appendix and Figure 4.2). CAM plants exhibit slightly enriched δD values. The plants from the greenhouse have been grown with water of similar isotopic composition and the absence of a δD difference between C3 and C4-CAM plants indicates a not evident isotope fractionation in the metabolic pathways for both groups. However, such a δD difference does exist in the CH_4 produced (see above), which implies either a different fractionation in the CH_4 formation mechanism between the plant categories, or differences in the source substrate (which is then not represented well by bulk biomass). In fact, δD measurements on bulk biomass are problematic to interpret, because they represent a mix of exchangeable and non-exchangeable hydrogen. The isotope discrimination for δD between CH_4 and bulk biomass is significantly more negative for C3-plants (ΔD=-280 (±25)‰ than for C4-CAM plants (ΔD=-202 (±26)‰) (see Table 5, Appendix), while for carbon, the isotope discrimination is similar for the two plant categories. As discussed for the absolute δD values, the reason for the difference between C3 and C4-CAM plants must either be a kinetic fractionation, or an isotope difference in the precursor compounds, which is not captured in the bulk δD, or both.

The incorporation of hydrogen in plants depends on various factors: water adsorption, evapotranspiration rates and on the type of metabolic pathways specific from specie to specie. Within the same group the isotopic fractionations for hydrogen can be diverse due to different kinetic isotope effects [*Ziegler et al.*, 1976].

In fact, a correlation plot between δD-bulk and δD-CH_4 shows a lot of scatter (Fig. 4.6). It is noted that δD(CH_4) vary over a much wider range than δD of the bulk biomass (180‰ versus 90‰, respectively). The principle feature is the strong enrichment in δD(CH_4) from C4-CAM plants compared to C3 plants. The slope of a linear fit is largely determined by the slightly enriched CAM plants mentioned above.

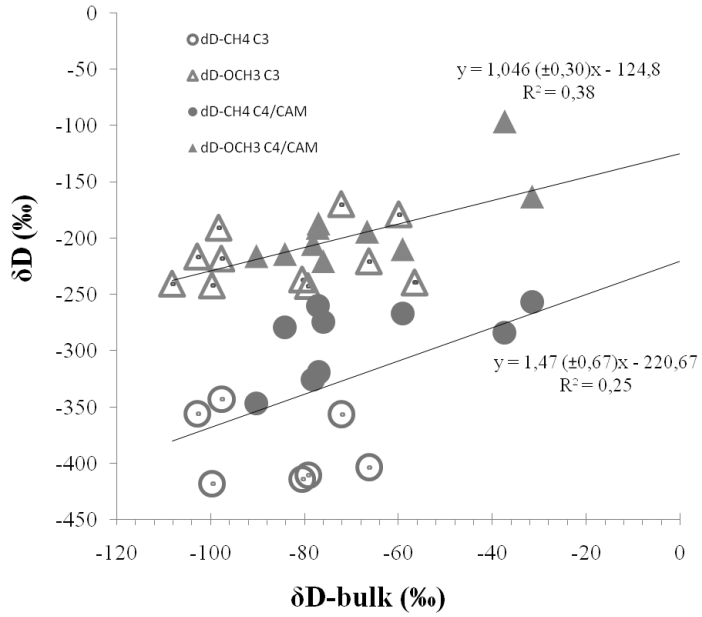

Figure 4.6 Relationship between δD bulk and δD of CH_4 and methoxyl-groups

Methoxyl groups contain non-exchangeable hydrogen [*Greule et al.*, 2008; *Keppler et al.*, 2007; *Keppler et al.*, 2008] and have been identified as a source substrate for CH_4 formation. Figure 4.6 shows that δD values of the OCH_3 groups are not significantly different for C3 and C4 plants, whereas again the CAM plants stand out slightly with elevated δD values for both bulk and OCH_3 groups. These CAM plants again mainly determine the slope of the linear fit line through all data points, whereas the remaining data show no significant correlation. The absence of a strong δD difference in the OCH_3 groups of C3 and C4-CAM plants indicates that the difference observed in the CH_4 also does not originate from the OCH_3 precursors. Since it is unlikely that kinetic fractionation processes alone could account for the differences between the plant categories, this also implies that there must be an additional isotopically distinct reservoir that acts as substrate for CH_4. We propose that the difference of δD(CH_4) between the plant groups originates from different relative fractions of CH_4 derived from OCH_3 groups and another isotopically distinct reservoir (with possible additional kinetic fractionations). For example, if this additional reservoir is more depleted than the OCH_3 groups, then C3 plants would produce relatively more CH_4 from this reservoir, and relatively less from OCH_3 groups, compared to C4 plants.

4.5 Emission rates

The concentration increase in the static setup allows for a straightforward calculation of CH_4 emission rates. It should be kept in mind that the UV intensity in all experiments was 5 times higher than the typical tropical levels, so the absolute emission rates can't be transferred to natural conditions. Nevertheless, we can examine differences between the individual species under constant high UV conditions. The precision in the determination of the emission rates from individual plants is ±20 ng/gDWh.
Table 6 in the Appendix and Figure 4.7 show that on first approach, emission rates are higher from C3 plants compared to C4-CAM plants with median values of 301 ng/gDWh and 180 ng/gDWh respectively.
Figure 5.7 shows the deuterium and carbon isotope discrimination between methane and the different plant compounds ($\Delta=\delta CH_4 - \delta_{plant}$) as a function of emission rate.

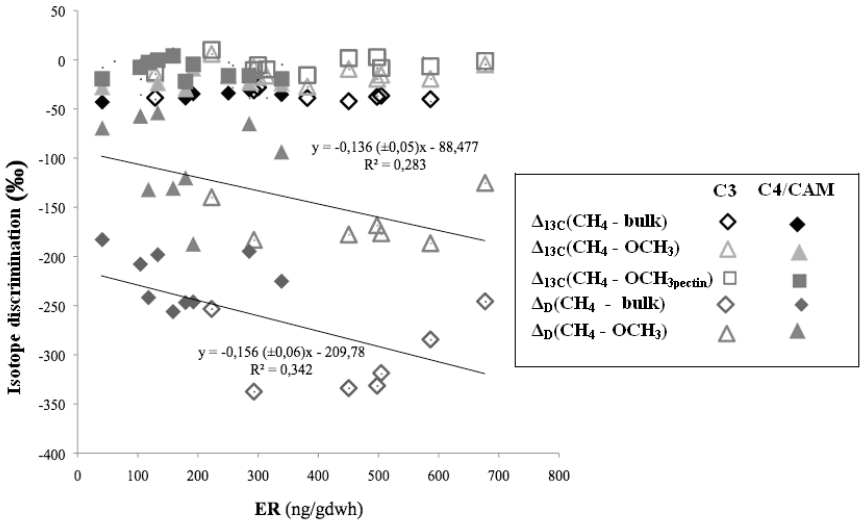

Figure 4.7 Isotope discriminations for C3 and C4/CAM plants versus CH_4 emission rates.

The fact that C3 and C4 plants differ in ER and in $\Delta_{CH4\text{-}bulk}$ leads to a correlation between these quantities. This is in qualitative agreement with the hypothesis presented above, that C3 emit relatively more from an additional source substrate than the OCH_3 groups, which then needs to be depleted in D. Further research should be carried out to identify this additional substrate.

4.6 Conclusions and outlook

The formation of methane when plant compounds are irradiated with UV light has now been reported from several research groups [*Keppler et al.*, 2008; *McLeod et al.*, 2008; *Messenger et al.*, 2009; *Vigano et al.*, 2008; *Wang et al.*, 2009].

The experiments presented above constitute further support for this CH_4 formation pathway from organic matter under aerobic conditions and provide several new insights.

Overall, CH_4 produced from plants under UV irradiation is strongly depleted in both D and ^{13}C. Thus isotopically light CH_4 is not an unambiguous fingerprint for bacterial sources, but can also be produced photochemically from plant matter. The CH_4 is even more depleted than the exceptionally depleted methoxyl groups of pectin, which only contain non-exchangeable hydrogen. The correlation of $\delta^{13}C$ in methoxyl groups and CH_4, as well as the strong difference in $\delta D(CH_4)$ between C3 and C4 plants require that at least one other source substrate is involved in CH_4 formation, and that CH_4 from this substrate is strongly depleted in δD. C3 plants would then emit relatively more CH_4 from this substrate than C4 plants, and in fact the average emission rates from C3 plants are higher than from C4 plants.

The isotopic signatures (both $\delta^{13}C$ and δD) of methane produced from plant material irradiated with UV light provide new parameters for the assessment of the role of this source in the global methane budget, since its effect on the isotope budget can be included. If vegetation is an important source of CH_4, it should be included in the interpretation of historic CH_4 isotope changes as reconstructed from ice core data [*Ferretti et al.*, 2005] on glacial-interglacial time scales. Recent isotope studies indicate the potential importance of shifting patterns of C3 and C4 vegetation for the isotope content of atmospheric CH_4 [*Schaefer and Whiticar*, 2008].

The overall scatter in CH_4 emitted from different plant species is considerable, and the origin of variations within the individual plant groups (C3, C4, CAM) is unclear The study could be extended to include more plant species in order to improve the understanding of the processes that lead to methane emission upon UV irradiation and also to classify the Biomes characterized by different plant communities. Furthermore, the difference in $\delta D(CH_4)$ between C3 and C4/CAM plants in the absence of a difference in the bulk material is intriguing, and the hypothesis of a second (depleted) substrate should be examined by using isotope labeling studies. The selective discrimination of hydrogen and carbon in plants with different metabolism (C3, C4 or CAM) may be used as additional tool for classification techniques.

Acknowledgments

We thank the gardeners of the Botanical Garden of the Utrecht University for the plant material analyzed and Cascamificio Vigano (Bergamo, Italy) for the cotton flowers from Tadzhikistan. This work was funded by the Dutch NWO project 016.071.605

Chapter 5

Water drives the deuterium content of the methane emitted from plants

The spatial distribution of the deuterium content of precipitation has a well-established latitudinal variation that is reflected in organic molecules in plants growing at different locations. Some laboratory and field studies have already shown that the deuterium content of methane emitted from methanogens can be partially related to δD variations of the water in the surrounding environment. Here we present a similar relation for the methane emitted from plant biomass under UV radiation. To show this relation, we determined the hydrogen isotopic composition of methane released from leaves of a range of plants grown with water of different deuterium content. The plant leaves were irradiated with UV light and the CH_4 isotopic composition was measured by continuous flow isotope ratio mass spectrometry (CF-IRMS). Furthermore, the deuterium content of bulk biomass and of the methoxyl groups of the biomass was measured. The D/H ratio successively decreases from the source water via bulk biomass and methoxyl groups to the CH_4 emitted. The latter has only about half of the deuterium of the source water. The range of isotope ratios in bulk biomass and OCH_3 groups is smaller than in the water used to grow the plants. OCH_3 groups, which contain only non-exchangeable water, can be used to assess the fraction of external water that was incorporated before OCH_3 groups were formed. Surprisingly, the CH_4 formed from UV irradiation has a wider isotopic range than the OCH_3 groups. These results are supported by analysis of the fractionation factors. Although the precise production pathway cannot be fully determined, the presented experiments indicate that methoxyl groups are not the only source substrate for CH_4, but that other sources, including very depleted ones, must contribute. The results imply that the deuterium content of the methane generated from plants under UV irradiation is closely linked to δD in precipitation, and this dependency should be included in global isotope models.

Submitted to *Geochimica et Cosmochimica Acta*, (2009), Ivan Vigano[1], Thomas Röckmann[1], Rupert Holzinger[1], Arnold van Dijk[2], Frank Keppler[3], Markus Greule[3], Willi A. Brand[4], Heike Geilmann[4] and Huib van Weelden[5].

[1]Institute for Marine and Atmospheric Research, Utrecht University, Utrecht, The Netherlands,
[2]Department of Earth Sciences, Utrecht University, Utrecht, The Netherlands
[3]Max Planck Institute for Chemistry, Mainz, Germany
[4]Max-Plank Institute for Biogeochemistry, Jena, Germany
[5]Department of Dermatology and Allergology, Utrecht University Medical Center, Utrecht, The Netherlands

5.1 Introduction

Greenhouse gases like methane (CH_4) have increased in the atmosphere over the past two centuries, mainly due to human activity. Records from air trapped in ice cores revealed that the magnitude and speed of the present changes is exceptional compared to other natural transitions recorded since the late Pleistocene [*Loulergue et al.*, 2008; *Petit et al.*, 1999; *Spahni et al.*, 2005; *Tzedakis et al.*, 2009].

Although its atmospheric concentration is about 200 times smaller than that of CO_2, methane is 25 times more efficient in adsorbing infrared radiation and its relative increase since pre-industrial times is about 150% compared to 35% for CO_2. Methane is the simplest and most abundant reduced organic compound in the atmosphere and an important component in atmospheric chemistry [*Badr et al.*, 1992b; *IPCC*, 2007].

Traditionally biogenic CH_4 was thought to be formed only from methanogens under strictly anaerobic conditions. The discovery of methane emissions from plants under aerobic conditions [*Keppler et al.*, 2006b] was a surprise and created a lot of controversy. Whereas subsequent studies did not confirm a significant production of CH_4 emitted from living plants [*Dueck et al.*, 2007], experiments on dry and fresh plant matter and plant structural components irradiated with UV light showed that CH_4 can be indeed produced under aerobic conditions [*McLeod et al.*, 2008; *Vigano et al.*, 2008]. Isotope labeling was used to prove that the methoxyl ($-OCH_3$) groups of esterified galacturonic acid, the building block of plant pectin, are a source of CH_4 formed at elevated temperatures or under UV irradiation [*Keppler et al.*, 2008]. Messenger et al. [*Messenger et al.*, 2009] showed that reactive oxygen species (ROS) are involved in the formation of CH_4. Although the relevance for the global CH_4 budget is less than initially thought, the existence of CH_4 formation from plants has been confirmed by several isotope studies, [*Bruggemann et al.*, 2009; *Greule et al.*, 2008; *Greule et al.*, 2009; *Keppler et al.*, 2008; *Vigano et al.*, 2008].

Vigano et al. [2009] showed that the CH_4 emitted upon irradiation with UV light is isotopically very depleted in both carbon and hydrogen. For ^{13}C that study clearly showed discrimination between CH_4, plant biomass and methoxyl groups. For deuterium, the results were less clear, at least partly due to considerable scatter between different plant species.

The goal of the present study was to shed more light on the CH_4 production process using deuterium measurements and plants with slightly different deuterium content. This was achieved by growing plants with isotopically different waters. Excluding some microbes that can utilize H_2, the primary hydrogen source of any organic compound in the biosphere is water and, especially for plant biomass, plant leaf water. The isotopic fractionation for hydrogen and oxygen in plant tissues depends on the initial isotopic content of the soil water (and thus precipitation), evapotranspiration, and isotope fractionation during biochemical synthesis [*White*, 1988; *Yakir and DeNiro*, 1990; *Yakir*, 1992].

The most important hydrogen carrier in the biosynthesis of organic compounds is NAD(P)H, which transfers H^+ from water into other molecules via photochemical reduction to H^-, bound in the form NAD(P)H [*Schmidt et al.*, 2003]. Part of the primary fixed hydrogen is re-exchanged with that of the water during subsequent reactions [*Yakir and DeNiro*, 1990].

Recent studies have demonstrated the tight correlation between the δD of methoxyl groups and δD in the precipitation in the area where the plants grew (the

latter was not directly measured, but calculated using the Online Isotope Precipitation Calculator, (OIPC) [*Keppler et al.*, 2007; *Keppler and Hamilton*, 2008]. This offers the potential to use the isotope signature of methoxyl groups as a paleoclimate proxy. Methoxyl groups, especially from lignin, are considered to be stable with no exchange of hydrogen with water. The isotope labeling study on polygalacturonic acid (PGA), the main constituent of plant pectin and lignin, has shown that at least half of the CH_4 that can be liberated from PGA under aerobic conditions originates from the methoxyl groups in PGA [*Keppler et al.*, 2008].
The isotopic composition of precipitation is monitored all around the globe by the Global Network of Isotopes in Precipitation (GNIP) [*Araguas et al.*, 1996; *GNIP et al.*, 2004]. Water vapour evaporating from the ocean is getting successively depleted in deuterium when moving to higher latitudes and into the continents [*Frankenberg et al.*, 2009], and the δD in precipitation collected usually ranges from ~-140‰ at boreal or subtropical latitudes up to ~+20‰ in the tropics. In the polar regions, cold temperatures together with low evapotranspiration, bring the δD values down to ~-250‰ [*Bowen and Revenaugh*, 2003].

Here we describe experiments on greenhouse-grown plants watered with slightly labeled water covering the natural range of δD values from tropical to temperate regions. The isotopic composition of the source water, the bulk plant material, the methoxyl groups and the CH_4 that is emitted upon irradiation with UV light show the transfer of hydrogen from the source water to the emitted CH_4.

5.2 Material and Methods

5.2.1 Preparation of isotopically different plant material

Different plant species (Table 7, Appendix) were grown from the seeds in the greenhouse of Utrecht University in a humid and well drained sandy soil under normal (not sterile) conditions. Plants of each species were watered from special tanks containing water of different δD content throughout their growing phase. Two species were first investigated with a suite of five isotopically different waters, and in a second experimental series, five species, including the first tow, were investigated with second series of five isotopically different waters. It is important for the discussion below that the plants were not grown isolated, but in a common greenhouse environment, which means that ambient water vapor is a second important source of water to the plant.

Plant leaves were collected after 4-6 weeks from the seedling. For the determination of the CH_4 isotope signatures, we used whole intact leaves dried at 60ºC for ten hours in an oven, as well as fresh leaves, while for the bulk and methoxyl-group analyses, the plant leaves were milled and sieved trough a 0.2mm filter in order to obtain fine and homogeneous material.

It should be noted that during the drying and milling process the exposed surface of the sample increased drastically. A fraction of the hydrogen atoms of the organic material could have been exchanged, for example with water retained in the material itself (depending on its hygroscopic strength) or present as water vapor in the surrounding environment [*Keppler et al.*, 2007; *Schmidt et al.*, 2003].

This exchange would certainly affect the δD-bulk analyses reported here, but it is expected that it does not affect the methoxyl group analyses, because the hydrogen there is considered non-exchangeable.

5.2.2 UV irradiation set-up

The irradiation setup was similar to that employed in the study of Vigano et al. [2009a, 2008] and here we only report a short summary. Plant leaves were placed in a leak tight 100ml volume reactor made from Suprasil (UV transparent). Before and after each experiment the reactor was flushed for at least 15 min. with 100ml/min of conventional compressed air (~1.9 ppm CH_4). During the experiment, the reactor was operated in static mode and the leaves were irradiated with a UV lamp (OSRAM Vitalux, 300W) for 1-3 hours. This type of lamp is commonly employed for medical purposes, with a UVA/UVB content comparable to solar radiation if the source is kept at appropriate distance. The total unweighted UVB radiation was determined with a calibrated Waldmann UV meter (Waldmann, Schwenningen, Germany). The relative spectral distribution measurements and the calibration of the Waldmann device were performed with a calibrated standard UV-visible spectro-radiometer (model 752, Optronic Laboratories Inc, Orlando, FL, USA) [Vigano et al., 2008]. We used 5 times the natural tropical UVB levels (20 W/m^2) in order to produce sufficiently high emission rates for precise characterization of the isotopic composition of the source by applying the Keeling plot analysis [*Pataki et al.*, 2003]. Temperature inside the quartz finger was monitored with a micro-thermocouple placed inside the vial and always kept below 30ºC by using a strong ventilator.

Before every run, the sample vial, including the sample, was pre-flushed with compressed air at ambient methane level (~1.9 ppm, $\delta D\text{-}CH_4$~-90‰) for at least 15 min. When the lamp is turned on, the amount of CH_4 increased linearly with irradiation time. After irradiation, the gas was sampled by expansion into a 100ml evacuated glass bottle.

5.2.3 Isotope Ratio Mass Spectrometry analyses of methane

The collected samples were analyzed on a continuous flow isotope ratio mass spectrometry (CF-IRMS) system for $\delta D\text{-}CH_4$ (reproducibility ~ ±2‰) [*Keppler et al.*, 2008; *Vigano et al.*, 2008]. The CF-IRMS analysis provides isotope values and concentrations derived from the peak areas of the chromatogram. Typically we irradiated the samples inside a leak tight quartz reactor for at least three different time periods (1h, 2h, 3h), as previously described by Vigano et al. [2009]. Keeling plots of isotopic composition versus inverse mixing ratio, $1/[CH_4]$, yield good linear correlations ($R^2 > 0.9$) and the isotope source signatures are derived by extrapolating to hypothetical $[CH_4] \Rightarrow \infty$ [*Vigano et al.*, 2009a]. The experimental setup allows determining source signatures from single species within 6h with an accuracy of ±5‰ for $\delta D\text{-}CH_4$.

δD values are the relative deviations of the D/H ratio in a sample relative to the international standard Vienna Standard Mean Ocean Water (VSMOW). The range of the isotopic values has been scaled according to previous studies on methane sources [*Bergamaschi et al.*, 1994; *Bergamaschi et al.*, 2000]. We report mean values and standard deviations for different plant groups in Table 7 of the Appendix.

In the discussion of the results we refer to the fractionation factor between two reservoirs a and b, which is defined as

$$\alpha_{D_{a/b}} = \frac{R_a}{R_b} = \frac{(\delta D_a + 1)}{(\delta D_b + 1)}$$

5.2.4 Bulk isotope analyses

Bulk δD was determined at the Stable Isotope Laboratory of the Max-Plank Institute for Biogeochemistry in Jena (Germany).

The method for bulk δD analysis using a High Temperature Conversion (HTC) mass spectrometric technique closely follows the procedure described for $\delta^{18}O$ determination in bulk material by Brand et al. [2009]. Samples are weighed into Ag-foil and positioned into an Autosampler ('Zero-Blank', Costech, Milan, Italy). Upon actuation, the packets drop into a helium flushed high temperature reactor (HTO, Hekatech, Wegberg, Germany) kept at 1450°C. The reactor has an outer SiC tube and an inner tube made from glassy carbon with reversed carrier gas flow to ensure that the full helium flux passes through the core of the reactor [*Gehre et al.*, 2004]. In addition, the inner tube is filled with glassy carbon chips up to the highest temperature zone where the reaction to CO, H_2, and carbon plus further unspecified reaction products and residues takes place. From the reactor, the sample gas passes a fine filter containing NaOH on pumice ('Ascarite') and $Mg(ClO_4)_2$ before entering a packed column (5-Å) gas chromatograph at 70°C for separating H_2 and CO. An open split interface ('ConFlo III', [*Werner et al.*, 1999]) provides the connection to a Delta$^+$XL stable isotope mass spectrometer (both from Thermo-Fisher Scientific, Bremen, Germany). By monitoring the ion currents at m/z 3 and 2, the hydrogen isotopic composition is analyzed. As primary reference for reporting on the VSMOW scale we used NBS22 oil with an assigned value of -118.5‰. Using this material, a local reference material 'PET-J1' (polyethylene, 'Uvasol', purchased from Merck, Darmstadt, Germany) was calibrated with a δD value of -80.75‰ vs. VSMOW.

Aliquots of these materials were interspersed together with the samples and analyzed in the same sequence. The reported sample results are based on the relative differences to the working reference material results. As a quality control reference we included one sample of IAEA-CH7 polyethylene in the daily sequence of measurements. IAEA-CH7 has an assigned value of -100.3‰ on the VSMOW scale.

5.2.5 Methoxyl-group analyses

The D/H isotope ratios of the plant methoxyl groups were analyzed according to Greule et al., (2008) and Greule et al., [2009]. In brief, methoxyl groups of plant

material are cleaved off with hydroiodic acid (HI) at 130°C in closed reaction vials. Subsequently a headspace analysis of the gaseous product methyl iodide (CH_3I) is carried out using gas chromatography pyrolysis/combustion isotope ratio mass spectrometry (GC-P/C-IRMS). This rapid and precise method enables the determination of δD values of plant methoxyl groups without any isotopic discrimination.

Plant methoxyl groups exist in two different types of chemical bondage, ester methoxyl groups (mainly appearing in pectin) and ether methoxyl groups (main sources in nature is lignin). In this study we have measured δD values of the total plant methoxyl pool including pectin and lignin type methoxyl groups.

5.3 Results and discussion

Figure 5.1 and Table 7 in the Appendix show the δD values determined on the plant bulk material, the OCH_3 groups, and the source signatures of CH_4 emitted upon irradiation with UV light, as function of the δD in the water that was used to grow the plants. Clearly, the CH_4 emitted is particularly depleted in deuterium compared to any other signature (Table 7, Appendix), in agreement with the previously reported isotope signatures from Vigano et al. [2009]. δD in the methoxyl groups is also lower than the bulk δD value.

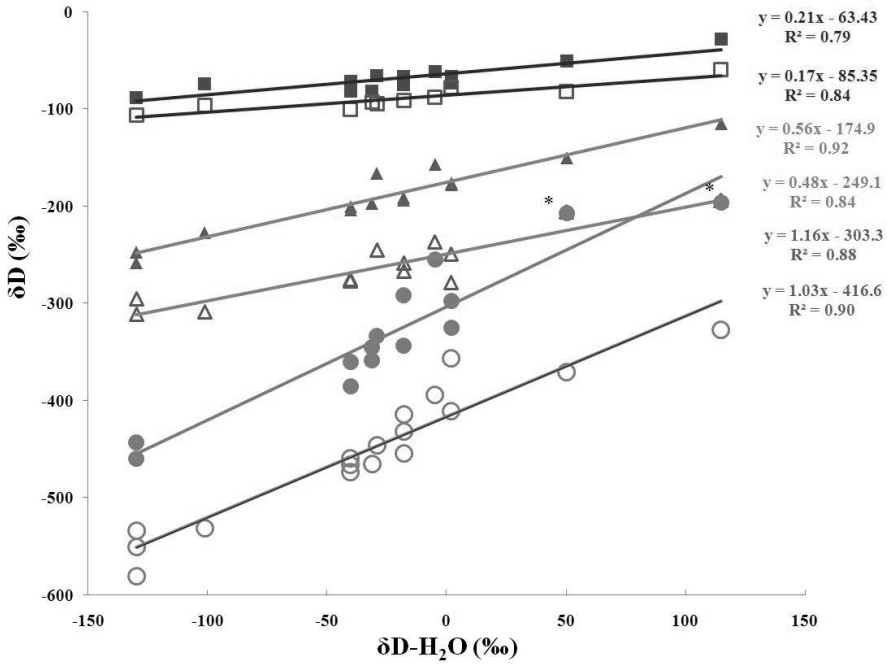

Figure 5.1 δD values for C3 (open symbols) and C4 (solid symbols) plants, of CH_4 , OCH_3 and bulk material as a function of δD-H_2O. Waters with δD values in the range -29.3‰ to -40.3‰ are common tap water. δD values between -40.3‰ and 114.8‰ were obtained by mixing pure D_2O (99.99%) with common tap water. Values between -101.2‰ and -114.8‰ were obtained by mixing water from Greenland ice cores (pure δD values ~ -300‰) with common tap water.
* δD values of OCH_3 and CH_4 overlap

The bulk values show only a relatively small fractionation compared to the source water. It should be kept in mind that the bulk plant material has probably a large fraction of exchangeable hydrogen [*Schimmelmann*, 2002], consequently the evaluations regarding the bulk analyses here are affected by large uncertainties.
Furthermore, the plants were not grown isolated, but were exposed to the air of the greenhouse. Therefore water vapor was exchanged via the stomata where it equilibrated with the leaf water [*Limm et al.*, 2009]. Leaves take up large amounts of water from the surrounding air [*Farquhar and Cernusak*, 2005] and $\delta D\text{-}H_2O$ in the leaf derives from a mix of H_2O present in ambient air with the water coming from the roots, and this mix it is affected by stomatal regulations. Unfortunately, leaf water δD was not measured in our study to assess this exchange directly, but δD of the methoxyl groups provides some indirect information (see below).

Despite these concerns, the generally tight correlations in Figure 5.1 ($r^2 > 0.79$) denote a clear effect of the deuterium content of the water on deuterium in bulk plant material, the methoxyl groups and emitted CH_4. This already confirms our initial hypothesis that the hydrogen signature from source water is transferred to plant components and emitted CH_4. Quantitative analysis, however, reveals some interesting and unexpected features.

As shown in Vigano et al. [2009], δD signatures of the emitted CH_4 are different between C3 and C4 plants. The differences increase in magnitude from the bulk material via OCH_3 groups to CH_4. The average C3 plant produces CH_4 with 43% less D than the source water, whereas it is only 32% less for C4 plants. Interestingly, this difference is found back in all individual fractionation constants. C4 plants fractionate ~2% less during the incorporation of D into bulk biomass (Figure 5.2), but also in the formation of the assumedly non-exchangeable OCH_3 groups (~8%), and in the production of CH_4 (~11%).

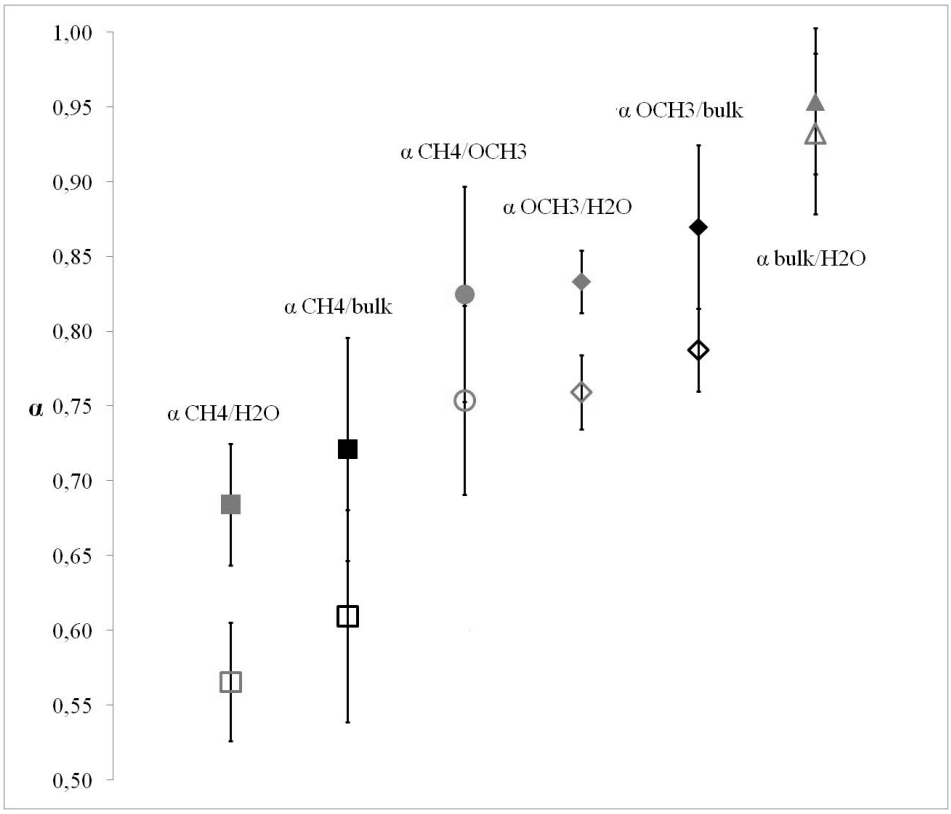

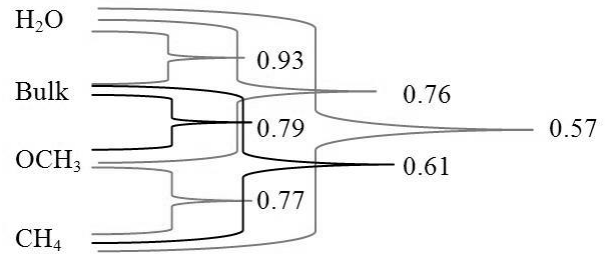

C3

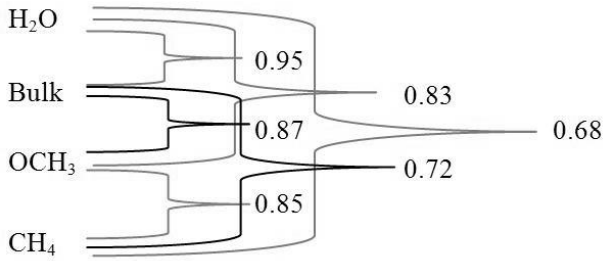

C4

Figure 5.2 Average fractionation factors between the analyzed hydrogen reservoirs for C3 (open symbols) and C4 (solid symbols) species. The upper part shows the relative magnitudes and 1σ error bars. The dendrograms illustrate the differences and similarities between C3 and C4 plants.

It is also worthwhile to explore the fractionation between bulk plant material, the plant methoxyl groups, and emitted CH_4. For C3 plants, the fractionation constant between OCH_3 and bulk biomass, $\alpha_{OCH3\text{-}bulk}$, is 0.79, which is close to the value for $\alpha_{CH4–OCH3}$ (0.77). Also for C4 plants, these two values are similar, but the fractionation is significantly smaller ($\alpha_{OCH3\text{-}bulk}$=0.87 and $\alpha_{CH4–OCH3}$=0.85). It is interesting to note that these two fractionation factors relate to totally different processes: $\alpha_{OCH3\text{-}bulk}$ quantifies the fractionation by metabolic processes between the OCH_3 groups and the bulk, whereas $\alpha_{CH4–OCH3}$ is believed to be characteristic for a non-metabolic, most likely photochemical process [Vigano et al., 2008]. Chemical fractionation factors are representative of the respective process and should not vary between different reservoirs. Therefore the difference between C3 and C4 plants indicates that 1) OCH_3 groups are not the only reservoir for CH_4 and 2) the other, unkown, reservoir has a different isotopic composition in C3 and C4 plants [*Sternberg et al.*, 1984]. Notably, Messenger et al. [2009] suggested that CH_4 can also be produced from *O*-acetyl groups of monosaccharides (e.g. mannose pentaacetate) upon UV irradiation and potentially might be a CH_4 source in plants. They further suggested that this source may account for discrepancies in previous isotope labelling experiments by Keppler et al. [2008].

The slopes of the regression lines in Figure 5.1 require further analysis. If the isotope signature of the source water was the only hydrogen reservoir and just transferred to the plant and finally to the CH_4 emitted, then we would expect a slope of 1 for all these correlation lines. However, this is only true for the relation between the δD of the water and the δD of the CH_4 emitted. For the bulk biomass, the slope is only 0.2, so the isotope signature of the water is only to a small part reflected by the bulk biomass. Two processes can be responsible for the difference. First, as mentioned above, the isotopically different plants were not grown in isolated chambers. Therefore, the liquid water used to grow the plants is not the only source of water Second, the drying and grinding process strongly increases the surface area of the material and exposes matter that may not have been in direct contact with the atmosphere to ambient water vapor. On the other hand, the data of bulk plant material and source water are still highly correlated (Figure 5.1). It appears that although only 20% of the hydrogen in the bulk material is from the original water, the other reservoir does not introduce large additional variability, suggesting that a common and rather constant source is shared by all plants, as expected for both the water vapor in the greenhouse and water exchange during the grinding process. It should be noted that the experiments presented here are particularly vulnerable to these two sources of external water since the source water was (in many cases) isotopically distinct from both the typical water in the greenhouse and the water in the laboratory where the bulk samples were prepared.

Whereas it is well-known that bulk δD measurements have to be interpreted with caution because of the influence of exchangeable hydrogen, this should not be the case for the OCH_3 groups. However, the slope of the correlation line between the isotopic composition of OCH_3 groups and the source water is only 0.5. There is some variability indicating differences in different individual plants, but the slope is significantly smaller than 1. The simplest explanation is that the water was already diluted before synthesis of the OCH_3 group and that only 50% of the source water signature is incorporated into the plant at this stage of biosynthesis.

The most surprising finding, however, is that CH_4 that is released upon UV irradiation (presumably with a significant proportion from OCH_3 groups) does show the full range of the isotope content of the source water again (slope ~1 in Figure 5.1).

It is not possible to widen a range of isotope compositions with pure kinetic fractionations, since kinetic fractionations act relative to the original reservoir. One possibility to explain this behavior is that the δD measurement on the OCH_3 groups does not reflect the true substrate from which the CH_4 product is formed. For example, the OCH_3 may consist of two fractions of equal magnitude. One is the substrate from which CH_4 is formed and does retain the full spread of δD from the source water. The second reservoir, which does not form CH_4 and is fully exchanged, i.e., has a constant isotope signal. However, prior research has shown that OCH_3 groups contain only non-exchangeable hydrogen [*Greule et al.*, 2008b; *Keppler et al.*, 2007a; *Keppler et al.*, 2007; *Vigano et al.*, 2009a]. In a recent study where we analyzed δD of OCH_3 of numerous wood samples from various regions, the isotope variability in the OCH_3 groups was more strongly linked to the one in the (in this case model predicted) δD of the source water [*Röckmann et al.*, 2009]. For these reasons we reckon that the hydrogen was exchanged before the OCH_3 groups have been synthesized.

A more likely process that may explain differences between the isotopic composition of the OCH_3 groups and the produced CH_4 is that CH_4 is formed not only from OCH_3, but in addition from an isotopically very distinct reservoir. The fit to the correlation between δD-CH_4 and δD-OCH_3 (Fig. 5.3) has a slope of roughly 0.45, and considering that methoxyl groups are not affected by exchange of hydrogen this suggests that they cannot be the sole substrate of the CH_4 formation. This is actually expected from other recent isotope labeling studies [*Keppler et al.*, 2007; *Messenger et al.*, 2009; *Vigano et al.*, 2009a].

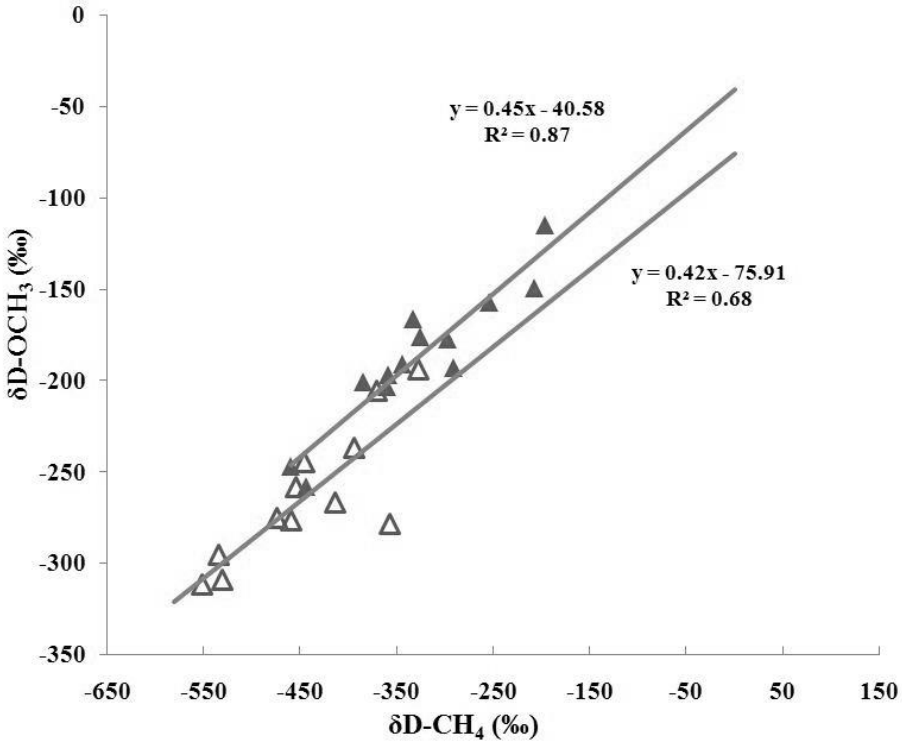

Figure 5.3 δD values of methoxyl groups and bulk against δD signatures of methane for C3 (open symbols) and C4 plants (solid symbols).

In this case, however, the relative fraction from the two reservoirs would have to depend on the isotopic composition of the source water in order to explain the increase in slope, i.e. the "heavier" reservoir would have to contribute more to the plants watered with "heavier" water than to the plants watered with "lighter" water. Given the very small isotope labeling in our study, metabolic effects of the isotopic composition of the source water can almost certainly be excluded.

Thus, the origin of the difference in the isotope correlation slopes for the OCH_3-H_2O and CH_4-H_2O systems, respectively, is not fully understood at present. It should further be noted that not only the isotopic composition of the other source substrate(s) is of interest, but also possible kinetic isotope effects, which are likely different for CH_4 formation from the different reservoirs. Identification of additional reservoirs is therefore important for a further understanding of the deuterium transfer processes.
Sharpatyi et al. [2007] described a probable radical reaction on cellulose induced by UV radiation, where the generation of a methyl radical is essential for the consecutive formation of CH_4. The formation of such methyl radicals could be induced through generation of •OH derived from singlet oxygen ($^1O_2$) as proposed by Messenger et al. (2009) in their study on reactive oxygen species. Still, the origin of the fourth hydrogen needed to form the methane molecule remains unclear. From deuterium labeling experiments, Keppler et al. [2008] proposed that under UV irradiation roughly 50% of the hydrogen is from methoxyl groups, while the rest is from the surrounding water or organic compounds or a mix of both reservoirs. According to the higher depletion in deuterium of the CH_4 emitted, the fourth hydrogen must come from a highly depleted pool or/and be affected by very strong isotopic fractionation. Extreme depletion at defined positions of isoprenoids has been reported by Schmidt et al (2003), and they have been used in order to explain the hydrogen isotope distribution in methoxyl groups (hypothetical assumed value ~-680‰) [*Keppler et al.*, 2007].

5.3.1 Fractionation factors and their dependence on δD of the source water

The average fractionation factors bulk/water for C3 and C4 plants, $\alpha^{C3}_{bulk/H2O}$ = 0.93±0.05 and $\alpha^{C4}_{bulk/H2O}$ = 0.95±0.05, respectively, have overlapping error bars. Nevertheless, investigation of the individual data points clearly shows a systematic offset (Figure 5.1). Therefore, further insight can be gained by investigation of the individual fractionation factors, and their dependence on the isotopic composition of the source water.

In Figure 5.4, the fractionation factors between the different reservoirs are plotted as a function of the isotopic composition of the water used to grow the plants. As mentioned above, it is not expected that the small change in water isotopic composition, which is close to the range actually occurring in precipitation on earth, would affect metabolic pathways. In an ideal system that is only governed by kinetic isotope effects, the fractionation factors should be independent of the isotopic composition of the source water. Therefore, the fractionation factor between the different reservoirs and water should be constant. However, Figure 5.4 shows that various dependencies are found between the different reservoirs. Although the absolute values are different between C3 and C4 plants, as discussed above, the slopes of the correlation lines are very similar for C3 and C4 plants and the systematic nature

indicates that they represent interfering effects which are important in our system, which can in many cases be related to the observations of the bulk values as discussed above.

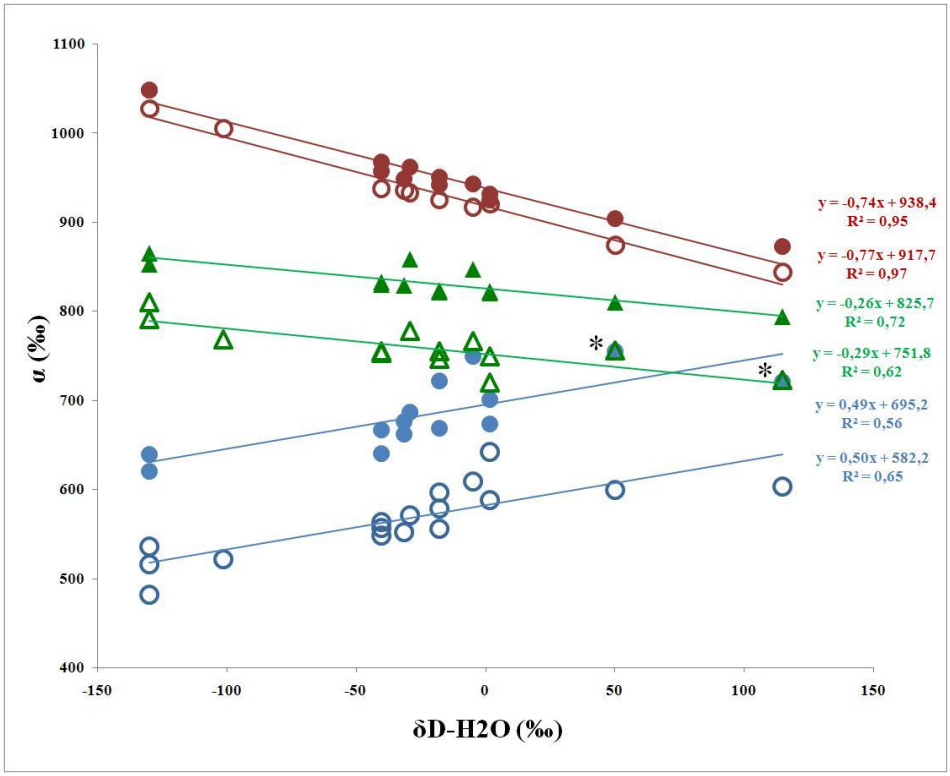

Figure 5.4 Changes of the fractionation factors reported in Table 1 for C3 (open symbols) and C4 plants (solid symbols) as function of δD-H_2O for CH_4 (blue), OCH_3 groups (green) and bulk biomass (red) relative to source water.
* δD values of OCH_3 and CH_4 overlap

A negative slope in Figure 5.4 means that the derived fractionation factor decreases when the source water becomes more enriched in deuterium. This is the case for the correlation between $\alpha_{bulk/H2O}$, and $\delta D_{H2O,}$ and $\alpha_{OCH3/H2O}$ and δD_{H2O}, respectively, and it indicates that the isotope signature of the source water is "diluted" in these reservoirs. For example, when δD in the water changes by +100‰, the corresponding change in $\alpha_{bulk/H2O}$ is -75‰. This means that only 25% of the shift in the source water is actually transferred to the bulk biomass. The corresponding change in $\alpha_{OCH3/H2O}$ is -28‰, which means that only 72% of the source water shift is transferred to the OCH_3 groups. The remaining hydrogen fraction (roughly 30% for OCH_3 groups and 75% for bulk biomass) must come from another reservoir, and the numbers agree reasonably with the numbers derived above from the different ranges of δD values covered. As OCH_3 groups contain only non-exchangeable hydrogen, the additional hydrogen must be mixed-in already before formation of these groups, most likely from the water vapor reservoir in the greenhouse, which exchanges with plant leaf water before the C-H bonds are formed. Another 50% of water can then be exchanged or added at later stages, either within the plant, or during the preparation of the samples to explain the bulk observations.

The fact that the slope of the fractionation factor is positive in the CH_4-H_2O system reflects the increase in the observed range of the δD values (Figure 5.5) again.

In the analysis of the fractionation factor, we actually see that the relative changes in $\delta D(CH_4)$ are even larger than in the pure source H_2O. The ~1:1 slope between $\delta D(CH_4)$ and $\delta D(H_2O)$ in Figure 1 is slightly misleading, because a 100‰ change at a level of ~-500‰ for CH_4 is in relative terms much larger than a 100‰ change for H_2O at ~0 ‰. This is reflected in the strong increase of $\alpha_{CH4/H2O}$ with δD_{H2O}. Different processes have been discussed above, but none can explain this positive slope of $\alpha_{CH4/H2O}$ satisfactorily. In isotope research, it is always possible to decrease differences, e.g., by contamination from an external reservoir as discussed for bulk and OCH_3 groups, by scale contraction in the mass spectrometer, or other effects, but it is very hardly possible to increase relative differences from a substrate to a product.
In summary, the investigation of the individual fractionation constants provides interesting information about the input of external hydrogen into the system, but the fractionations in the processes that lead to CH_4 cannot yet be fully explained and need further research.

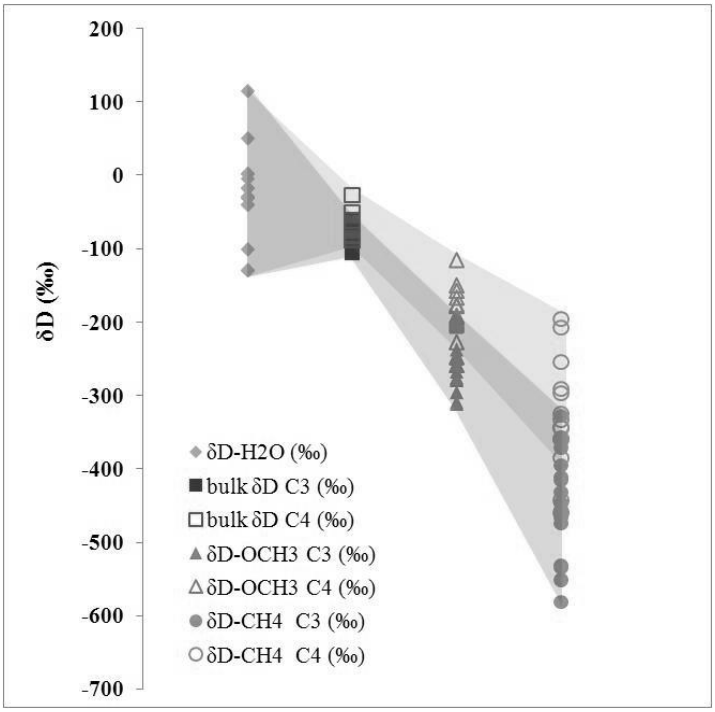

Figure 5.5 Spreading of the isotope values of the different analyses of C3 and C4; the δD-CH_4 covers the widest range.

5.4 Conclusions

Our results show that the D content of the water utilized by plants affects the δD of the methane produced upon irradiation with UV light. The deuterium content of the source water is transferred (and transformed through strong kinetic fractionations) to the CH_4 that is finally produced. In this respect, this source behaves similar to microbial sources [*Schoell*, 1988; *Schoell et al.*, 1988; *Waldron et al.*, 1999]. Since we did not sterilize our plants, we cannot exclude a priori a microbial interference here, but the non-bacterial origin of CH_4 produced by UV radiation in our analytical setup

has been demonstrated in previous investigations [*Vigano et al.*, 2008; *Vigano et al.*, 2009a].

Additional isotope measurements on the bulk biomass and OCH_3 groups are useful in elucidating the import of external water sources into the system. The most surprising finding is, however, that this dilution effect due to external hydrogen does not show up in the final CH_4 product, whereas it is visible in one of its main precursors, the OCH_3 groups. For the future, the next step should be identify the missing precursors compounds (both carbon and hydrogen(s)) and the related isotope fractionations.

Acknowledgments

We thank the gardeners of the Botanical Garden of Utrecht University for the plant material analyzed, Arndt Schimmelmann for the very useful advice concerning leaf water exchange issues and Martin Schoell for insightful discussions. This work was funded by the Dutch NWO project 016.071.605.

Chapter 6

Methoxyl groups of plant pectin as a precursor of atmospheric methane: evidence from deuterium labelling studies

This is a study where my main contribution was the determination of the deuterium isotopic composition in CH_4.

The observation that plants produce methane (CH_4) under aerobic conditions has caused considerable controversy in the scientific community and the general public. It not only led to much discussion and debate on its contribution to the global CH_4 budget but also on the authenticity of the observation itself. Previous results suggested that methoxyl groups of the abundant plant structural component pectin might play a key role in the in situ formation process of CH_4 Here we investigate this effect with an isotope labelling study.

Polysaccharides, pectin and polygalacturonic acid, with varying degrees of deuterium labelled methoxyl groups were investigated for CH_4 formation under UV irradiation and heating

A strong deuterium signal in the emitted CH_4 was observed from these labelled polysaccharides

Results clearly demonstrate that ester methyl groups of pectin can serve as a precursor of CH_4 supporting the idea of a novel chemical route of CH_4 formation in plants under oxic environmental conditions. Furthermore the results suggest that other carbon moieties in pectin also contribute to the observed emissions.

Published in *New Phytologist*, **doi**: 10.1111/j.1469-8137.2008.02411.x, as co-author with Frank Keppler[1], John T. G. Hamilton[2], W. Colin McRoberts[2],Marc Braß[3] and Thomas Röckmann[3]

[1]Max-Planck-Institute for Chemistry, Joh.-Joachim-Becher-Weg 2, 55128 Mainz, Germany;
[2]Agri-Food and Biosciences Institute, Newforge Lane, Belfast BT95PX, UK;
[3]Institute for Marine and Atmospheric Research Utrecht, Utrecht University, Princetonplein 5, 3584CC Utrecht, the Netherlands;

6.1 Introduction

It is well known that plants emit a wide range of volatile organic compounds (VOCs), such as isoprenoids and oxygenated compounds (e.g. methanol and acetone), to the atmosphere [*Loreto et al.*, 2008]. However, it was only recently found that plants also produce CH_4 when we showed that intact living plants, as well as plant litter, produce this important greenhouse gas in an oxygen rich environment and release it to the atmosphere [Keppler et al., 2006]. We also reported that CH_4 emissions were sensitive to both temperature and natural sunlight irradiation. The fact that plants produce CH_4 under aerobic environmental conditions is a surprising finding because prior to our observations biological formation was only considered to occur under strictly anaerobic conditions, in environments such as wetlands. Our controversial findings have led to considerable discussion and debate as to their authenticity and their implications for the CH_4 global budget and global warming [*Dueck et al.*, 2007; *Evans*, 2007; *Hopkin*, 2007; *Kirschbaum et al.*, 2006; *Schiermeier*, 2006]. Most importantly, Dueck *et al*. [2007], using ^{13}C-labelled plants reported that they could not detect substantial emissions of CH_4 from living plants casting further serious doubt on our work. On the other hand, published study by Wang et al. (2007) showed emissions of methane from several shrubs of the Mongolian Steppe confirming the finding of aerobic methane formation in plants.

Interestingly very recently, via a personal communication, we became aware of work conducted in the late 1950's at the Academy of Sciences of Georgia (Tbilisi) on emissions of VOCs from leaves of *Populus simonii* Carr. and *P. Sosnowskyi* Grossh [*Sanadze and Dolidze*, 1960]. In that study the researchers suggested that plants could emit CH_4 as well as ethane, propane, isoprene and several other volatile organic components. However no follow up studies on CH_4 release were undertaken as this group very successfully focussed on isoprene emissions instead.

As a first step it is important to gain information about precursor compounds in plants that could give rise to CH_4. Based on previous results we suggested the possibility of the involvement of the methyl moiety of the esterified carboxyl group (methoxyl group) of pectin [Keppler et al, 2004]. Indeed, in experiments with apple pectin we not only observed emission of CH_4 but also noted that the emission rate was broadly similar to that measured with detached leaves [Keppler et al. 2006]. However, even though those results indicated a role for pectin they provide no proof for the involvement of the pectin methoxyl group in CH_4 formation.

Stable isotope analysis is a powerful tool which we recently employed to demonstrate that plant pectin and lignin methoxyl groups have unique carbon isotope signatures [Keppler et al., 2004], and to also establish the relationship between hydrogen isotopes of wood lignin methoxyl groups and meteoric water [Keppler et al. 2007]. In this investigation we again use this technique together with pectin and polygalacturonic acid (Fig. 6.1), modified to contain varying degrees of deuterium labelled esterified methyl groups, to prove that plant pectin methoxyl groups are a precursor of CH_4 and thus could be a source of it in an oxic environment.

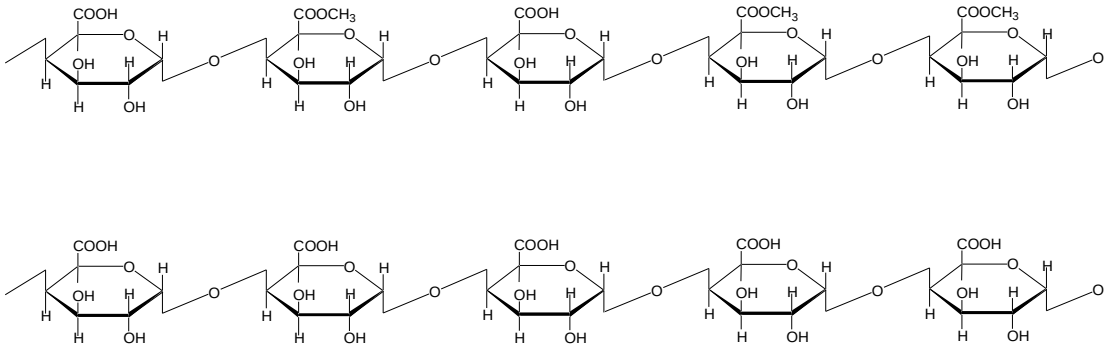

Figure 6.1 Chemical structure of pectin (upper graph) and PGA (lower graph)

6.2 Materials and methods

Isotopic labelling of pectin and polygalacturonic acid

All reagents were purchased from Sigma-Aldrich Company Ltd except for low methoxyl pectin (GENU® pectin LM-101 AS), which was a gift from CP Kelco Ltd., Denmark and methyl D-galactopyranoside which was purchased from CMS Chemicals, Oxfordshire, UK.

Methyl esterification

Methyl esterification was performed essentially as described by van Alebek [2000]. Briefly, samples of polygalacturonic acid (2g ± 0.01g) were weighed into 100 ml volumetric flasks and solutions of anhydrous methanolic H_2SO_4 (0.02 N, 100 ml) containing either 0%, 5% or 20% tetradeuterated methanol (v/v) added. Samples were incubated at 4°C for 47 days with occasional shaking and then centrifuged (2000 rpm, 10 minutes). The methanolic H_2SO_4 was decanted and the remaining sample washed with propan-2-ol (3 x 40 ml), with the supernatant being discarded following centrifugation.

The samples were left over night at room temperature to allow evaporation of the remaining propan-2-ol and then distilled water (20 ml) was added to the samples, which were then thoroughly mixed, frozen and lyophilised over a 6 day period. Dried samples were ground to a powder using a pestle and mortar. Low methoxyl pectin was methylated by the procedure described above but only 5% tetradeuterated methanol was used for derivatisation and the incubation period was 14 days.

Determination of deuterium label in pectin and polygalacturonic acid

Methoxyl content was determined by measuring the release of methyl iodide (CH_3I) using the Zeisel technique as described by Keppler et al. [2006]. Incorporation of deuterium label of the ester group in pectin and modified PGAs was also determined using CH_3I. For both quantification and measurement of label gas chromatography - mass spectrometry (GC/MS) were employed. The GC oven was equipped with a PoraPLOT Q column (12.5 m x 0.25 mm x 8 μm) and programmed to hold at 80°C for 1 min and then ramp at 10°C/min to 160°C. The injector port was maintained at 250°C and the sample (50 μl) was injected split at a ratio of 100:1. The mass spectrometer was operated in the selected ion monitoring (SIM) mode measuring ion currents at *m/z* 127, 142 and 145. CH_3I was quantified by direct comparison of sample peak areas for ion current *m/z* 145 with a standard curve obtained with authentic standard. % Label was calculated as (integral of ion current at *m/z* 145/sum of integrals at ion currents *m/z* 142 and 145) *100.
Methoxyl content and degree of labelling for esterified polygalacturonic acids and pectin are presented in Table 1.

Temperature and illumination experiments

Lypholised milled samples (~200 mg) in glass vials (fused quartz, 40ml) sealed with caps containing a PTFE lined silicone septa were heated for 24h at 40, 60, and 80°C or illuminated with an 250W Osram Vitalux lamp (UVA 320-400 nm, UV-B 280-320 nm). For more details we refer to the paper of Vigano et al. [2008]. All experiments were performed in laboratory ambient air so thus the initial CH_4 concentration in the vial was approximately 1800 to 2000 ppb with δ^2H values around −90‰. δ^2H of CH_4 was measured by GC-IRMS at the end of each experiment. For blank measurements empty vials (only containing laboratory ambient air) were prepared at the same time as the samples and treated under identical conditions.

For the light experiments vials were placed approximately 35 cm below the lamp and temperature measured during experiments was in the range between 30 and 38°C. The total unweighted UV-B radiation was ~3.7 W/m^2 and UV-A radiation was ~42 W/m^2. The UV content (UV-A and UV-B separately) was determined with a Waldmann UV meter (Waldmann, Schwenningen, Germany).

Isotope ratio monitoring mass spectrometry for determination of δ^2H values on CH_4

Gas samples were transferred from the vials to an evacuated 40 cm^3 sample loop. CH_4 was trapped on Hayesep D, separated by gas chromatography from interfering compounds and transferred via an open split to the isotope ratio mass spectrometer (ThermoFinnigan Delta^{plus} XL). Concentration (reproducibility ± 20 ppb at ambient concentration) and δ^2 H values were determined using a methane standard with known concentration and isotopic composition as internal reference, and a measurement of the inlet pressure in the sample loop. Values of δ^2 H (‰) relative to that for VSMOW are defined by the equation δ^2H (‰) = $(^2H/^1H_{sample}/^2H/^1H_{standard} - 1)$ x 1000‰. Throughout the paper we use the form $\delta D(CH_4)$ values instead of $\delta^2H_{methane}$ values.

A GC-FID instrument for grab sample analysis (reproducibility ± 10 ppb) was additionally used for verification of the IRMS concentration measurements.

6.3 Results and discussion

In a first approach we employed pectin containing a low degree (0.05 %) of deuterium labelled methoxyl groups (Table 8, Appendix) for heating experiments at 80°C. The emission rate was measured to be ~2.5 ng g^{-1} dw h^{-1} and the δ^2 H values of CH_4 ($\delta D(CH_4)$ values) changed from ~−83‰ to 1‰ within 14 hours. Calculation of the change in δ^2 H values together with the change in CH_4 concentration in the vials reveal that at least 80% of the emitted CH_4 must have been derived from the methoxyl groups of pectin. These first results provided strong evidence of the involvement of pectin methoxyl groups in CH_4 formation. However, because of the complexity of the pectin polymer it was somewhat difficult to fully decipher the isotope information and understand why methoxyl groups could only account for 80% of emitted methane. Therefore, as pectin is a polysaccharide composed primarily of partially esterified α-(1-4) linked galacturonic acid units we decided to employ polygalacturonic acid for further experiments. Using polygalacturonic acid (PGA) as a model compound has a couple of major advantages over pectin itself. Firstly, since it contains no methoxyl groups it could be used as the control compound to determine if CH_4 formation can also occur from the free acid and secondly, as it is easily methyl esterified with methanol, ester derivatives with known deuterium label content could be conveniently prepared.

Results from experiments where labelled and untreated PGA samples were incubated at temperatures between 40 and 80°C are shown in Figure 2. As was expected high $\delta D(CH_4)$ values were measured for the labelled PGA samples (up to 1400000‰, see Table 9, Appendix) and thus it was essential that ambient laboratory air (~1900 ppb with $\delta D(CH_4)$ values in the range of –90‰) was used for headspace in the reaction vials so as to avoid massive contamination and memory effects in the analytical system. Headspace from both labelled PGA samples (6 and 22% deuterium label) showed a continuous increase in the $\delta D(CH_4)$ values with increasing temperature (Figure 6.2a) whereas with the unlabelled methyl esterified PGA sample a slight decrease in $\delta D(CH_4)$ values with increasing temperature (Figure 6.2b) was noted.

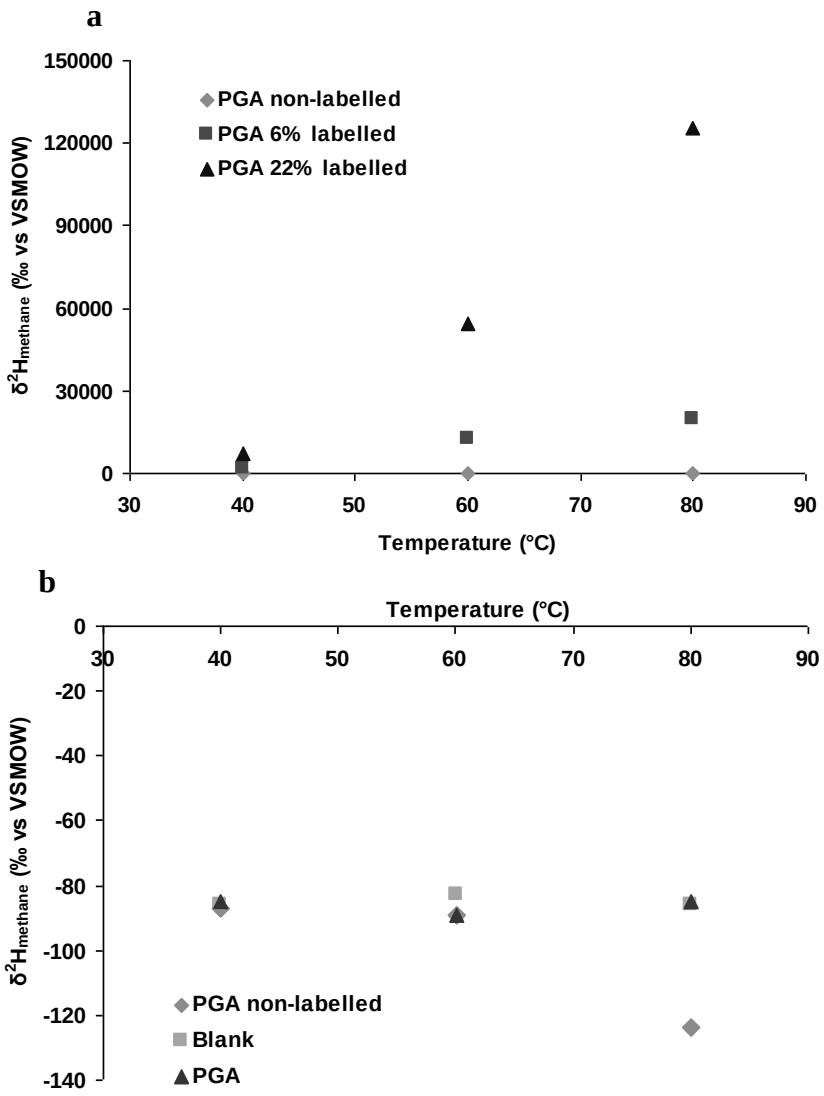

Figure 6.2 Heating experiments with PGA and methyl esterified PGAs. (a) $\delta^2H_{methane}$ values of methyl esterified PGAs. (b) $\delta^2 H_{methane}$ values of blank, PGA and non labelled methyl esterified PGA.

Relative to the labelled samples, the $\delta D(CH_4)$ values of the untreated PGA sample only differed marginally from that of laboratory air. The strong increase in the $\delta D(CH_4)$ values for labelled PGA samples is accompanied by an increase in emission rates at higher temperatures. Emission rates for the esterified PGAs were found to range between 0.3 and 0.7 ng g^{-1} dw h^{-1} at 40°C and 1.3 and 3.1 ng g^{-1} dw h^{-1} at 80°C, rates in a similar range to that recently reported for apple pectin (Keppler et al. 2006). Formation of CH_4 from untreated PGA was much lower, ~0.2 and 0.7 ng g^{-1} dw h^{-1} at 40 and 80°C, respectively. The calculated ratio of label between PGA sample with 22% and PGA sample with 6% label is 3.7 (22.6/6.1) and this ratio is generally reflected for the calculated ratios of $\delta D(CH_4)$ values of PGA 22% and PGA 6% after the incubation periods. Based on the $\delta D(CH_4)$ values and the increase in headspace CH_4 concentration in the incubation vials during the incubation period it is possible to calculate the percentage of CH_4 arising directly from the methyl moiety of the

methoxyl group (see Fig. 6.3). This calculation shows that, on average, about two thirds of CH_4 is formed from methoxyl groups with a range of 48 to 68% observed.

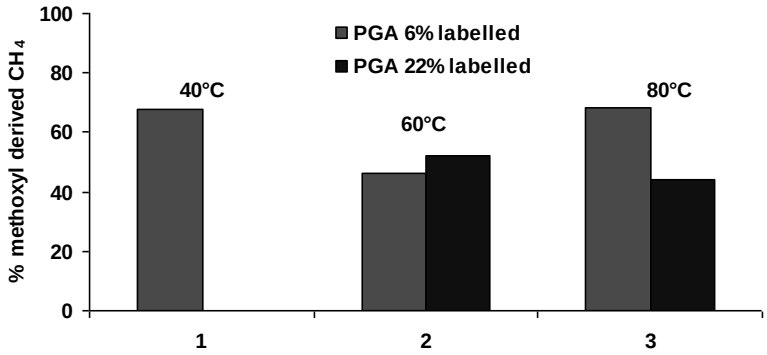

Figure 6.3 Percentage of CH_4 formed from methoxyl groups of PGA.

One possible explanation for this observation is that the methyl moiety is not transferred intact during CH_4 formation. Using GC/MS, with the instrument employed in the selected ion monitoring mode, headspace from labelled PGA (22% deuterium) which had been incubated at 80°C was shown to have peaks at both m/z 16 and 19 at the expected retention of an authentic CH_4 standard. The presence of a peak at m/z 19, which was absent in the unlabelled methyl esterified PGA sample, indicated the presence of CH_4 containing three deuterium atoms clearly shows that the methyl group from methylated PGA was transferred intact during the heating process. So now, interestingly, when this finding is combined with the IR/MS results, it is apparent that methoxyl groups cannot be responsible for all CH_4 formed during the heating experiments and approximately one third must originate from other carbon moieties within methyl esterified PGA. An alternative explanation could be the release of methane due to desorption processes, as recently suggested by Kirschbaum et al. [2007], although the results obtained in this study with the untreated PGA would not support such a contention. Much more likely there would appear to be a second pathway of CH_4 production, which becomes even more evident whenever we discuss the data from the light experiments below.

In addition to heating, natural sunlight has been shown to have an even more pronounced effect on CH_4 emissions from pectin [Keppler et al. 2006]. Moreover with the recent studies of McLeod et al. [2007] and Vigano et al. [2007] it has now become more evident that UV-light plays an important role in the production of CH_4 from plant matter and for more detailed information about this we refer readers to their work. Thus in a second set of experiments we decided to investigate the influence of UV radiation on isotopically labelled PGA samples. We used a 250W Osram 'Vitalux' lamp that produces UV-A (320-400 nm), UV-B (280-320 nm) and barely detectable traces of UV-C (<280 nm) [*Vigano et al.*, 2008]. For our experiments we used a total unweighted UV-B irradiance of ~3.7 W/m^2 which is similar to typical UV-B irradiances found in the tropics. Typical ambient (non-weighted) summer UV-B irradiances near the Earth surface range from 2 W/m^2 at mid latitudes to 4 W/m^2 in the tropics [Bernhard et al. 1997]. This present study aimed to demonstrate mechanisms and the molecular source for aerobic production of methane from pectin and the potential role of UV radiation. Realistic environmental UV exposure requires careful attention to spectral distribution and the spectral weighting of experimental lamps [Bjorn & Teramura 1993], so further studies are required to ensure accurate

simulation of ambient UV exposures and the extent and quantification of these processes in natural sunlight.

Similar to the heating experiments, both labelled PGA samples (6 and 22% deuterium label) showed an increase in the $\delta D(CH_4)$ values with increasing irradiation time (Figure 6.4a) reaching values of methane of up to ~ 230000‰ after 14h whilst the unlabelled methyl esterified PGA sample showed a significant decrease from -−101 to−189‰ over the same time period (Figure 6.4b). $\delta D(CH_4)$ values of the untreated PGA did not differ significantly from that of laboratory air.

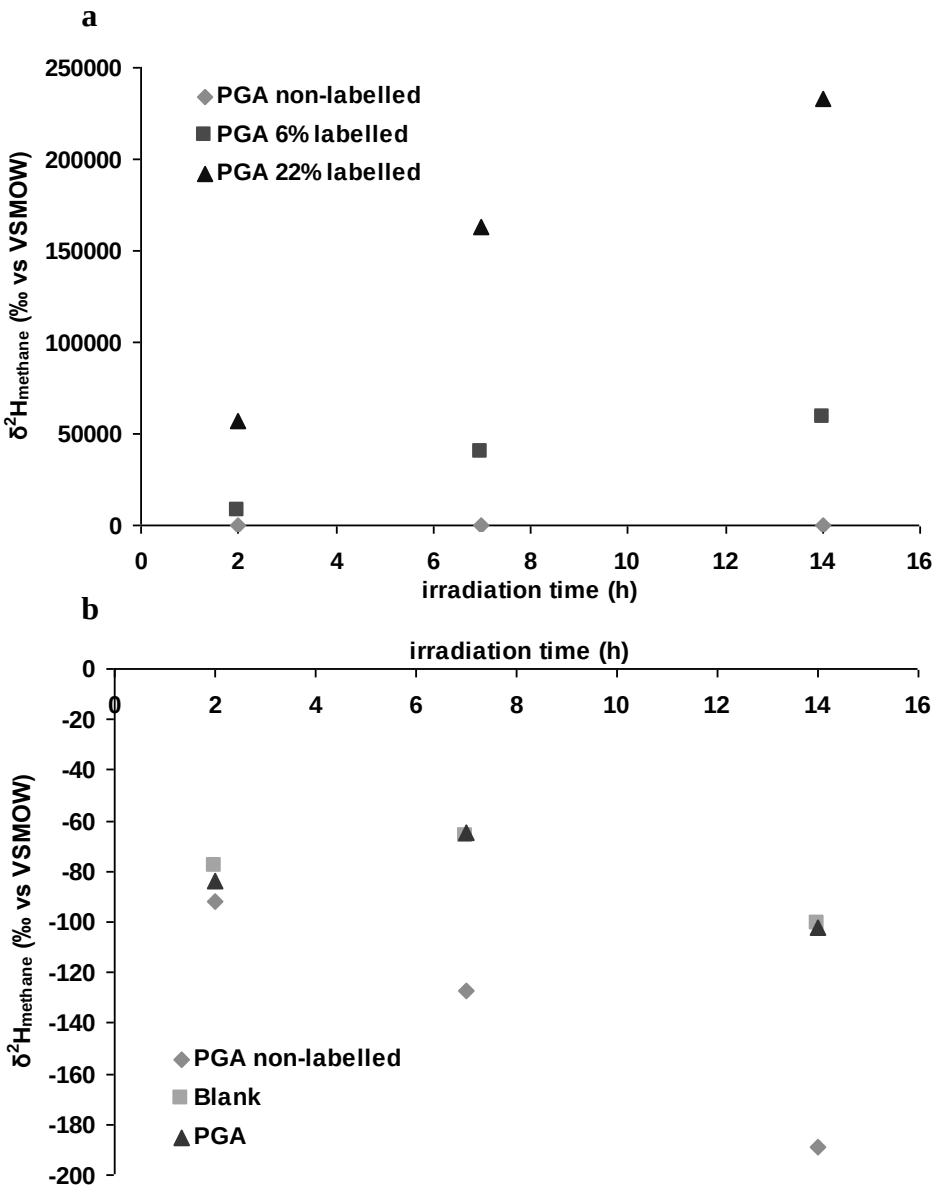

Figure 6.4 Irradiation experiments with PGA and methyl esterified PGAs. (a) $\delta^2 H_{methane}$ values of methyl esterified PGAs. (b) $\delta^2 H_{methane}$ values of blank, PGA and non labelled methyl esterified (c) Percentage of CH_4 formed from methoxyl groups of PGA.

Emission rates from untreated PGA were found to range from 2 to 3 ng g^{-1} dw h^{-1} whilst, in contrast, rates for all methylated PGAs were found to range between 9.2 and 36 ng g^{-1} dw h^{-1}, which is one to two orders of magnitude higher than the rates measured during heating experiments at 40°C. With light the percentage of CH_4 calculated to be directly derived from methoxyl groups ranged from 28 to 41% (Fig. 6.5), with on average one third found to originate from this source. This proportion differs significantly from that observed for the temperature experiments, possibly indicating different pathways involved in CH_4 formation in the two processes.

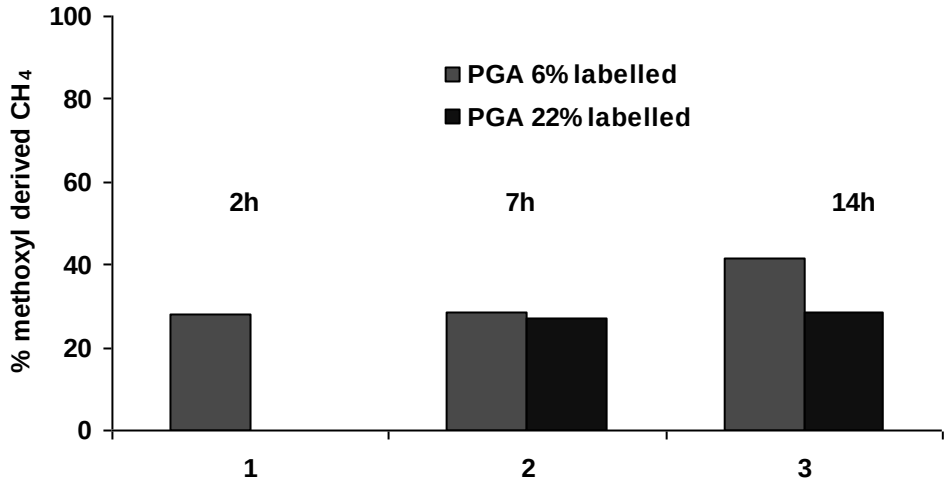

Figure 6.5 Percentage of CH_4 formed from methoxyl groups of PGA.

It should be mentioned that the CH_4 fraction not originating directly from the methyl moiety of the methoxyl pool cannot be fully explained by formation from non esterified PGA as those emission rates are almost an order of magnitude lower than the rates observed for methoxylated PGAs. Therefore it would appear that esterification of pectin is also important for the secondary CH_4 formation process also observed with pectin in that once the methyl group is removed it increases the possibility of CH_4 formation from other carbon atoms within the sugar structure. An example for a free radical process leading to formation of CH_4 during photochemical induced degradation of polysaccharides was recently presented by Sharpatyi [2007].

6.4 Conclusions

Our results provide unambiguous isotope evidence that methoxyl groups of pectin can act as a source of atmospheric CH_4 under aerobic conditions. They further suggest that other carbon moieties in pectin can also contribute to the observed CH_4 emissions particularly with photochemical treatment, possibly by a free radical mechanism similar to that recently suggested by Sharpatyi [2007].

As previously shown [Keppler et al. 2006] emissions of CH_4 from pectin are strongly dependent on temperature and exposure to light, in particular in the UV range. For more detailed studies on the light-effect we would refer readers to the studies of McLeod et al. [2007] and Vigano et al. [2008] in which the role of UV light on the formation of methane from dried and fresh detached leaves is described in considerable detail.

Chapter 7

Eddy covariance methane measurements at a Ponderosa pine plantation in California

In this study I was responsible for the logistic and for the set up of the equipment as well as for the data storage.

Long term methane flux measurements have been mostly performed with plant or soil enclosure techniques on specific components of an ecosystem. New fast response methane analyzers make it possible to use the eddy covariance (EC) technique instead. The EC technique is advantageous because it allows continuous flux measurements integrating over a larger and more representative area including the complete ecosystem, and allows fluxes to be observed as environmental conditions change naturally without disturbance. We deployed the closed-path Fast Methane Analyser (FMA) from Los Gatos Research Ltd and demonstrate its performance for EC measurements at a Ponderosa pine plantation at the Blodgett Forest site in central California. CH_4 concentrations measured at 10 Hz showed a relatively high noise level that was caused by a software related problem. Nevertheless, in the frequency range important for turbulent exchange, the cospectra of CH_4 compare very well with all other scalar cospectra confirming the quality of the FMA measurements are good for the EC technique. The low-pass filtering characteristics of our closed-path system and the use of the Webb-Pearman-Leuning (WPL) corrections for a combination of open and closed-path sensors are discussed using a large ensemble of cospectra. The diurnal variation of the methane concentration was up to 60 ppbv with an average of 1843 ppbv. Concentrations increased from morning to late afternoon as upslope flow from the valley below carried polluted air to the site, and then decreased through the night as downslope flow carried cleaner air from aloft. The fluxes were consistently directed downward with a well defined diurnal pattern, averaging -35 ± 40 ngm^{-2} s^{-1} during the daytime. The detection limit of the system was estimated at 22 ngm^{-2} s^{-1}. The average CH4 deposition during the daytime was higher than the average value for warm temperate forests in a recent global inventory and the results from a process-based model study.

Published in *Atmos. Chem. Phys.*, 9, 5201-5229, 2009, as co-author with C. J. P. P. Smeets[1], R. Holzinger[1], A. H. Goldstein[2], and T. Röckmann[1]

[1]Institute for Marine and Atmospheric Research Utrecht, Utrecht University, Princetonplein 5, 3584CC Utrecht, the Netherlands;

[2]University of California, Berkeley, Department of Environmental Science, Policy and Management, USA;

7.1 Introduction

We will briefly describe here the observations made from 11 to 19 August 2007, above a Ponderosa pine plantation owned by Sierra Pacific Industries, adjacent to the University of California at Berkeley's Blodgett Forest Research Station.

Long term methane flux measurements have been mostly performed with plant or soil enclosure techniques on specific components of an ecosystem. The fast response methane analyzers make it possible to use the eddy covariance (EC) technique instead. The EC technique is advantageous because it allows continuous flux measurements integrating over a larger and more representative area including the complete ecosystem, and allows fluxes to be observed as environmental conditions change naturally without disturbance. Development of closed-path Fast Methane Analyser (FMA) from Los Gatos Research Ltd (previously described), demonstrate its performance for EC measurements at a Ponderosa pine plantation at the Blodgett Forest site in central California. The diurnal variation of the methane concentration was up to 60 ppbv with an average of 1843 ppbv.

Concentrations increased from morning to late afternoon as upslope flow from the valley below carried polluted air to the site, and then decreased through the night as downslope flow carried cleaner air from aloft. The fluxes were consistently directed downward with a well defined diurnal pattern, averaging -35 ± 40 ngm^{-2} s^{-1} during the daytime. The detection limit of the system was estimated at 22 ngm^{-2} s^{-1}. The average CH4 deposition during the daytime was higher than the average value for warm temperate forests in a recent global inventory and the results from a process-based model study. For details regarding the evaluation of the EC data quality,and processing when applying Webb-Pearman-Leuning (WPL) corrections,[*Webb*, 1982]we refer to the published work of Smeets et al. (2009).

7.2 Description of the measurement site

The site is situated on the western slope of the Sierra Nevada mountains in California (38.90_ N, 120.63_W, and 1315m elevation), 75 km downwind (northeast) of Sacramento and receives anthropogenically impacted air masses rising from the valley below during the day. The site was planted with *Pinus ponderosa* L. in 1990, interspersed with a few individuals of Douglas fir, white

fir, California black oak, and incense cedar. Average canopy height in July 2007 was about 8 m, and the leaf area index was estimated as 3.2 m_2 m_{-2}. The understory was composed primarily of manzanita (*Arctostaphylos* spp.) and whitethorn (*Ceonothus cordulatus*) shrubs. A detailed description of the site is provided by [*Goldstein et al.*, 2000; *Misson et al.*, 2005].

The eddy covariance (EC) technique is ideally suited for continuous flux measurements integrating over a larger and more representative area including the complete ecosystem, allowing fluxes to be observed as environmental conditions change naturally without disturbance. Recently, methane analyzers have become available that have a fast enough response time to perform EC flux measurements of methane [e.g.Hendriks et al., 2008; Kroon et al., 2007; Wille et al., 2008]. We tested the DLT-100 Fast Methane Analyser (FMA) from Los Gatos Research (LGR) Ltd

incorporated for EC flux measurements over a Ponderosa pine plantation at the Blodgett Forest site on the western slope of the Sierra Nevada Mountains in California. In the near future we plan to test the recent hypothesis of higher methane emissions in the Amazon basin. The FMA is a closed path methane analyzer with a response rate up to 20 Hz and is comparatively easy to use, relatively inexpensive, and stable over longer periods [*Hendriks et al.*, 2008].

7.3 Experimental setup

The Eddy covariace measurements were carried out at the top of a 13.5m high scaffolding tower. The instrumentation consisted of a Campbell CSAT3 sonic anemometer, a Campbell FW3 Type E thermocouple, a LI-COR LI7500 open-path hygrometer, and a Fast Methane Analyzer (FMA, Los Gatos Research). Raw data was sampled at 10 Hz using a Campbell CR1000 datalogger and stored on a laptop. The FMA was operated in a closed-path EC set-up that carries the sampled air through a 20m long PVC tube with a 1 cm inner diameter. The tube inlet was shielded from rain by a funnel that was mounted 0.2m behind the sonic anemometer and close to the LI7500. Before the air enters the cavity it passes a Swagelok SS-4FW4 internal filter with a 2 μm pore size.

The pump is a high flow dry scroll pump XDS-35i from BOC Edwards with a maximum pumping capacity of 580 $lmin^{-1}$ that is placed behind the FMA. The FMA and dry scroll pump were placed in water resistant and ventilated aluminium boxes. The resistance within the system reduces the pumping speed and from the time lag between the sonic anemometer and the FMA signal we estimated it to be about 40 l min^{-1}. The EC measurements were installed 5.5m above a medium dense canopy at a height of about z=13.5m.

7.4 Results

In Fig.7.1 the mixing ratios of CH_4 and CO_2 are plotted together with the meteorological variables temperature, wind speed, relative humidity, net-radiation and wind direction. The timelines of CH_4 and CO_2 closely follow each other which suggests that both gases originate from the same source regions (Central valley/Sacramento region) and that their mixing ratios are mainly controlled by the diurnal flow patterns. The meteorological variables show a clear diurnal variation that illustrates the very regular upslope/downslope flow, described in detail by [*Dillon et al.*, 2002; *Lamanna and Goldstein*, 1999]. During summer this circulation is very persistent and present for 72% of the time [*Carroll and Dixon*, 2002].
During the daytime, upslope flow from the warm Central valley rises along the Western slope of the Sierra Nevada. After sunset a shallow stable boundary layer develops due to radiative cooling of the surface and a layer of cold air flows downslope. Along with this regular wind pattern, the Sacramento urban plume is transported up into the foothills of the Sierra Nevada during daytime. After sunset, the pollutants are flushed back towards Central Valley, being replaced by cleaner regional background air from aloft. Early in the morning, together with the onset of the

upslope flow as indicated by the first vertical solid line in Fig. 7.1 (at 07:30 h), the concentrations of CH_4 and CO_2 increase simultaneously untill the flow turns downslope again at sunset (second vertical solid line at 18:00 h). This diurnal cycle for CH_4 and CO_2 resembles the results from Lamanna and Goldstein [1999] for anthropogenically emitted hydrocarbons.

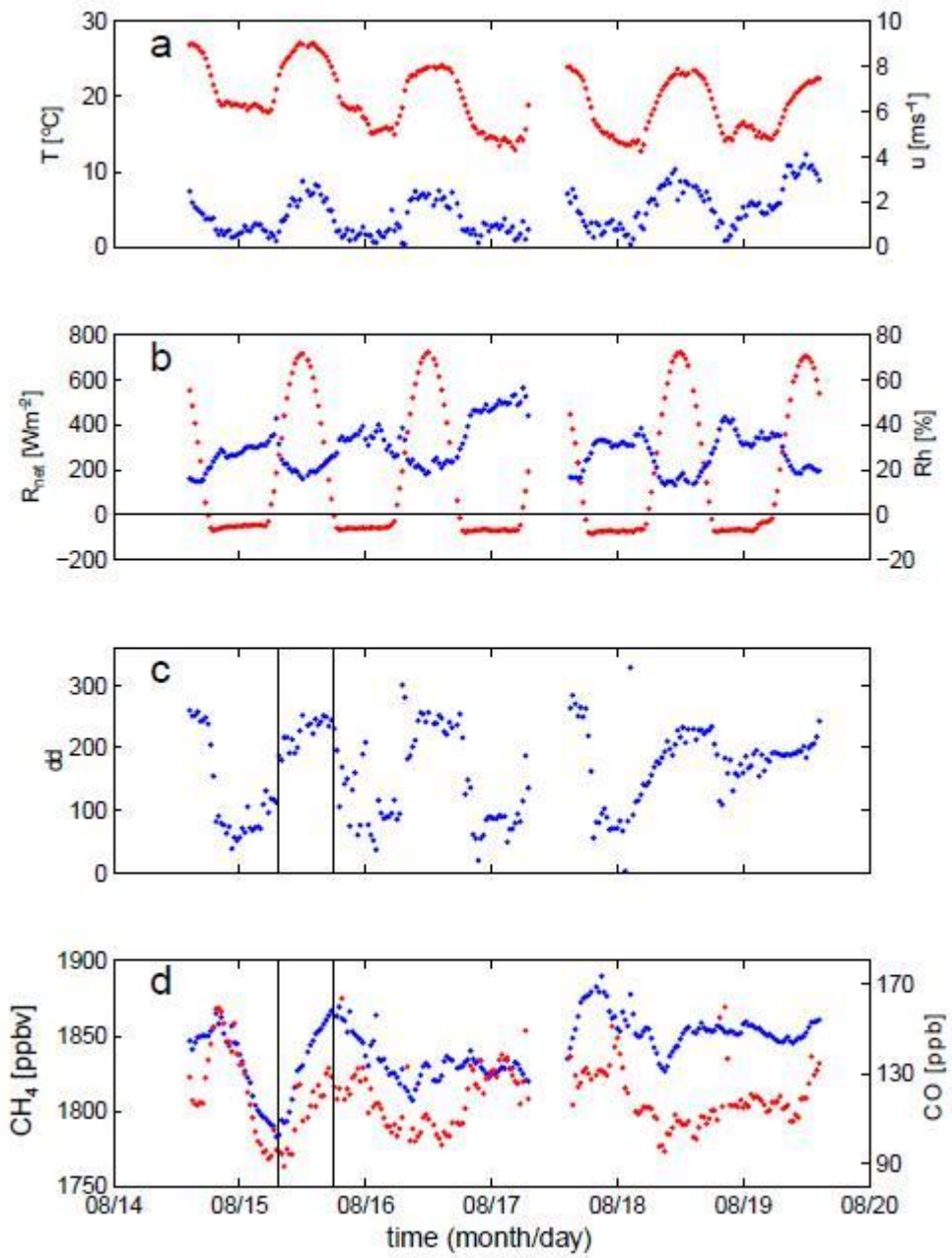

Figure 7.1 Time series of **(a)** temperature (*T* , red) and wind speed (*u*, blue), **(b)** net-radiation (*R*net, red) and relative humidity (RH, blue), **(c)** wind direction (*dd*), and **(d)** CH_4 (blue) and CO_2 (red) concentrations as a function of time. The vertical lines in plot (c) and (d) mark the start and reversal of the upslope flow.

The identical behaviour for CH_4 and CO_2 demonstrates that CH_4 originates from the anthropogenic sources around the Sacramento area. While CO_2 emissions mainly originate from combustion, the majority of CH_4 emissions in California comes from landfills (42%) and agricultural livestock (38%) [*Franco*, 2002]. The latter is heavily concentrated in the Central Valley which makes it probably the most important contributor.

The CH_4 concentrations vary around the California ambient air background value of about 1835 ppbv [*Rigby et al.*, 2008] with higher values occurring in the pollution plume from the Sacramento area (late afternoon) and lower ones for the regional background air originating from higher in the Sierra Nevada (just before sunset).

The time series of the various fluxes are plotted in Fig. 7.2. The sensible heat, latent heat and CO_2 fluxes all show a clear daily cycle in accord with the fair weather conditions. At night, all fluxes become negligible as the atmosphere becomes stable and turbulence ceases. The methane fluxes show the same diurnal pattern and are consistently directed downward during daytime. The night time CH_4 fluxes have noticeable more scatter than all other fluxes, which relates to the higher uncertainty of the CH_4 measurements.

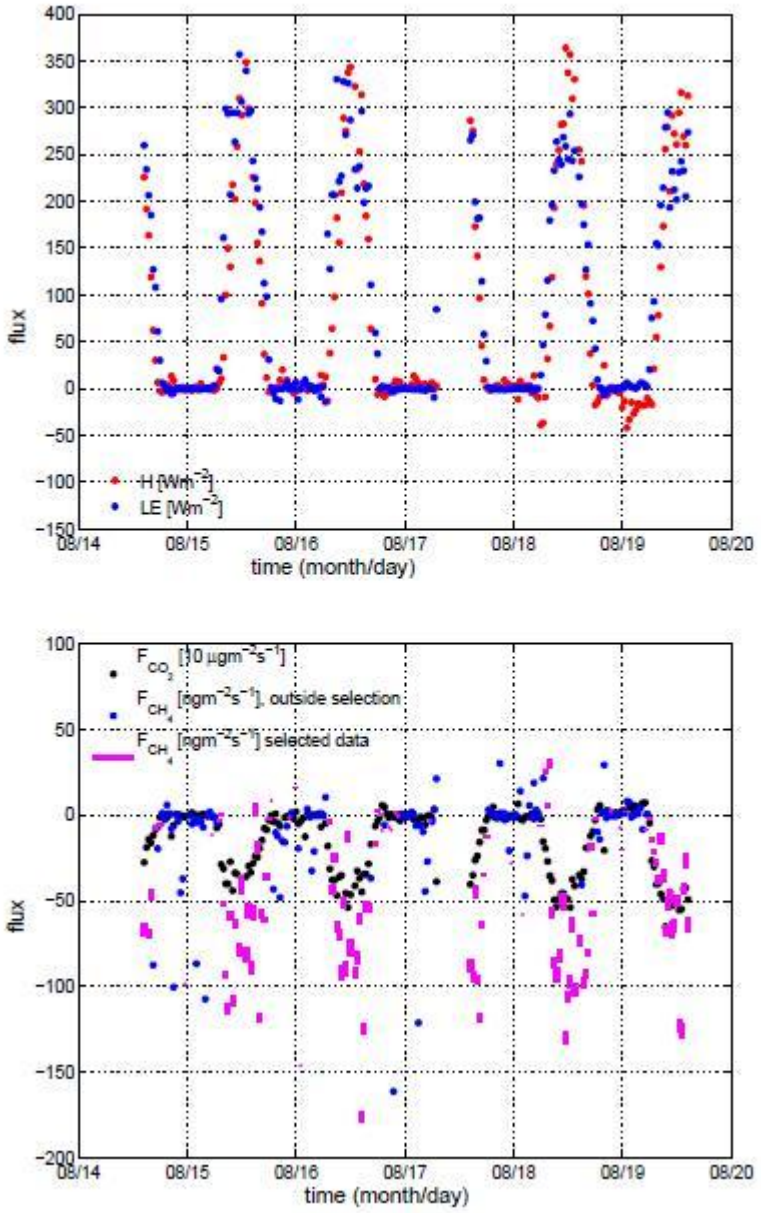

Figure 7.2 The time series of the various fluxes. For CH_4 fluxes (pink bars) we only plotted those runs for which a realistic phase shift was obtained from the maximization of covariances (a time lag between 2.2 and 3.0 s). The size of the pink bars illustrates the effect of a water vapor phase shift in the WPL corrections (i.e. with and without phase effect corresponds to the largest and smallest negative values of a bar, respectively). The CH_4 fluxes outside the selection are plotted as blue dots.

The daily maximum (downward) CH_4 flux varies around 100 ngm^{-2} s^{-1} (or 10 8.6mgm^{-2} day^{-1}) and the daily average is about 35 ngm^{-2} s^{-1} (3.0mgm^{-2} day^{-1}). These values were calculated accounting for water vapor phase effects in the WPL corrections assuming RH=35%. The CH_4 fluxes obtained during the Blodgett forest campaign are higher than those from observational and model estimates. A recent global inventory of field measurements conducted in temperate forests estimates an annual average uptake of 1.6 mgm^{-2} day^{-1} [*Dutaur and L.V*, 2007; *Ridgwell et al.*, 1999](used a process-based model to calculate the consumption of atmospheric CH_4

by soils, and their average grid cell value for the experimental region in the month of July is about −1 mgm^2 day^{-1}.Verchot et al. (2000) and Dutaur and Verchot (2007) suggest that soil texture is an important biochemical control of CH_4 oxidation in soils with coarse textured soils consuming CH_4 most efficient.

Given the very dry conditions at the Blodget forest site throughout summer, it is likely that during our measurements the CH_4 uptake by the soil was not limited by oxidation reactions in the soil but through its gas-phase transport capacity, i.e., how well the ground is drained [*Verchot et al.*, 2000]. In line with this, the diurnal variation of sub-surface temperatures and humidity were not found to correlate with the measured CH_4 fluxes. Since the soil at the Blodgett forest site is very porous (up to 65% by volume, Goldstein et al., 2000) we therefore expect a high gas diffusivity that is likely to support the observation of relatively high CH_4 fluxes.

Most results from other studies using EC systems to measure CH_4 fluxes were obtained under conditions providing much higher fluxes, e.g. an average of 480 ngm^{-2} s^{-1} over a peat meadow area [*Hendriks et al.*, 2007], 50 to 350 ngm^{-2} s^{-1} over Arctic tundra [*Wille et al.*, 2008], and an average of 680 ngm^{-2} s^{-1} over peat grassland [*Kroon et al.*, 2007]. We analyzed the detection limit for our CH_4 fluxes following the method described by Wienhold et al. [1995] and also used by Kroon et al. [2007].

The average probable detection limit for the ensemble of 87 runs is estimated at 22 ngm^{-2} s^{-1} with a standard deviation of 12 ngm^{-2} s^{-1}. The uncertainty of fluxes above the detection limit is on average 26%. As a comparison, the uncertainty for all other fluxes obtained with the same method is about 6%, a factor 4 lower. Note, as mentioned before, that the results for CH_4 are influenced by large instrumental noise resulting from outdated instrument software. Implementation of new software reduces the signal-to-noise ratio of the FMA a factor 5 and is expected to lower the detection limit.

7.5 Conclusions

The observations at the Blodget forest site show that the CH_4 concentrations vary diurnally with the upslope flow from the polluted valley below in the day, and the downslope flow of cleaner air from aloft during the night with an average value of about 1843 ppbv. The CH_4 fluxes were consistently directed downward and followed a clear diurnal pattern. Based on an ensemble of 87 30-min flux measurements the average during the daytime was 35±40 ngm^{-2} s^{-1} and the maximum values varied around 100 ngm^{-2} s^{-1}. These values are higher than recent estimates from a global inventory of field measurements in temperate forests [*Dutaur and L.V*, 2007] and a processbased model study [*Ridgwell et al.*, 1999]. The very dry conditions and porous soil texture at the Blodgett Forest site support a high gas diffusivity of the soil resulting in Current estimates of upward directed CH4 fluxes over tropical forest ecosystems by Braga do Carmo et al. [2006], Miller et al. [2007] and Sinha et al. [2007] give values of about 20 to 210, 280, and 80 ngm^{-2} s^{-1}, respectively.

There is no direct evidence of methane emissions from plants occurring during the warm and dry summer associated with elevated, although not measured UV irradiance.

The presence of the aerobic emission under UV has been also discussed by [*Bowling et al.*, 2009] in a recent study on a subalpine forest, where the strength of the soil sink does not allow the determination of the weak plant source. The role of the soil seems

to be of primary importance as already reported by several studies. Flooded terrain are known for being large sources[*Devol et al.*, 1988; *Watanabe et al.*, 2009] in the biosphere, and the role of the plants as in situ mediator for the transport of methane has been investigated as well [*Bazhin*, 2004; *Ding and Cai*, 2003; *Nouchi et al.*, 1990; *Ramachandran Purvaja*, 2004]. The plant source, probably due to the low emission rates cannot be well defined with eddy covariance field measurements covering a large area, but it should be measurable with enclosed techniques where, for example, part of branches can be sealed into special dynamic chamber [*Ortega and Helmig*, 2008; *Ortega et al.*, 2008]. The air can be sampled and analyzed for methane concentrations and isotope ratio with the techniques described in chapter 2.

Chapter 8

Main findings, final discussions and future perspectives

8.1 Outlook

The main work that is described in this dissertation concerns the aerobic methane production from plant matter. This is a follow up research based on the previous results of Keppler et al. [2006] in which they reported methane emissions from plants under aerobic conditions. Following studies showed contradictory findings as some research groups could not detect any methane production from ^{13}C labeled living plants [*Dueck et al.*, 2007]. Although the studies were performed with different measurement techniques, the topic of methane production under aerobic conditions has been heavily discussed and it is still the subject of an intense debate.

The review of the literature in chapter 1 leads to the conclusion that the discovery of aerobic methane production itself is now confirmed by several experimental studies, although with still large uncertainties. In particular, it is important to make a difference between methane emission from intact living plants and from plant litter. The previous values reported for living plants in Keppler et al. [2006] and the crude upscaling suggested a source strength up to 30% of the global budget. These high values have not been reproduced and other studies come up with emission rates that are 10 to 100 times lower than Keppler et al. [2006]. One reason could be that the measurement techniques are not adequate. The preferred method for biological studies is to use dynamic chambers in continuous flow mode, in order to avoid non-natural conditions from build-up of plant products of depletion of CO_2, for example. The use of static chambers [*Keppler et al.*, 2006; *Qaderi and Reid*, 2009] is good first approach to qualify the compounds in the air sampled but not to quantify them [*Ortega and Helmig*, 2008; *Ortega et al.*, 2008].

From the studies of Smeets et al. [2008] and Bowling et al. [2009], it was clear that even in forests subjected by relatively high UV levels during summer, the aerobic methane emission seems to be too smoothly distributed and cannot be detected with Eddy Covariance techniques.

With respect to these findings, the role of UV radiation leading the aerobic methane emissions from plant matter has been investigated, and additional research has been done in this direction to establish the isotope signature of the methane emitted and how water affects the deuterium content.

Concerning the first experiments, the experiments were always carried out in a dynamic setup in order to avoid potential artifacts and to better quantify the emission

rates of the methane produced from dry or fresh detached leaves, and from other parts of the plant like the bark. The subsequent isotope studies were performed in closed (static) reactors as the main task was to determine with more accuracy the isotope strength of any methane produced. In dynamic reactors the increase of methane concentrations is not substantial enough to be used for the determination of the isotopic fingerprints.

The entirety of the research performed is summarized below, with the main findings for each chapter printed in italics.

In the work presented in chapter 3 the main task of this dissertation was achieved, which was *the role of UV radiation and temperature in aerobic methane production*. A multitude of experiments has been developed in order to precisely characterize the strength of this new source and determine how it depends on the spectral distribution of the light source. We have been able to characterize emission rates from numerous leaves of different plant species and also from structural plant compounds. In this study a special setup utilizing cavity ring-down laser spectroscopy was adopted, where a continuous monitoring of the CH_4 concentrations at different flow rates was possible for the first time, allowing high precision measurements of emission rates as described in chapter 2.

The research was started by simply employing some dry leaves collected in the field and successively irradiating these with strong UVC penray lamps. The emission rates measured with common compressed air at 20% of oxygen were exceptionally high but comparable to the previous findings of Keppler et al. [2006]. Despite knowing that such wavelengths are not reaching the earth surface because of ozone absorption, we regarded them as an indication for the existence of the pure chemical-physical reaction. Knowing the wavelength spectrum of incoming solar radiation, it was worth to move forward and to investigate the difference between various UV wavelengths. Most of the incoming UV radiation that reaches the Earth surface is UVA radiation and only 1% is UVB radiation (see Appendix). From experiments carried out with different UV lamps on a sample of dry grass, it was demonstrated that *UVB is the most effective in inducing CH_4 emission, giving first qualitative information on the action spectrum of the reaction*.

The use of light in the visible spectrum, vital for the photosynthetic respiratory chain, did not reveal CH_4 production, suggesting that this mechanism is probably a degradation process rather than a biochemical one.

Following an identical procedure several dry and fresh detached leaves were analyzed, as well as structural compounds like pectin, cellulose and lignin, which denoted characteristic and different CH_4 production rates. Natural UV levels were also applied in order to estimate potentially emission rates which might occur in a natural environment. The emission rates from dry leaves under UV irradiation are higher than those measured in the experiments with dry leaves carried out by Keppler et al. However, compared to living plants, the rates are at least 10 times lower than the estimates of Keppler et al. [2006]. Since higher emission rates have also not been found in other studies with living plants, or other sources could have been involved or the experimental methods adopted with static chambers may have been affected by unidentified artifacts.

It was also clarified that the methane produced is not from desorption of gases present in the plant tissues as suggested by Kirshbaum et al. [2007]. In brief, the methane

production was of the same magnitude when the leaf sample was irradiated in compressed air flow or in methane free air. Furthermore, long term measurements over one month of continuous irradiation surprisingly showed a constant production of CH_4 indicating that the reservoir that can be released as methane from the plant matter is larger than can be explained by adsorption-desorption processes.
Further experiments displayed how fast the reaction can be, and in fact *the instantaneous CH_4 production rules out any biological activity*.
Another set of results was obtained by looking at the effects of the temperature on the methane release and on the effect of UV light with temperature changes. An important finding is that *without light the CH_4 production abruptly starts when the temperature exceeds 70°C*, proving that a certain energy barrier needs to be exceeded. Another interesting observation is that *under UV light the CH_4 emission seems to begin around 0°C*. For temperatures below 0°C, with UV light, and without light below 70°C, it was not possible to detect relevant emission rates with the cavity ring-down spectroscopy.
To improve the detection limit and to search for very small emission rates, we employed subsequently isotope techniques on pure ^{13}C labeled plant leaves of *Zea Mais.* Plants were simply incubated in a static glass reactor with common compressed air at 20°C, and then the $\delta^{13}C$-CH_4 of the air was monitored weekly with IRMS (Chapter 3). The changes in the $\delta^{13}C$-CH_4 revealed that even *without light and at ambient temperature the aerobic process driving the methane formation is still present*. The emission rates derived from the change of the isotopic composition of the CH_4, are small and so far the lowest reported in literature. The high sensitivity reachable with the Isotope ratio Mass Spectrometry techniques, allows the determination of very small emission rates.
All these experiments present clear evidence for the existence of aerobic methane production.

Chapter 4 present an analysis aimed at defining the stable isotope signature of the CH_4 emitted from the plant leaves when irradiated by UV light. Stable isotope signatures of methane are characteristic for different sources, with usually enriched values in ^{13}C and D for geological and biomass burning emissions and more depleted values for natural emission due to anaerobic production [*Quay et al.*, 1999]. The first values of $\delta^{13}C$ for the methane emission from plants were experimentally obtained by Keppler et al. [2006] and δD assumptions were made by Whiticar et al. [2007]; these assessed the isotopic signature for CH_4 from plants at ~-58‰ for $\delta^{13}C$ and ~-270‰ for δD. In our study we wanted to determine the isotopic composition of CH_4 from organic matter under the influence of UV light. This composition does not need to be identical to the composition measured by of Keppler et al., because also the values of emission rates differ substantially from the living plant emissions of Keppler et al. [2006] from where the first ^{13}C signatures derive, and for these emissions UV radiations could not have been the only cause of CH_4 production [*Vigano et al.*, 2008].
The most surprising finding is that the isotope signature of the CH_4 produced from the plant matter irradiated is strongly depleted in both ^{13}C and D, with values of ~60‰ and~-340‰ respectively.
The isotope signatures of ^{13}C are generally in agreement with the first findings of Keppler et al. [2006], but *the deuterium signatures are so far the most depleted in nature according to published data of Quay et al. [1999]. The reason for such high depletion is still unknown.* In addition to strong kinetic isotope effects which are involved, there are indications that during the formation of methane from methoxyl

groups or other chemical moieties, there is incorporation of hydrogen from a very depleted pool; this is better described in chapter 6.
The study is not only reporting the isotope signatures from several plant leaves but also carbon and deuterium isotopic analyses of methoxyl groups and bulk matter, in order to gain more information on the possible reaction pathway involved. *In fact the correlation between $\delta^{13}C$ of methoxyl groups and $\delta^{13}C$-CH_4, and the strong deuterium depletion in CH_4 relative to OCH_3, suggest that another substrate is involved in the CH_4 production.*
Notwithstanding the emission rates derived from these experiments are not representative for natural conditions, due to the use of high UV levels and static reactors, it is worth to mention that *the overall CH_4 production calculated was higher for C3 plants than for the C4-CAM plants*. Further investigation has been done looking at the relative discrimination of the heavy isotopes in methane relative to the bulk matter ($\Delta = \delta CH_4 - \delta_{plant}$). The deuterium data indicate that the difference in emission rates between C3 and C4-CAM plants is in qualitative agreement with the hypothesis that C3 plants emit relatively more from an additional depleted substrate more depleted in D.
The analyses reported reflect also the selective discrimination in deuterium and carbon for the plants with different metabolism (C3, C4 and CAM) which can be used as additional tool for classification strategies.

Chapter 5 presents an investigation of the role of water in determining the deuterium content of the methane emitted from plants. The question is: If water affects the isotope balance of the chemical plant compounds, can this information be retrieved from the methane produced?
The goal of the research was achieved by growing several plants with water of different deuterium content. A range of δD values was used which can be representative of that found in natural precipitation. It is known that the δD of precipitation changes from polar to equatorial latitudes due to evapotranspiration processes [*Araguas et al.*, 1996], and previous studies revealed that the δD of methane emitted from microbial sources is related to the δD of the water [*Schoell*, 1988; *Schoell et al.*, 1988; *Waldron et al.*, 1999]. In our study, leaves of each plant were collected and irradiated with UV light and the CH_4 analyzed for δD as described in chapter 4. In addition, deuterium analyses of bulk and methoxyl groups were also performed in order to obtain more information on how those substrates are involved in the CH_4 production.
The most intriguing result was that the δD of the methane emitted has a 1:1 correlation with the deuterium isotope content of the source water, while the isotope correlations of the source water with methoxyl groups and bulk analyses have a lower slope. One possible explanation is that methoxyl groups cannot be the only substrate of the CH_4 produced as already discussed, and there should be another depleted pool in order to explain the higher degree of deuterium depletion in CH_4. As suggestion for further research, the theory proposed by Sharpatyi [2006] concerning a radical mechanism for CH_4 emission from cellulose should be investigated with isotope labeling experiments.
The repercussions of this study should be tested on the field for a better understanding of the global isotope budget of methane, which is still surrounded with large uncertainties.

Chapters 6 and 7 are two complete different studies, one is a lab research and the other one is a field measurement. I wanted to briefly describe this two as I contributed directly in developing the CH_4 measurements (for the lab experiments) and in organizing and setting up the equipment as well as the data collecting (for the field measurement).

The chapter 6 is regarding the deuterium labeling experiments on methoxyl groups (-OCH_3), where it is shown that these moieties are precursors of the aerobic methane and that they contribute for about 50% to the methane released.

Heating and UV experiments were carried out on special labeled compounds with molecular structures similar to the one of the pectin but with deuterated methoxyl groups (-OCD_3).

The change of the deuterium isotopic values obtained for the methane emitted was a robust confirmation that indeed such chemical groups are involved in the methane formation although they are not the only substrate.

Potential other candidates can be for example cellulose or lignin, also present in the cell walls like pectin. A potential radical mechanism for methane formation has been proposed by Sharpatiy et al. [2007], but an experimental investigation is necessary.

The chapter 7 is dealing with field measurements based on the Eddy Covariance technique for the determination of CH_4 fluxes. The study was conducted in Blodgett Forest, an afforested area owned by the University of Berkley in California. The site is roughly 100km east of Sacramento, Sierra Nevada, Ca, U.S.). The *Ponderosa pine* is the main plant species present in that area and this was the first methane flux measurement carried out in that region. The Eddy Covariance methods has been utilized for several years to study CO_2 fluxes in different ecosystem, and the same setup was adopted for CH_4 in principle (see section 7.2). The measurements were carried out during the second and third week of august 2007, characterized by exceptionally dry conditions, warm temperature and clear sky conditions with consequently relatively high UV levels.

The role of temperature and UV for the aerobic methane formation could have been of significance in that area, but the final fluxes values did not demonstrate this.

In fact, for the whole measurement time, the fluxes of CH_4 were directed towards the surface, due to the strong soil sink effect under dry conditions.

The aerobic emission from plants derived from the UV irradiation and high temperatures should be therefore of much smaller magnitude than the soil sink.

It is important to notice that a step is missing here: from lab to field measurements we are jumping from a really small scale directly to an open natural environment. As mentioned at the end of this chapter, it should be worthwhile to carry out an in situ measurement focused on a single plant to better identify the aerobic methane release.

8.2 Consequences

According to the latest published data [*IPCC*, 2007], the major methane sources from the biosphere are wetlands, rice paddies and marshes located in tropical, sub-tropical and boreal ecosystems.

It is well known that the methane derived from those sources is mainly produced anaerobicaly from microbial degradation of the organic matter. A minor but still not quantified contributor originates from aerobic production, which can be considered as a degradation process driven by UV radiation and temperature. Those factors can act simultaneously, but it has been observed that such emissions occur even at room

temperature without light, indicating that this "aging" process is always present at least if the temperatures are above 0ºC [*Vigano et al.*, 2008].
Several old and new studies have shown how plants can modulate methane fluxes in different ecosystems [*Bazhin*, 2004; *Nisbet et al.*, 2008; *Zeikus*, 1974] and how emission rates depend on evapotranspiration processes due to the fact that the plant can facilitate the transport of methane from the rhizosphere up to the atmosphere via xylem flow [*Nouchi et al.*, 1990].
In the recent years studies confirmed the presence of methanotrophic bacteria in the plant tissues [*Doronina et al.*, 2004] and aerobic methylotrophic bacteria in association with plants have been discovered, and experimental results confirmed their key role in providing peculiar substances like hormones and vitamins for optimal growth [*Ivanova et al.*, 2006; *Ivanova et al.*, 2007].
It is still unknown how and if these bacteria communities interact with the methane released from the tissues due to evapotranspiration processes or via the UV-temperature degradation effect. It is certain from the results presented in this thesis that water is affecting the hydrogen isotope balance in the plant and consequently also the δD of the methane emitted [*Vigano et al.*, 2009]. Whether this depends on bacterial metabolism or not is beyond the scope of this study, but more biological and biochemical examinations should be done to better apprehend the hydrogen isotope fractionation.
Precipitation around the globe is well monitored in the last years due to an established network which also routinely includes stable isotope analyses on oxygen and hydrogen [*Araguas et al.*, 1996; *IAEA/WMO*]. The δD in precipitation denotes variations ranging from enriched values close to 10‰ at tropical latitudes toward a depletion of ~-200‰ at the poles, with almost a symmetrical trend on both hemispheres. The δD of methane has a typical interhemispheric gradient [*Quay et al.*, 1999], depending on magnitude and location of sources and sinks.
Two third of the emerged Earth surface is located on the northern hemisphere where also the majority of the bacterial sources and sinks are located. Concerning bacterial sources there is indeed an important contribution from boreal ecosystems like Taiga and Tundra and from wetlands and rice paddies at subtropical-tropical latitudes.
Experimental and field studies on isotope fractionation have been done and confirm that the isotopic composition of water influences the isotopic composition in methanogenesis and that almost 50 % of variations in hydrogen in the methane formation can be explained by the δD in the precipitation [*Waldron et al.*, 1999]. The isotopic hydrogen influence of precipitation has been found in other plant compounds [*Keppler et al.*, 2007; *Keppler and Hamilton*, 2008; *Weiguo Liu*, 2008]. The methane generation under UV radiation or temperature can be derived from different substrates with diverse hydrogen discriminations with respect to water.
Water and methane seem to have a peculiar interconnection not only here regarding their hydrogen stable isotopic composition, but it is also very well known that water can affect the emission rates of this greenhouse gas in different ecosystem [*Crutzen*, 1991; *Le Mer and Roger*, 2001]. Passing from dry-desert environments to wetlands characterized by flooded terrains, we have completely different properties: sinks in dry locations [*Bowling et al.*, 2009; *Smeets et al.*, 2009; *Striegl and McConnaughey*, 1992] and sources in wetland locations, respectively [*Nouchi et al.*, 1990; *Walter et al.*, 2006]. In addition we have to consider also the role of temperature modulating these effects previously described, and their magnitude depend on seasons and on local meteorology.

At this point the evidence of the aerobic methane production [*Vigano et al.*, 2008] which has a peculiar isotopic fingerprint [*Vigano et al.*, 2009a], coupled with the isotopic dependence on precipitation [*Vigano et al.*, 2009b], can be a meaningful tool for quantifying the role of the biosphere in the global methane budget.

Further research should be done at least to clarify the following questions:

1. Are living plants emitting significant amounts of methane?
2. What are the precursors of aerobic methane besides methoxyl groups?
3. If the process is strictly non microbial, is it present even under anaerobic conditions?
4. How can this new source be quantified better?
5. Is this process present on other planets?

The first question is still an open debate between different research groups, which are reporting values that are not in agreement. To resolve this issue, it is deemed necessary to convene a consortium of scientists from both "sides", as this has potentially a big impact in climate change.
The second question has been answered partially in chapter 4, 5 and 6, where is clear that roughly 50% of the CH_4 produced is coming from $-OCH_3$. The third question needs to be investigated in parallel with the first one by applying dedicated lab experiments. For example CH_4 formation from cellulose and from sterile material under anoxic environments should be studied.
The fourth question is the most demanding since an accurate global quantification should not rely on work of only a single research group but it should involve a wider group of experts, with different methods. For example, as mentioned in chapter 2, when going from lab experiments to field measurements we are probably missing a step, i.e. the detailed experiment in the field, under natural conditions.
The last question is intriguing considering the fact that there have been already studies on organic molecules irradiated with high energy UV radiation, and results already showed that methane is one of the primary products as mentioned in chapter 4. Can such processes partially explain e.g. the presence of methane in Mars? Is it of interest to notice that the highest concentrations on Mars are found in equatorial latitudes where the UV irradiance is high, but also the CH_4 radical destruction, so there must be a source of significant magnitude in order to explain the observed levels.
.

Appendix

The UV radiation

Ultraviolet (UV) light is electromagnetic radiation with a wavelength shorter than that of visible light, but longer than soft X-rays. It is so named because the spectrum consists of electromagnetic waves with frequencies higher than those that humans identify as the color violet (purple). The electromagnetic spectrum of ultraviolet light can be subdivided in a number of ways. The draft ISO standard on determining solar irradiances (ISO-DIS-21348) describes the following ranges:

Name	**Abbreviation**	**Wavelength**
Ultraviolet A	UVA	400 nm- 315 nm
Near	NUV	400 nm – 300 nm
Ultraviolet B	UVB	315 nm – 280 nm
Middle	MUV	300 nm – 200 nm
Ultraviolet C	UVC	280 nm – 100 nm
Far	FUV	200 nm – 122 nm
Vacuum	VUV	200 nm – 10 nm
Extreme	EUV	121 nm – 10 nm

Although in medicine the UVA-UVB are discriminated at 320 nm, but this is because it refers to the action spectrum of DNA damage.
The Sun emits ultraviolet radiation in the UVA, UVB, and UVC bands, but because of absorption in the atmosphere's ozone layer, 98.7% of the ultraviolet radiation that reaches the Earth's surface is UVA. Some of the UVB and UVC radiation is responsible for the generation of the ozone layer.
Ordinary glass is partially transparent to UVA but is opaque to shorter wavelengths while Silica or quartz glass, depending on quality, can be transparent even to vacuum UV wavelengths. Ordinary window glass passes about 90% of the light above 350 nm, but blocks over 90% of the light below 300 nm.

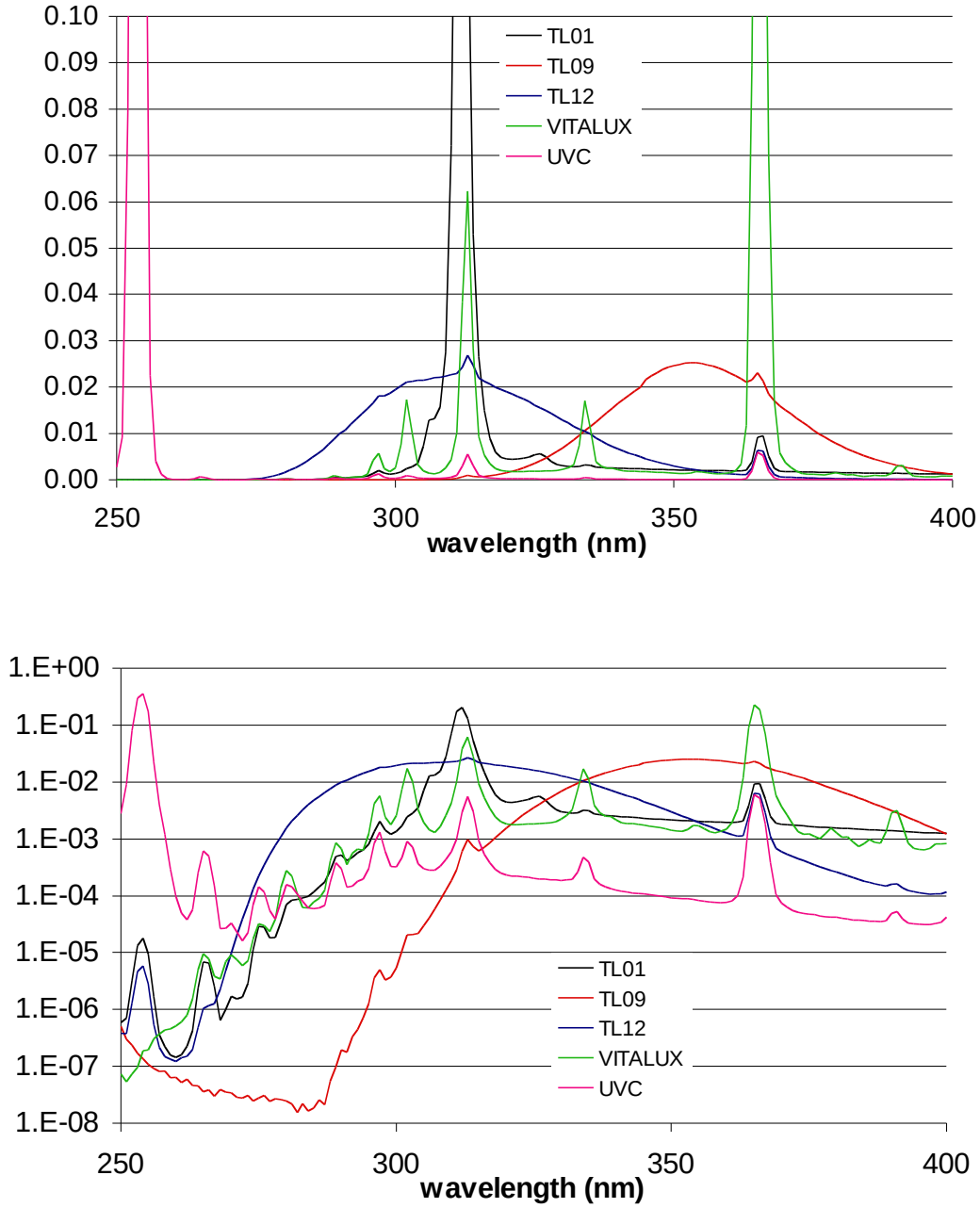

Figure 1 UV spectra of the light sources employed in our study, obtained with a calibrated standard UV-visible spectroradiometer (model 752, Optronic Laboratories Inc, USA). Top, linear scale, bottom, logarithmic scale. The spectra are normalized to yield the same total (250 – 400 nm) UV emission.

Table 1. Dome Concordia firn air samples: isotope values and concentrations [*Braunlich et al.*, 2001].

	MPI-C									LGGE	
Sample	depth			$\delta D_{V\text{-}SMOW}$	$\delta^{13}C_{V\text{-}PDB}$	AES-014		NOAA 2			$\delta^{13}C_{V\text{-}PDB}$
	[m]		[m]	[‰]	[‰]	ppb	±	ppb	±	[m]	[‰]
Dome-6	0	SM 77	0,1	-71,3	-46,99	1718,4	0,6	1694,8	1,2	0,3	-47,09
	6									5,9	-46,71
Dome-1	10	SM 74	10,3	-72,8	-46,90	1719,7	0,1	1695,7	1,2	10,3	-46,89
	15									15,4	-47,06
Dome-2	20	SM 80	20,2	-73,4	-47,13	1712,9	0,2	1689,1	1,5	20,0	-47,13
Dome-3	30	SM 79	29,8	-74,7	-47,24	1701,3	0,1	1677,3	1,1	30,0	-47,24
Dome-4	40	SM 75	40,1	-74,3	-47,33	1689,3	0,1	1665,2	1,1	40,3	-47,33
Dome-5	50	SM 76	50,0		-47,58	1684,1	0,1	1660,4	1,5	50,0	-47,38
Dome-7	60	SM 78	60,0	-76,3	-47,59	1667,6	0,0	1644,4	1,1	60,2	-47,54
Dome-8	70	SM 73	69,9	-75,4	-47,75	1655,5	0,1	1632,4	1,5	69,9	-47,84
Dome-9	80	SM 71	79,7	-77,9	-48,02	1642,0	0,4	1618,9	1,3	79,7	-47,96
	85									84,9	-48,09
Dome-10	90	SM 72	89,6	-78,8	-48,24	1622,6	0,1	1599,9	1,2	89,6	-48,33
Dome-11	95	SMG 63	94,4	-79,2	-48,72	1603,7	0,3	1581,5	1,4	94,6	-48,79
Dome-14	96	SMG 57	95,8	-79,9	-49,24	1560,3	0,1	1538,4	1,2	96,9	-50,26
Dome-12	96,8	SMG 65	96,5	-79,9	-49,83	1485,1	0,1	1464,3	1,2	96,7	-50,32
Dome-13	97,3	SMG 22	97,1	-81,9	-49,99	1476,0	0,1	1455,1	1,4	97,3	-50,34
	99									99,0	-50,49

Table 2. List of selected CH_4 production experiments carried out with UV radiation.

Plant leaves common name (species)	Temp. (ºC)	Lamp	UVA (W/m^2)	UVB (W/m^2)	Total UV (W/m^2)	Emission rate (ng CH_4 g^{-1}dw h^{-1})	Notes
Perennial ryegrass (Lolium perenne)	30	Vitalux	37	12	49	40	fresh
	25	Vitalux	21	9	30	50	dry
	n.m.	Vitalux	120	17	137	200	dry milled
	20	UVB nb TL01	1	29	30	90	dry
	25	UVB nb TL01	2	7	8	25	fresh
	30	NaHPS	n.d.	n.d.	n.d.	0	fresh
	20	UVB bb TL12	11	19	30	100	dry
	25	UVB bb TL12	13	25	38	60	fresh
	20	UVA TL09	28	0	29	15	dry
	25	UVA TL09	50	1	50	15	fresh
	n.m.	UVB bb TL12	1	2	3	5	fresh
	n.m.	UVB bb TL12	2	3	5	12	fresh
	n.m.	UVB bb TL12	2	4	6	14	fresh
	n.m.	UVB bb TL12	3	5	8	17	fresh
	n.m.	UVB bb TL12	1	2	3	4	dry
	n.m.	UVB bb TL12	2	3	5	9	dry
	n.m.	UVB bb TL12	2	4	6	10	dry
	n.m.	UVB bb TL12	3	5	8	13	dry
	35	UVC	n.m.	n.m.	n.m.	1517	dry
Sweet vernal grass (Anthoxanthum odoratum L.)	30	Vitalux	37	12	49	200	fresh
Switchgrass (Panicum virgatum)	30	Vitalux	37	12	49	100	fresh
Maize (Zea mays)	30	Vitalux	37	12	49	26	dry
	30	Vitalux	37	12	49	50	fresh
Banana (Musa acuminata)	25	Vitalux	21	6	27	140	dry
	25	Vitalux	21	6	27	48	fresh
	30	NaHPS	n.d.	n.d.	n.d.	0	fresh
	35	UVC	n.m.	n.m.	n.m.	1012	dry
Hinoki cypress (Chamaecyparis obtusa)	35	UVC				1423	dry
Guzmania (Guzmania lingulata)	25	UVB bb TL12	14	24	38	67	fresh
	n.m.	UVC	n.m.	n.m.	n.m.	4300	fresh
Spanish moss (Tilandsia usneoides)	20	UVB bb TL12	14	24	38	40	fresh
	25	UVA TL09	66	1	67	45	dry
	30	NaHPS	n.d.	n.d.	n.d.	0	fresh
	n.m.	UVA TL09	62	1	63	30	dry

Plant leaves common name (species)	Temp. (ºC)	Lamp	UVA (W/m^2)	UVB (W/m^2)	Total UV (W/m^2)	Emission rate (ng CH_4 $g^{-1}dw$ h^{-1})	Notes
	n.m.	UVC	n.m.		n.m.	250	dry
Sunflower (Helianthus annuus)	25	UVB bb TL12	14	24	38	12	fresh
Cannabis (Cannabis sativa)	25	UVB bb TL12	14	24	38	40	fresh
Ponderosa pine (Pinus ponderosa)	25	UVB bb TL12	14	24	38	55	fresh
Yaw (Taxus cuspidata)	25	Vitalux	21	6	27	44	dry
Fig (Ficus benjamini)	25	UVB bb TL12	14	24	38	125	dry
	25	UVB bb TL12	14	24	38	80	fresh
	40	UVB bb TL12	14	24	38	120	fresh
	n.m.	UVC	n.m.	n.m.	n.m.	998	dry
	30	NaHPS	n.d.	n.d.	n.d.	0	fresh
Nettle (Urtica dioica)	25	UVB bb TL12	14	24	38	67	fresh
Bamboo (Phyllostachys aurea)	30	UVB bb TL12	14	24	38	56	dry
	30	UVB bb TL12	14	24	38	134	fresh
Rhododendron (Rhododendron maximum)	25	Vitalux	21	6	27	16	dry
Different Plant material							
Cotton (Gossypium hirsutum)	25	UVB bb TL12	14	24	38	22	flower
	25	Vitalux	21	6	27	393	flower
Ponderosa Pine (Pinus ponderosa)	25	UVB bb TL12	14	24	38	10	bark
	25	Vitalux	21	6	27	50	bark
Sequoia (Sequoia sempervirens)	25	UVB bb TL12	14	24	38	7	bark
Robinia (Robinia pseudoacacia)	25	UVB bb TL12	14	24	38	9	bark
moss (Hylocomium splendens)	30	UVB bb TL12	14	24	38	75	dry leaves
	40	UVB bb TL12	14	24	38	150	dry leaves
Structural Plant Compounds							
Cellulose	n.m.	Vitalux	120	17	137	8	dry
	35	UVB bb TL12	14	24	38	32	dry
Citrus Pectin 90% esterified	30	UVB bb TL12	14	24	38	60	dry

Plant leaves common name (species)	Temp. (ºC)	Lamp	UVA (W/m^2)	UVB (W/m^2)	Total UV (W/m^2)	Emission rate (ng CH_4 g^{-1}dw h^{-1})	Notes
Apple Pectin							
	25	UVB bb TL12	14	24	38	20	dry
	n.m.	UVB bb TL12	1	2	3	4	dry
	n.m.	UVB bb TL12	2	3	5	5	dry
	n.m.	UVB bb TL12	2	4	6	6	dry
	n.m.	UVB bb TL12	3	5	8	9	dry
	n.m.	UVC	n.m.	n.m.	n.m.	190	dry
	n.m.	Vitalux	120	17	137	85	dry
	30	NaHPS	n.d.	n.d.	n.d.	0	dry
Lignin	25	UVB bb TL12	14	24	38	16	dry
	n.m.	UVB bb TL12	1	2	3	0.5	dry
	n.m.	UVB bb TL12	2	3	5	0.7	dry
	n.m.	UVB bb TL12	2	4	6	2	dry
	n.m.	UVB bb TL12	3	5	8	3	dry
	n.m.	Vitalux	120	17	137	32	dry
Palmitic acid	30	UVB bb TL12	14	24	38	0	dry
	30	Vitalux	39	12	51	0	dry
	n.m.	UVC	n.m.	n.m.	n.m.	15	dry

n.m.: not measured

n.d.: not determined

Table 3. List of materials analyzed with relative isotopic analysis (‰) and emission rates (ng/gDWh)

Plants-Compounds		$\delta^{13}C$-CH_4	bulk $\delta^{13}C$	$\delta^{13}C$-OCH_3	Pectin-$\delta^{13}C$-OCH_3	δD-CH_4	bulk δD	δD-OCH_3	ER
Lignin	commercial	-53. 30	-23.32	-16.76	n.m.	-201.7	-150.6	-306.5	n.d.
Pectin	commercial	-55.69	-26.99	n.m.	n.m.	-393.0	-29.3	n.m.	n.d.
Cellulose	commercial	-81.14	-25.69	n.m.	n.m.	-428.9	-67.4	n.m.	n.d.
Perennial ryegrass (Lolium perenne)	C3	-64.50	-27.92	-49.20	-56.22	-418.3	-99.7	-241.9	504.5
Sweet vernal grass (Anthoxanthum odoratum L.)	C3	-67.10	-29.49	-47.86	-69.78	-410.7	-79.3	-242.5	497.6
Madagascar dragon tree (Dracaena marginata)	C3	-56.38	n.m.	n.m.	n.m.	n.m.	n.m.	n.m.	573.8
Oil tree (Pentaclethra macroloba)	C3	-73.50	-31.36	-64.15	-75.17	-414.4	-80.5	-236.7	450.5
Weeping fig (Ficus benjamina)	C3	-69.74	-29.69	-50.39	-63.05	-356.7	-72.2	-170.1	586.3
(Crinum lily)	C3	-67.03	-28.39	-52.92	-54.13	n.m.	-59.9	-179.1	128.8
Planes (Platanus orientalis L.)	C3	-65.33	n.m.	-49.22	-55.50	n.m.	-108.2	-240.4	314.0
Maple (Acer pseudoplatanus)	C3	-67.57	n.m.	-62.95	-66.23	-343.4	-97.7	-218.2	677.2
Rosmary (Rosmarinus officinalis)	C3	-64.65	n.m.	n.m.	n.m.	n.m.	n.m.	n.m.	60.8
Ash (Fraxinus xanthoxyloides)	C3	-67.05	n.m.	-73.09	-77.10	-356.2	-102.8	-216.4	222.6
Salvia (Salvia argentea)	C3	-62.72	n.m.	n.m.	n.m.	n.m.	n.m.	n.m.	225.1
Ginger (Costus scaber)	C3	-64.90	n.m.	n.m.	n.m.	-360.8	n.m.	n.m.	222.2
Barbados nut (Jatropha curcas)	C3	-72.50	n.m.	n.m.	n.m.	n.m.	n.m.	n.m.	38.9
Schefflera actinophylla (Octopus tree)	C3	-72.15	n.m.	n.m.	n.m.	-343.1	n.m.	n.m.	329.0
Palma imperial (Ceratozamia mexicana)	C3	-68.09	-29.24	-40.75	-52.47	n.m.	-56.5	-239.3	381.7
Bananas (Musa acuminata)	C3	-60.52	-29.53	-52.38	-50.11	-403.7	-66.3	-220.6	292.9
Bamboo (Phyllostachys aurea)	C3	-60.54	-32.40	-43.12	-54.96	n.m.	-98.3	-190.9	299.8
Scarlet star (Guzmania lingulata)	CAM	-61.70	n.m.	n.m.	n.m.	n.m.	n.m.	n.m.	257.2
Snake plant (Sanseviera trifasciata)	CAM	-50.59	-15.94	-41.56	-45.89	-283.6	-37.4	-96.4	192.1
Shirley temple airplant (Tilandsia xerographica)	CAM	-52.50	-17.10	-28.22	-33.03	-256.6	-31.5	-163.1	338.9
Spanish moss (Tilandsia usneoides)	CAM	-55.58	n.m.	-48.69	-47.95	-267.0	-59.1	-209.9	104.3
Switchgrass (Panicum virgatum)	C4	-55.90	-12.90	-28.14	-36.56	-260.1	-77.3	-190.9	40.9
Sorghum a (Sorgum bicolor)	C4	-48.43	n.m.	-24.90	-47.95	-274.3	-76.1	-220.6	133.1
Orzaga (atriplex halimus)	C4	-47.55	n.m.	-52.79	-51.52	-346.5	-90.4	-216.0	158.7
Red amarant (Amaranthus cruentus)	C4	-59.92	n.m.	-56.37	-57.28	-318.9	-77.1	-187.1	117.7
Sorghum b (Sorgum drummondii)	C4	-47.55	-13.60	-30.84	-31.33	n.m.	-66.7	-194.3	250.5
Lemon grass (Cymbopogon flexuosus)	C4	-52.30	-13.30	-22.72	-30.28	-325.2	-78.3	-205.3	179.3
Maize (Zea mais)	C4	-42.37	-11.78	-19.23	-26.21	-279.1	-84.3	-214.2	285.2
Cotton flower (Gossipium hirsutum)*	C3	-69.90	n.m.	n.m.	n.m.	-653.3	-25.4	n.m.	n.d.

(n.m.: not measured; n.d.: not determined)

*Cotton flowers from Tadzhikistan

Standard deviation for δD-CH_4 and $\delta^{13}C$-CH_4 signatures are: 5‰ and 0.5‰ respectively.

Standard deviation for Bulk $\delta^{13}C$ analyses is ~ 0.5‰, while for bulk δD is ~5‰.

Standard deviation for Methoxyl-groups analyses is ~0.5‰.

Emission rates are derived from the peak area of the Isotope Ratio Mass Spectrometer by using ISODAT® software; standard deviation is ~20ng/gDh

Table 4. Median values for δ values and emission rates of C3 and C4/CAM plants

	C3	C4-CAM
$\delta^{13}C\text{-}CH_4$ (‰)	-67.0 (±4.5)	-52.3 (±5.5)
$\delta^{13}C_{bulk}$ (‰)	-29.5 (±1.5)	-13.5 (±2.0)
$\delta^{13}C\text{-}OCH_3$ (‰)	-50.4 (±9.6)	-29.5 (±13.4)
$\delta^{13}C\text{-}OCH_{3pectin}$ (‰)	-56.2 (±9.4)	-36.5 (±11.0)
$\delta D\text{-}CH_4$ (‰)	-360 (±32)	-279(±32)
δD_{bulk} (‰)	-80 (±18)	-77 (±19)
$\delta D\text{-}OCH_3$ (‰)	-220 (±26)	-200 (±37)
ER (ng/gDWh)*	301 (±187)	180 (±88)

* Emission rates in nano-gram per gram of dry weight per hour. Standard deviations given in brackets.

Table 5. Average values for δ values of C4 and CAM plants

	C4	CAM
$\delta^{13}C\text{-}CH_4$ (‰)	-50.7 (±5.6)	-55.1 (±4.8)
$\delta^{13}C_{bulk}$ (‰)	-12.9 (±0.8)	-16.5 (±0.8)
$\delta^{13}C\text{-}OCH_3$ (‰)	-33.6 (±14.8)	-39.5 (±10.4)
$\delta^{13}C\text{-}OCH_{3pectin}$ (‰)	-40.1 (±12.1)	-40.5 (±10.5)
$\delta D\text{-}CH_4$ (‰)	-300 (±34)	-270(±13)
δD_{bulk} (‰)	-78 (±7)	-42 (±14)
$\delta D\text{-}OCH_3$ (‰)	-204 (±13)	-156 (±57)

Standard deviations given in brackets.

Table 6. Carbon and deuterium Δ isotope discrimination

Δ Isotope discrimination (‰) (δa - δb)*	C3	C4-CAM
Δ_{13C}(CH4 - bulk)	-37.5 (±3.0)	-38.8 (±3.7)
Δ_{13C} (CH4 - OCH_3)	-16.6 (±7.1)	-22.7 (±9.4)
Δ_{13C} (CH4 - $OCH_{3pectin}$)	-10.8 (±6.9)	-15.7 (±8.3)
Δ_{13C} (bulk - OCH_3)	20.8 (±5.5)	21.2 (±7.7)
Δ_{13C} (bulk - $OCH_{3pectin}$)	26.7 (±5.4)	23.1 (±6.5)
Δ_{13C} (OCH_3 - $OCH_{3pectin}$)	10.9 (±9.5)	7.0 (±12.2)
Δ_D(CH_4 - bulk)	-280 (±25)	-202 (±26)
Δ_D (CH_4 - OCH_3)	-140 (±32)	-100 (±34)
Δ_D (bulk - OCH_3)	137 (±22)	123 (±28)

* Subtraction between median values of Table 1. Standard deviations given in brackets.

Table 7. List of plant leaves analyzed, relative isotopic analyses and fractionation factors α.

Plants-Compounds	δD-CH_4 (‰)	*δD-H_2O (‰)	bulk δD (‰)	δD-OCH_3 (‰)	α CH_4/H_2O	α CH_4/OCH_3	α CH_4/bulk	α OCH_3/H_2O	α OCH_3/bulk	α bulk/H_2O
Perennial ryegrass (*Lolium perenne,C3*)	-531.1	-101.2	-96.1	-309.0	0.52	0.68	0.52	0.77	0.76	1.01
	-445.7	-29.3	-94.0	-245.0	0.57	0.73	0.61	0.78	0.83	0.93
	-394.4	-4.9	-87.4	-237.0	0.61	0.79	0.66	0.77	0.84	0.92
	-370.4	50.2	-81.8	-206.0	0.60	0.79	0.69	0.76	0.86	0.87
	-327.3	114.8	-59.3	-194.0	0.60	0.83	0.72	0.72	0.86	0.84
	-551.0	-129.9	-105.7	-311.6	0.52	0.65	0.50	0.79	0.77	1.03
	-459.6	-40.3	-100.0	-276.8	0.56	0.75	0.60	0.75	0.80	0.94
	-465.3	-31.3	-93.0	n.m.	0.55	-	0.59	-	-	0.94
	-454.5	-17.9	-91.2	-258.7	0.56	0.74	0.60	0.75	0.82	0.93
	n.d.	1.9	-77.7	-249.3	-	-	-	0.75	0.81	0.92
Bean (*Phaseolus vulgari,C3*)	-580.6	-129.9	n.m.	n.m.	0.48	-	-	-	-	-
	-465.9	-40.3	n.m.	n.m.	0.56	-	-	-	-	-
	n.d.	-31.3	n.m.	n.m.	-	-	-	-	-	-
	-431.5	-17.9	n.m.	n.m.	0.58	-	-	-	-	-
	-410.9	1.9	n.m.	n.m.	0.59	-	-	-	-	-
Rockcress (*Arabidopsis thaliana,C3*)	-534.0	-129.9	n.m.	-295.4	0.54	0.66	-	0.81	0.70	-
	-473.8	-40.3	n.m.	-275.3	0.55	0.73	-	0.76	0.72	-
	n.d.	-31.3	n.m.	n.m.						
	-414.2	-17.9	n.m.	-267.2	0.60	0.80	-	0.75	0.73	-
	-356.7	1.9	n.m.	-278.9	0.64	0.89	-	0.72	0.72	-
Maize (*Zea mais,C4*)	n.d.	-101.2	-74.2	-226.8				0.86	0.84	
	-333.2	-29.3	-65.7	-166.3	0.69	0.80	0.71	0.86	0.89	0.96
	-254.5	-4.9	-61.2	-157.0	0.75	0.88	0.79	0.85	0.90	0.94
	-207.3	50.2	-50.5	-149.6	0.75	0.93	0.83	0.81	0.90	0.90
	-196.0	114.8	-27.3	-115.2	0.72	0.91	0.83	0.79	0.91	0.87
	-460.0	-129.9	-87.9	-247.1	0.62	0.72	0.59	0.87	0.83	1.05
	-359.9	-40.3	-81.7	-203.3	0.67	0.80	0.70	0.83	0.87	0.96
	-358.8	-31.3	-81.1	-197.2	0.66	0.80	0.70	0.83	0.87	0.95
	-291.5	-17.9	-74.5	-193.3	0.72	0.88	0.77	0.82	0.87	0.94
	-297.5	1.9	-73.2	-177.8	0.70	0.85	0.76	0.82	0.89	0.93
Sorghum (*Sorghum drummondii,C4*)	-443.4	-129.9	-87.7	-258.0	0.64	0.75	0.61	0.85	0.81	1.05
	-385.2	-40.3	-71.3	-200.6	0.64	0.77	0.66	0.83	0.86	0.97
	-345.0	-31.3	n.m.	n.m.	0.68	-	-	-	-	-
	-343.6	-17.9	-66.1	-190.9	0.67	0.81	0.70	0.82	0.87	0.95
	-325.3	1.9	-66.2	-176.0	0.67	0.82	0.72	0.82	0.88	0.93
				Average C3	0.57	0.75	0.61	0.76	0.79	0.93
				Average C4	0.68	0.83	0.72	0.83	0.87	0.95
				St.dev. C3	0.04	0.07	0.07	0.02	0.05	0.05
				St.dev. C4	0.04	0.06	0.07	0.02	0.03	0.05

*The δD-H2O is referring to the deuterium content of the water provided during the growing of the plants in spring-summer.
n.d. : not determined; n.m. : not measured

Table 8. List of conducted experiments for the deuterium labelling studies

Component	Temperature (°C)	Lamp (Vitalux)	Duration (h)	Blank (ppb)	$\delta D(CH_4)$ blank (‰)	End (ppb)	$\delta D(CH_4)$ end (‰)	$\delta D(CH_4)$ theoretical* (‰)	Emission rate (ng g^{-1} dw h^{-1})
Pectin untreated	80	-	14	1855	−83	2181	−107		3.7
Pectin label 0.05%	80		14	1855	−83	2074	1	18	2.5
PGA untreated	40	-	24	1937	−86	1962	−85		0.2
PGA methyl esterified 0% label	40	-	24	1937	−86	1981	−87	-	0.3
PGA methyl esterified 6% label	40	-	24	1937	−86	2029	1860	2740	0.7
PGA methyl esterified 22% label	40	-	24	1937	−86	n.d.	7310	-	n.d.
PGA untreated	60	-	24	1896	−83	1983	−89		0.7
PGA methyl esterified 0% label	60	-	24	1896	−83	2012	−89		0.9
PGA methyl esterified 6% label	60	-	24	1896	−83	2139	12800	27500	2.0
PGA methyl esterified 22% label	60	-	24	1896	−83	2051	54600	10500	1.2
PGA untreated	80	-	24	1877	−86	1960	−85		0.6
PGA methyl esterified 0% label	80	-	24	1877	−86	2225	−124		2.2
PGA methyl esterified 6% label	80	-	24	1877	−86	2075	20000	29400	1.3
PGA methyl esterified 22% label	80	-	24	1877	−86	2365	126000	284000	3.1
PGA untreated	30-38	X	2	1918	−78	n.d.	−84		n.d.
PGA methyl esterified 0% label	30-38	X	2	1918	−78	2048	−92		9.2
PGA methyl esterified 6% label	30-38	X	2	1918	−78	2104	7800	27600	13.8
PGA methyl esterified 22% label	30-38	X	2	1918	−78	n.d.	57500		n.d.
PGA untreated	30-38	X	7	1937	−65	2067	−66	-	2.6
PGA methyl esterified 0% label	30-38	X	7	1937	−65	2893	−127	-	18
PGA methyl esterified 6% label	30-38	X	7	1937	−65	3510	39500	138000	16
PGA methyl esterified 22% label	30-38	X	7	1937	−65	3397	163000	600000	15
PGA untreated	30-38	X	14	1943	−101	2196	−102	-	2.7
PGA methyl esterified 0% label	30-38	X	14	1943	−101	3755	−189	-	19
PGA methyl esterified 6% label	30-38	X	14	1943	−101	3574	59000	142000	33
PGA methyl esterified 22% label	30-38	X	14	1943	−101	4710	233000	825000	58

* theoretical value was calculated by the assumption that the increase of the mixing ratio in the vial (End – Blank) comes from methane that is entirely derived from labelled methoxyl groups (see theoretical methane values in Table 1)

Table 9. Methoxyl content and degree of labelling for esterified polygalacturonic acids and pectin are presented.

Sample	Methoxyl content (%)	Deuterium label %	Theoretical $\delta D(CH_4)$ (‰ vs VSMOW)*
Polygalacturonic acid esterified with unlabelled methanol	1.44	-	-
Polygalacturonic acid esterified with 5% CD_3OD labelled methanol	1.48	6.1	312000
Polygalacturonic acid esterified with 20% CD_3OD labelled methanol	2.30	22.6	1410000
Pectin treated with 5% CD_3OD labelled methanol	4.08	0.05	1660

* calculated using the following equation: δ^2H (‰) = (($^2H/^1H_{methoxyl}$ * 0.75) + ($^2H/^1H_{standard}$ *0.25) − $^2H/^1H_{standard}$))/ $^2H/^1H_{standard}$ x 1000‰ and the assumption that for the four hydrogen atoms of the formed CH_4 three hydrogen atoms (75%) are derived from the methoxyl group (OCH_3) and one (25%) comes either from surrounding water or the organic model compound with a theoretical value of δ^2H of 0 ‰ ($^2H/^1H_{standard}$).

Bibliography

Abrajano, T. A., et al. (1988), Methane-hydrogen gas seeps, Zambales Ophiolite, Philippines: Deep or shallow origin?, *Chemical Geology*, *71*(1-3), 211-222.
Anderson, D. Z., et al. (1984), Mirror reflectometer based on optical cavity decay time, *Appl. Opt.*, *23*(8), 1238-1245.
Araguas, L. A., et al. (1996), Global monitoring of the isotopic composition of precipitation, *J. Radioanal. Nucl. Chem.-Artic.*, *205*(2), 189-200.
Aselmann, I., and P. J. Crutzen (1989), Global distribution of natural freshwater wetlands and rice paddies, their net primary productivity, seasonality and possible methane emissions, *Journal of Atmospheric Chemistry*, *8*(4), 307-358.
Avissar, R., et al. (2002), The Large-Scale Biosphere-atmosphere Experiment in Amazonia (LBA): Insights and future research needs, *Journal of Geophysical Research-Atmospheres*, *107*(D20).
Bachelet, D., and H. U. Neue (1993), Methane emissions from wetland rice areas of Asia, *Chemosphere*, *26*(1-4), 219-237.
Badr, O., et al. (1991), Atmospheric methane: Its contribution to global warming, *Applied Energy*, *40*(4), 273-313.
Badr, O., et al. (1992a), Sinks for atmospheric methane, *Applied Energy*, *41*(2), 137-147.
Badr, O., et al. (1992b), Methane: A greenhouse gas in the Earth's atmosphere, *Applied Energy*, *41*(2), 95-113.
Baer, D. S., et al. (2002), Sensitive absorption measurements in the near-infrared region using off-axis integrated-cavity-output spectroscopy, *Applied Physics B: Lasers and Optics*, *75*(2), 261-265.
Barker, J. F., and P. Fritz (1981), Carbon isotope fractionation during microbial methane oxidation, *Nature*, *293*(5830), 289-291.
Bartlett, K. B., and R. C. Harriss (1993), Review and assessment of methane emissions from wetlands, *Chemosphere*, *26*(1-4), 261-320.
Bazhin, N. M. (2004), Influence of plants on the methane emission from sediments, *Chemosphere*, *54*(2), 209-215.
Beerling, D. J., et al. (2008), Missing methane emissions from leaves of terrestrial plants, *Global Change Biology*, *14*(0), 1-6.
Bergamaschi, P., et al. (1994), - High-precision direct measurements of 13CH4/12CH4 and 12CH3D/12CH4 ratios in atmospheric methane sources by means of a long-path tunable diode laser absorption spectrometer, - *33*(- 33), - 7716.
Bergamaschi, P., et al. (2000), Measurements of the carbon and hydrogen isotopes of atmospheric methane at Izana, Tenerife: Seasonal cycles and synoptic-scale variations, *J. Geophys. Res.*, *105*.
Bergamaschi, P., et al. (2006), Methane Emissions from Terrestrial Plants - On the discovery of CH4 emissions from terrestrial plants and its potential implications – comments on the paper of Keppler et al. [Methane emissions from terrestrial plants under aerobic conditions, Nature, 439, 2006], *DG Joint Research Centre, Institute for Environment and Sustainability, Scientific and Technical Research series, EUR 22240 EN*, ISBN 92-79-02007-02002, 02006 pp.
Bergamaschi, P., et al. (2007), Satellite chartography of atmospheric methane from SCIAMACHYon board ENVISAT: 2. Evaluation based on inverse model simulations, *J. Geophys. Res.*, *112*(D2), doi: 10.1026/2006JD007268.
Bernhard, G., et al. (1997), Measurements of spectral solar UV irradiance in tropical Australia, *J. Geophys. Res.*, *102*(D7), 8719-8730.
Bosse, U., and P. Frenzel (1998), Methane emissions from rice microcosms: The balance of production, accumulation and oxidation, *Biogeochemistry*, *41*(3), 199-214.
Bousquet, P., et al. (2006), Contribution of anthropogenic and natural sources to atmospheric methane variability, *Nature*, *443*(7110), 439-443.
Bowen, G. J., and J. Revenaugh (2003), Interpolating the isotopic composition of modern meteoric precipitation, *Water Resour. Res.*, *39*(10), 13.
Bowling, D. R., et al. (2009), Soil, plant, and transport influences on methane in a subalpine forest under high ultraviolet irradiance, *Biogeosciences*, *6*(7), 1311-1324.
Braunlich, M., et al. (2001), Changes in the global atmospheric methane budget over the last decades inferred from 13C and D isotopic analysis of Antarctic firn air, *J. Geophys. Res.*, *106*.
Breas, O., et al. (2002), The global methane cycle: Isotopes and mixing ratios, sources and sinks, *Isotopes in Environmental and Health Studies*, *37*(4), 257-379.
Brenninkmeijer, C. A. M., et al. (2003), Isotope effects in the chemistry of atmospheric trace compounds, *Chem. Rev.*, *103*(12), 5125-5161.

Bruggemann, N., et al. (2009), Nonmicrobial aerobic methane emission from poplar shoot cultures under low-light conditions, *New Phytologist*, *182*(4, doi:10.1111/j.1469-8137.2009.02797.x), 912-918.
Butenhoff, C. L., and M. A. K. Khalil (2007), Global Methane Emissions from Terrestrial Plants, *Environ. Sci. Technol.*, *41*(11, DOI: 10.1021/es062404i), 4032-4037.
Cantrell, C. A., et al. (1990), Carbon Kinetic Isotope Effect in the Oxidation of Methane by the Hydroxyl Radical, *J. Geophys. Res.*, *95*.
Cao, G., et al. (2008), Methane emissions by alpine plant communities in the Qinghai–Tibet Plateau, *Biol. Lett.*(doi: 10.1098/rsbl.2008.0373).
Carroll, J. J., and A. J. Dixon (2002), Regional scale transport over complex terrain, a case study: tracing the Sacramento plume in the Sierra Nevada of California, *Atmospheric Environment*, *36*(23), 3745-3758.
Christophe Gueret, M. D. a. F. B. (1997), Methane pyrolysis: thermodynamics, *chemical engineering science*, *52*(5), 815-827.
Cicerone, R. J., and R. S. Oremland (1988), Biogeochemical Aspects of Atmospheric Methane, *Global Biogeochem. Cycles*, *2*.
Collins, W. D., et al. (2006), Radiative forcing by well-mixed greenhouse gases: Estimates from climate models in the Intergovernmental Panel on Climate Change (IPCC) Fourth Assessment Report (AR4), *J. Geophys. Res.*, *111*(D14317, doi:10.1029/2005jd006713).
Craig, H. (1961), Isotopic Variations in Meteoric Waters, *Science*, *133*(3465), 1702-1703.
Crill, P. M., et al. (1987), Tropospheric Methane From an Amazonian Floodplain Lake, *J. Geophys. Res.*, *93*.
Criss, R. E., and J. Farquhar (2008), Abundance, notation, and fractionation of light stable isotopes, edited by G. J. MacPherson, et al., pp. 15-30, Mineralogical Soc Amer.
Crutzen, P., et al. (2006), Methane production from mixed tropical savanna and forest vegetation in Venezuela, *Atmos. Chem. Phys. Disc.*, *6*, 1-5.
Crutzen, P. J. (1991), Methane's sinks and sources, *Nature*, *350*, 380-381.
Davidson, E. A., and P. Artaxo (2004), Globally significant changes in biological processes of the Amazon Basin: results of the Large-scale Biosphere-Atmosphere Experiment, *Global Change Biology*, *10*(5), 519-529.
Delmas, R. (1994), An overview of present knowledge on methane emission from biomass burning, *Nutrient Cycling in Agroecosystems*, *37*(3), 181-190.
Devol, A. H., et al. (1988), Methane Emissions to the Troposphere From the Amazon Floodplain, *J. Geophys. Res.*, *93*.
Dillon, M. B., et al. (2002), Chemical evolution of the Sacramento urban plume: Transport and oxidation, *J. Geophys. Res.*, *107*.
Ding, W., and Z. Cai (2003), [Effect of plants on methane production, oxidation and emission], *Ying Yong Sheng Tai Xue Bao*, *14*(8), 1379-1384.
Dlugokencky, E. J., et al. (1998), Continuing decline in the growth rate of the atmospheric methane burden, *Nature*, *393*(6684), 447.
Dlugokencky, E. J., et al. (2001), Measurements of an Anomalous Global Methane Increase During 1998, *Geophys. Res. Lett.*, *28*.
Dlugokencky, E. J., et al. (2003), Atmospheric methane levels off: Temporary pause or a new steady-state?, *Geophys. Res. Lett.*, *30*.
do Carmo, J. B., et al. (2006), A source of methane from upland forests in the Brazilian Amazon, *Geophys. Res. Lett.*, *33*(4), L04809, doi:04810.01029/02005GL025436.
do Carmo, J. B. e. a. (2006), A source of methane from upland forests in the Brazilian Amazon, *Geophysical Research Letters*, *33*(L04809, doi:10.1029/2005GL025436).
Doronina, N. V., et al. (2004), Methanotrophs and methylobacteria are found in woody plant tissues within the winter period, *Microbiology*, *73*(6), 702-709.
Dueck, T., and A. van der Werf (2008), Are plants precursors for methane?, *New Phytologist*, *178*(4, doi:10.1111/j.1469-8137.2008.02468.x), 693-695.
Dueck, T. A., et al. (2007), No evidence for substantial aerobic methane emission by terrestrial plants: a ^{13}C-labelling approach *New Phytologist*, *175*, 29-35, doi : 10.1111/j.1469-8137.2007.02103.x.
Dueñas, C., et al. (1994), Consumption of methane by soils, *Environmental Monitoring and Assessment*, *31*(1), 125-130.
Dutaur, L., and V. L.V (2007), A global inventory of the soil CH4 sink, *global biogeochemical cycles*, *21*.
Ehhalt, D. H., and U. Schmidt (1978), Sources and sinks of atmospheric methane, *Pure and Applied Geophysics*, *116*(2), 452-464.

Etiope, G., et al. (2008), Reappraisal of the fossil methane budget and related emission from geologic sources, *Geophysical Research Letters*, *35*(9), 5.
Evans, J. R. (2007), Resolving methane fluxes, *New Phytologist*, *175*(1), 1-4.
FAO (2000), Global Forest Resources Assessment 2000—Main Report, *FAO Forestry Paper No. 140, Food and Agriculture Organization of the United Nations, Rome, 2001*.
Farquhar, G. D., et al. (1989), Carbon isotope discrimination and photosynthesis, *Annu. Rev. Plant Physiol. Plant Molec. Biol.*, *40*, 503-537.
Farquhar, G. D., and L. A. Cernusak (2005), On the isotopic composition of leaf water in the non-steady state, *Functional plant biology 32*(4), 293-303.
Feil, S. (2006), Plants surprise as methane producers, *Chemie in Unserer Zeit*, *40*(3), 158-158.
Ferretti, D., et al. (2006), Stable isotopes provide revised global limits of aerobic methane emissions from plants, *Atmos. Chem. Phys. Discuss.*, *6*, 5867-5875.
Ferretti, D. F., et al. (2005), Unexpected Changes to the Global Methane Budget over the Past 2000 Years, *Science*, *309*(5741), 1714-1717.
Fischer, H., et al. (2008), Changing boreal methane sources and constant biomass burning during the last termination, *Nature*, *452*(7189), 864-867.
Forster, P., et al. (2007), Changes in Atmospheric Constituents and in Radiative Forcing, in *Climate Change 2007: The Physical Science Basis. Contribution of Working Group I to the Fourth Assessment Report of the Intergovernmental Panel on Climate Change* edited by S. Solomon, et al., Cambridge University Press, Cambridge, United Kingdom and New York, NY, USA.
Franco, G. (2002), Inventory of California greenhouse gas emissions and sinks: 1990–1999., edited by S. California Energy Commission, CA (2002).
Frankenberg, C., et al. (2005), Assessing methane emissions from global space-borne observations, *Science*, *308*(5724), 1010-1014.
Frankenberg, C., et al. (2006), Satellite chartography of atmospheric methane from SCIAMACHY on board ENVISAT: Analysis of the years 2003 and 2004, *J. Geophys. Res.*, *111*(D7), D07303, 07310.01029/02005JD006235.
Frankenberg, C., et al. (2008), Tropical methane emissions: A revised view from SCIAMACHY onboard ENVISAT, *Geophys. Res. Lett.*, *35*(L1581, doi:10.1029/2008gl034300), 5.
Frankenberg, C., et al. (2009), Dynamic Processes Governing Lower-Tropospheric HDO/H2O Ratios as Observed from Space and Ground, *Science*, *325*(5946), 1374-1377.
Games, L. M., et al. (1978), Methane-producing bacteria: natural fractionations of the stable carbon isotopes, *Geochimica et Cosmochimica Acta*, *42*(8), 1295-1297.
Garnet, K. N., et al. (2005), Physiological control of leaf methane emission from wetland plants, *Aquatic Botany*, *81*(2), 141-155.
Gehre, M., et al. (2004), Continuous Flow 2H/1H and 18O/16O Analysis of Water Samples with Dual Inlet Precision, *Rapid Communications in Mass Spectrometry*, *18*(22, doi: 10.1002/rcm.1672), 2650-2660.
GNIP, et al. (2004), Global Network of Isotopes in Precipitation: The GNIP Database, edited, p. http://isohis.iaea.org, IAEA, Vienna.
Goldstein, A. H., et al. (2000), Effects of climate variability on the carbon dioxide, water, and sensible heat fluxes above a ponderosa pine plantation in the Sierra Nevada (CA), *Agric. For. Meteorol.*, *101*(2-3), 113-129.
Goldstein, A. H., and S. L. Shaw (2003), Isotopes of volatile organic compounds: An emerging approach for studying atmospheric budgets and chemistry, *Chem. Rev.*, *103*(12), 5025-5048.
Greule, M., et al. (2008), A rapid and precise method for determination of D/H ratios of plant methoxyl groups, *Rapid Commun. Mass Spectrom.*, *22*(doi:10.1002/rcm.3817), 3983-3988.
Greule, M., et al. (2009), A simple rapid method to precisely determine 13C/12C ratios of plant methoxyl groups, *Rapid Communications in Mass Spectrometry*, *23*(11, doi:10.1002/rcm.4057), 1710-1714.
Hackstein, J. H., and C. K. Stumm (1994), Methane production in terrestrial arthropods, *Proc Natl Acad Sci U S A*, *91*(12), 5441-5445.
Hansen, J., et al. (1997), Radiative forcing and climate response, *Journal of Geophysical Research-Atmospheres*, *102*(D6), 6831-6864.
Hao, W. M., and D. E. Ward (1993), Methane Production From Global Biomass Burning, *J. Geophys. Res.*, *98*.
Hendriks, D. M. D., et al. (2007), The full greenhouse gas balance of an abandoned peat meadow, *Biogeosciences*, *4*(3), 411-424.

Hendriks, D. M. D., et al. (2008), A compact and stable eddy covariance set-up for methane measurements using off-axis integrated cavity output spectroscopy, *Atmospheric Chemistry and Physics*, *8*(2), 431-443.
Herbelin, J. M., et al. (1980), Sensitive measurement of photon lifetime and true reflectances in an optical cavity by a phase-shift method, *Appl. Opt.*, *19*(1), 144-147.
Herzberg, G. (1972), Spektroskopische Untersuchung von Molek¸lstrukturen (Nobel-Vortrag), *Angewandte Chemie*, *84*(23), 1126-1142.
Hobbie, E. A., and R. A. Werner (2004), Intramolecular, compound-specific, and bulk carbon isotope patterns in C-3 and C-4 plants: a review and synthesis (vol 161, pg 371, 2004), *New Phytologist*, *161*(1, doi: 10.1046/j.1469-8137.2004.00970.x), 371-385.
Hopkin, M. (2007), Missing gas saps plant theory, *Nature*, *447*.
Houweling, S., et al. (2008), Early anthropogenic CH_4 emissions and the variation of CH_4 and C^{13}-CH_4 over the last millennium, *Global Biogeochemical Cycles*, *22*(1).
Houweling, S., et al. (2000), The modeling of tropospheric methane: How well can point measurements be reproduced by a global model?, *J. Geophys. Res.-Atmos.*, *105*(D7, doi: 10.1029/1999jd901149), 8981-9002.
Houweling, S., et al. (2006), Atmospheric constraints on global emissions of methane from plants, *Geophys. Res. Lett.*, *33*, L15821, doi:15810.11029/12006GL026162.
Houweling, S., et al. (2007), Early anthropogenic emissions and the variation of CH_4 and $^{13}CH_4$ over the last millennium, *Glob. Biogeochem. Cycl.*, *in press*.
Hut, G. (1987), Consultants' group meeting on stable isotope reference samples for geochemical and hydrological investigations, Report to the Director General, International Atomic Energy Agency, Vienna.
IAEA/WMO The Internetional Atomic Energy Agency (IAEA) and the World Meteorological Organizaton (WMO) of Global network for isotopes in precipitation. The GNIP Database (http://www-naweb.iaea.org/napc/ih/GNIP/IHS_GNIP.html), edited.
Ingall, E. D. (2008), Oceanography: Making methane, *Nature Geosci*, *1*(7), 419-420.
IPCC (2007), IPCC fourth assessment Report, Working group 3.
Irving, F., et al. (1982), Two New Carbonate Stable-Isotope Standards, *Geostandards and Geoanalytical Research*, *6*(1), 11-12.
Ishizuka, S., et al. (2005), The variation of greenhouse gas emissions from soils of various land-use/cover types in Jambi province, Indonesia, *Nutrient Cycling in Agroecosystems*, *71*(1), 17-32.
Ivanova, E., et al. (2006), Production of vitamin B12 in aerobic methylotrophic bacteria, *Microbiology*, *75*(4), 494-496.
Ivanova, E., et al. (2007), Hansschlegelia plantiphila gen. nov sp nov., a new aerobic restricted facultative methylotrophic bacterium associated with plants, *Systematic and Applied Microbiology*, *30*(6), 444-452.
Jacob, D. J., et al. (1990) Summertime Photochemistry of the Troposphere at High Northern Latitudes, *J. Geophys. Res.*, *97*.
Johnson, D. E., and G. M. Ward (1996), Estimates of animal methane emissions, *Environmental Monitoring and Assessment*, *42*(1), 133-141.
Kaiser, J. (2008), Reformulated 17O correction of mass spectrometric stable isotope measurements in carbon dioxide and a critical appraisal of historic [`]absolute' carbon and oxygen isotope ratios, *Geochimica et Cosmochimica Acta*, *72*(5), 1312-1334.
Karl, D. M., et al. (2008), Aerobic production of methane in the sea, *Nature Geosci*, *1*(7), 473-478.
Keppler, F., et al. (2000), Halocarbons produced by natural oxidation processes during degradation of organic matter, *Nature*, *403*(6767), 298-301.
Keppler, F., et al. (2004), Carbon isotope anomaly in the major C1 pool and its global biogeochemical implications, *Biogeosciences*, *1*, 123-131.
Keppler, F., et al. (2006), Methane emissions from terrestrial plants under aerobic conditions, *Nature*, *439*, 187-191, doi:110.1038/nature04420.
Keppler, F., et al. (2007), Stable hydrogen isotope ratios of lignin methoxyl groups as a paleoclimate proxy and constraint of the geographical origin of wood, *New Phytologist*, *176*(3, doi:10.1111/j.1469-8137.2007.02213.x), 600-609.
Keppler, F., and J. Hamilton (2008), Tracing the geographical origin of early potato tubers using stable hydrogen isotope ratios of methoxyl groups, Taylor & Francis Ltd.
Keppler, F., et al. (2008), Methoxyl groups of plant pectin as a precursor of atmospheric methane: evidence from deuterium labelling studies, *New Phytologist*, *178*(4, doi: 10.1111/j.1469-8137.2008.02411.x), 808-814.

Khalil, M. A. K., and R. A. Rasmussen (1983), Sources, Sinks, and Seasonal Cycles of Atmospheric Methane, *J. Geophys. Res.*, *88*.
Khalil, M. A. K., and R. A. Rasmussen (1985), Causes of increasing atmospheric methane: Depletion of hydroxyl radicals and the rise of emissions, *Atmospheric Environment (1967)*, *19*(3), 397-407.
Khalil, M. A. K., and R. A. Rasmussen (1987), Atmospheric methane: Trends over the last 10,000 years, *Atmospheric Environment (1967)*, *21*(11), 2445-2452.
Kirschbaum, M. U. F., et al. (2006), A comment on the quantitative significance of aerobic methane release by plants, *Functional Plant Biology*, *33*(6), 521-530.
Kirschbaum, M. U. F., et al. (2007), How Important is Aerobic Methane Release By Plants?, *Functional Plant Science and Biotechnology*, *1*(1), 138-145.
Kirschbaum, M. U. F., and A. Walcroft (2008), No detectable aerobic methane efflux from plant material, nor from adsorption/desorption processes, *Biogeosciences Discuss.*, *5*(4), 2773-2794.
Kitaoka, S., et al. (2007), Methane emission from Leaves of Larch, Birch and Oak Samplings Grown at Elevated CO2 Concentration in Northern Japan; Preliminary Study, *J. Agric. Meteorol.*, *63*(4), 201-206.
Konhauser, K. O., et al. (2009), Oceanic nickel depletion and a methanogen famine before the Great Oxidation Event, *Nature*, *458*(7239), 750-753.
Kroon, P. S., et al. (2007), Suitability of quantum cascade laser spectroscopy for CH4 and N2O eddy covariance flux measurements, *Biogeosciences*, *4*(5), 715-728.
Lamanna, M. S., and A. H. Goldstein (1999), In situ measurements of C2-C10 volatile organic compounds above a Sierra Nevada ponderosa pine plantation, *J. Geophys. Res.*, *104*.
Lassey, K. R., et al. (2007), Centennial evolution of the atmospheric methane budget: what do the carbon isotopes tell us?, *Atmospheric Chemistry and Physics*, *7*(8), 2119-2139.
Le Mer, J., and P. Roger (2001), Production, oxidation, emission and consumption of methane by soils: A review, *European Journal of Soil Biology*, *37*(1), 25-50.
Lelieveld, J., and P. J. Crutzen (1992), Indirect chemical effects of methane on climate warming, *Nature*, *355*(6358), 339.
Lelieveld, J., et al. (1998), Changing concentration, lifetime and climate forcing of atmospheric methane, *Tellus Series B-Chemical and Physical Meteorology*, *50*(2), 128-150.
Lelieveld, J. (2006), Climate change: A nasty surprise in the greenhouse, *Nature*, *443*, 405-406.
Lelieveld, J., et al. (2008), Atmospheric oxidation capacity sustained by a tropical forest, *Nature*, *452*(7188), 737-740.
Lima, I., et al. (2008), Methane Emissions from Large Dams as Renewable Energy Resources: A Developing Nation Perspective, *Mitigation and Adaptation Strategies for Global Change*, *13*(2), 193-206.
Limm, E., et al. (2009), Foliar water uptake: a common water acquisition strategy for plants of the redwood forest, *Oecologia*, *161*(3), 449-459.
Loreto, F., et al. (2008), Volatile organic compounds in the biosphere-atmosphere system: a preface, *Plant Biology*, *10*(1), 2-7.
Loulergue, L., et al. (2008), Orbital and millennial-scale features of atmospheric CH4 over the past 800,000[thinsp]years, *Nature*, *453*(7193), 383-386.
Lowe, D. C. (2006), Global change: A green source of surprise, *Nature*, *439*(7073), 148-149.
Matthews, E., and I. Fung (1987), Methane Emission From Natural Wetlands: Global Distribution, Area, and Environmental Characteristics of Sources, *Global Biogeochem. Cycles*, *1*.
Mayer, E. W., et al. (1982), Methane: Interhemispheric concentration gradient and atmospheric residence time, *Proc Natl Acad Sci U S A*, *79*(4), 1366-1370.
McLeod, A., et al. (2008), Ultraviolet radiation drives methane emission from terrestrial plant pectins, *New Phytologist*, *180*(DOI: 10.1111/j.1469-8137.2008.02571.x), 124-132.
McMahon, J., et al. (1972), The effect of pressure and temperature on the half-width of the methane absorption at 3.39[mu], *Journal of Quantitative Spectroscopy and Radiative Transfer*, *12*(5), 797-805.
Melack, J. M., et al. (2004), Regionalization of methane emissions in the Amazon Basin with microwave remote sensing, *Global Change Biology*, *10*(5), 530-544.
Messenger, D. J., et al. (2009), The role of ultraviolet radiation, photosensitizers, reactive oxygen species and ester groups in mechanisms of methane formation from pectin, *Plant Cell and Environment*, *32*(1), 1-9.
Miller, J. B., et al. (2002), Development of analytical methods and measurements of C-13/C-12 in atmospheric CH4 from the NOAA Climate Monitoring and Diagnostics Laboratory global air sampling network, *Journal of Geophysical Research-Atmospheres*, *107*(D13).
Miller, J. B., et al. (2007), Airborne measurements indicate large methane emissions from the eastern Amazon basin, *Geophys. Res. Lett.*, *34*(10), doi: 10.1029/2006GL029213.

Misson, L., et al. (2005), Influences of recovery from clearcut, climate variability, and thinning on the carbon balance of a young ponderosa pine plantation, *Agr. Forest Meteorol.*, *130*, 207-222.
Myhre, G., et al. (1998), New estimates of radiative forcing due to well mixed greenhouse gases, *Geophysical Research Letters*, *25*(14), 2715-2718.
Nisbet, R. E. R., et al. (2008), Emission of methane from plants, *Proc. R. Soc. B*.
Nouchi, I., et al. (1990), Mechanism of Methane Transport from the Rhizosphere to the Atmosphere through Rice Plants, *Plant Physiol*, *94*(1), 59-66.
O'Keefe, A., and D. A. G. Deacon (1988), Cavity ring-down optical spectrometer for absorption measurements using pulsed laser sources, *Review of Scientific Instruments*, *59*(12), 2544-2551.
Ortega, J., and D. Helmig (2008), Approaches for quantifying reactive and low-volatility biogenic organic compound emissions by vegetation enclosure, *Chemosphere*, *72*(3), 343-364.
Ortega, J., et al. (2008), Approaches for quantifying reactive and low-volatility biogenic organic compound emissions by vegetation enclosure, *Chemosphere*, *72*(3), 365-380.
P. J. Crutzen, E. S. C. A. M. B. (2006), Methane production from mixed tropical savanna and forest vegetation in Venezuela, *Atmospheric Chemistry and Physics Discussions (ACPD)*, *6*, 3093-3097.
Parsons, A. J., et al. (2006), Scaling methane emissions from vegetation, *Trends in Ecology & Evolution*, *21*(8), 423-424.
Pataki, D. E., et al. (2003), The application and interpretation of Keeling plots in terrestrial carbon cycle research, *Global Biogeochemical Cycles*, *17*(1).
Petit, J. R., et al. (1999), Climate and atmospheric history of the past 420,000 years from the Vostok ice core, Antarctica, *Nature*, *399*(6735), 429-436.
Phillips, D. L., and J. W. Gregg (2001), Uncertainty in source partitioning using stable isotopes, *Oecologia*, *127*(2), 171-179.
Piccot, S. D., et al. (1996), Global methane emissions from minor anthropogenic sources and biofuel combustion in residential stoves, *J. Geophys. Res.*, *101*.
Pickering, N. (1996), Physics of climate : J. P. Peixoto and A. H. Oort. New York, USA: American Institute of Physics, 1992. 520 pp. Price: US$ 45.00 (paperback). ISBN 0 88318 712 4, *Agricultural Systems*, *51*(2), 248-250.
Potter, C. S., et al. (1996), Estimation of global biogeochemical controls and seasonality in soil methane consumption, *Chemosphere*, *32*(11), 2219-2246.
Quay, P., et al. (1999), The isotopic composition of atmospheric methane, *Global Biogeochemical Cycles*, *13*(2), 445-461.
Ramachandran Purvaja, R. R. P. F. (2004), Plant-mediated methane emission from an Indian mangrove, *Global Change Biology*, *10*(11), 1825-1834.
Ramos, F., et al. (2009), Methane stocks in tropical hydropower reservoirs as a potential energy source, *Climatic Change*, *93*(1), 1-13.
Rasmussen, R. A., and M. A. K. Khalil (1981), Atmospheric Methane (CH4): Trends and Seasonal Cycles, *J. Geophys. Res.*, *86*.
Rasmussen, R. A., and M. A. K. Khalil (1983), Global production of methane by termites, *Nature*, *301*(5902), 700-702.
Rasmussen, R. A., and M. A. K. Khalil (1984a), Atmospheric Methane in the Recent and Ancient Atmospheres - Concentrations, Trends, and Interhemispheric Gradient, *Journal of Geophysical Research-Atmospheres*, *89*(ND7), 1599-1605.
Rasmussen, R. A., and M. A. K. Khalil (1984b), Atmospheric Methane in the Recent and Ancient Atmospheres: Concentrations, Trends, and Interhemispheric Gradient, *J. Geophys. Res.*, *89*.
Rasmussen, R. A., and M. A. K. Khalil (1986), Atmospheric Trace Gases: Trends and Distributions Over the Last Decade, *Science*, *232*(4758), 1623-1624.
Rice, A. L., et al. (2001), High-precision continuous-flow measurement of delta C-13 and delta D of atmospheric CH4, *Analytical Chemistry*, *73*(17), 4104-4110.
Ridgwell, J. R., et al. (1999), Consumption of atmospheric methane by soils: a process-based model, *Global Biogeochem. Cy.*, *13*(1), 59-70.
Rigby, M., et al. (2008), Renewed growth of atmospheric methane, *Geophys. Res. Lett.*, *35*.
Röckmann, T., et al. (2009), The isotopic composition of H2 from biomass burning - dependency on combustion efficiency, moisture content and δD of local precipitation, *J. Geophys. Res., submitted*.
Sanadze, G. A., and G. M. Dolidze (1960), Concerning the question of the chemical nature of the volatile substances in the leaves of some plants. [Salix alba; Populus simonii; Populus sosnowskyi], *Journal Name: Dokl. Bot. Sci. (Engl. Transl.); (United States); Journal Volume: 134:1-6; Other Information: Translated from Dokl. Akad. Nauk SSSR; 134: No. 1, 214-216(Apr 1960)*, Medium: X; Size: Pages: 203-204.

Sanhueza, E., and L. Donoso (2006), Methane emission from tropical savanna Trachypogon sp. grasses, *Atmos. Chem. Phys.*, *6*, 5315-5319.
Saueressig, G., et al. (1996), D/H Kinetic Isotope Effect in the Reaction CH4 + Cl, *Geophys. Res. Lett.*, *23*.
Schaefer, H., et al. (2006), Ice Record of $\delta^{13}C$ for Atmospheric CH_4 Across the Younger Dryas–Preboreal Transition, *Science*, *313*, 1109-1112.
Schaefer, H., and M. J. Whiticar (2008), Potential glacial-interglacial changes in stable carbon isotope ratios of methane sources and sink fractionation, *Global Biogeochemical Cycles*, *22*(1).
Schiermeier, Q. (2006a), Methane finding baffles scientists, *Nature*, *439*(7073), 128-128.
Schiermeier, Q. (2006b), The methane mystery, *Nature*, *442*(7104), 730-731.
Schimmelmann, A. (2002), Determination of the concentration and stable isotopic composition of nonexchangeable hydrogen in organic matter, *Analytical Chemistry*, *63*(21), 2456-2459.
Schmidt, H.-L., et al. (2003), Systematics of 2H patterns in natural compounds and its importance for the elucidation of biosynthetic pathways, *Phytochemistry Reviews*, *2*(1), 61-85.
Schoell, M. (1988), Multiple origins of methane in the Earth, *Chemical Geology*, *71*(1-3), 1-10.
Schoell, M., et al. (1988), Origin of methane in Lake Kivu (East-Central Africa), *Chemical Geology*, *71*(1-3), 257-265.
Scurlock, J. M. O., et al. (2001), Worldwide Historical Estimates and Bibliography of Leaf Area Index, 1932-2000, *ORNL Technical Memorandum TM-2001/268, Oak Ridge National Laboratory, Oak Ridge, Tennessee, U.S.A. , TM-2001/268*.
Sessions, A. L., et al. (2000), Determination of the H3 Factor in Hydrogen Isotope Ratio Monitoring Mass Spectrometry, *Analytical Chemistry*, *73*(2), 200-207.
Sharpatyi, V. A. (2007), On the mechanism of methane emission by terrestrial plants, *Oxidation Communications*, *30*(1), 48-50.
Sheppard, J. C., et al. (1981), Inventory of Global Methane Sources and Their Production Rates, *J. Geophys. Res.*, *87*.
Sinha, V., et al. (2007), Methane emissions from boreal and tropical forest ecosystems derived from in-situ measurements, *Atmos. Chem. Phys. Discuss.*, *7*(5), 14011-14039.
Smeets, C. J. P. P., et al. (2009), Eddy covariance methane measurements at a Ponderosa pine plantation in California, *Atmos. Chem. Phys.*, *9*(1), 5201-5229.
Smith, B. N., and H. Ziegler (1990), Isotopic fractionation of hydrogen in plants, *Bot. Acta*, *103*(4), 335-342.
Sowers, T. (2006), Late Quaternary Atmospheric CH4 Isotope Record Suggests Marine Clathrates Are Stable, *Science*, *311*(5762), 838-840.
Spahni, R., et al. (2005), Atmospheric Methane and Nitrous Oxide of the Late Pleistocene from Antarctic Ice Cores, *Science*, *310*, 1317-1321, DOI: 1310.1126/science.1120132.
Stadtman, T. C. (1967), Methane Fermentation, *Annual Review of Microbiology*, *21*(1), 121.
Steele, L. P., et al. (1987), The global distribution of methane in the troposphere, *Journal of Atmospheric Chemistry*, *5*(2), 125-171.
Sternberg, O. L., et al. (1984), Isotope Ratios of Cellulose from Plants Having Different Photosynthetic Pathways, *Plant Physiol*, *74*, 557-561.
Steudler, P. A., et al. (1996), Consequence of forest-to-pasture conversion on CH4 fluxes in the Brazilian Amazon Basin, *Journal of Geophysical Research-Atmospheres*, *101*(D13), 18547-18554.
Stoker, C. R., and M. A. Bullock (1997), Organic degradation under simulated Martian conditions, *J. Geophys. Res.-Planets*, *102*(E5), 10881-10888.
Striegl, R. G., and T. A. McConnaughey (1992), Consumption of atmospheric methane by desert soils, *Nature*, *357*(6374), 145.
Thurlow, M., et al. (1995), Methane uptake by unflooded paddy soils - the influence of soil - temperature and atmospheric methane concentration, *Soil Science and Plant Nutrition*, *41*(2), 371-375.
Toman, B., et al. (2006), New Guidelines for Î´13C Measurements, edited.
Tyler, S. C., et al. (2007), Stable isotope ratios in atmospheric CH4: Implications for seasonal sources and sinks, *Journal of Geophysical Research-Atmospheres*, *112*(D3).
Tzedakis, P. C., et al. (2009), Atmospheric methane, southern European vegetation and low-mid latitude links on orbital and millennial timescales, *Earth Planet. Sci. Lett.*, *277*(3-4), 307-317.
Vaghjiani, G. L., and A. R. Ravishankara (1991), New measurement of the rate coefficient for the reaction of OH with methane, *Nature*, *350*(6317), 406.
Verchot, L. V., et al. (2000), Land-use change and biogeochemical controls of methane fluxes in soils of eastern Amazonia, *Ecosystems*, *3*(1), 41-56.
Vigano, I., et al. (2008), Effect of UV radiation and temperature on the emission of methane from plant biomass and structural components, *Biogeosciences*, *5*(3), 937-947.

Vigano, I., et al. (2009b), Water drives the deuterium content of the methane emitted from plants, *Geochim. Cosmochim. Acta, submitted manuscript*.
Vigano, I., et al. (2009a), The stable isotope signature of methane emitted from plant material under UV irradiation, *Atmos. Environ., doi:10.1016/j.atmosenv.2009.07.046*.
Vogels, G. D. (1979), The global cycle of methane, *Antonie van Leeuwenhoek*, *45*(3), 347-352.
von Lerber, T., and M. W. Sigrist (2002), Cavity-Ring-Down Principle for Fiber-Optic Resonators: Experimental Realization of Bending Loss and Evanescent-Field Sensing, *Appl. Opt.*, *41*(18), 3567-3575.
Wahlen, M. (1993), The global methane cycle, *Annual Review of Earth & Planetary Sciences*, *21*, 407-426.
Waldron, S., et al. (1999), The global influence of the hydrogen isotope composition of water on that of bacteriogenic methane from shallow freshwater environments, *Geochimica et Cosmochimica Acta*, *63*(15), 2237-2245.
Walter, K. M., et al. (2006), Methane bubbling from Siberian thaw lakes as a positive feedback to climate warming, *Nature*, *443*(7107), 71-75.
Wang, Z.-P., et al. (2007), Aerobic methane emission from plants in the inner Mongolia steppe, *Env. Sci. Technol.*, doi:10.1021/es071224l.
Wang, Z. P., et al. (2008), Aerobic methane emission from plants in the Inner Mongolia steppe, *Environ. Sci. Technol.*, *42*(1), 62-68.
Wang, Z. P., et al. (2009), Physical injury stimulates aerobic methane emissions from terrestrial plants, *Biogeosciences Discuss.*, *6*(1), 1403-1420.
Watanabe, T., et al. (2009), Distinct members of a stable methanogenic archaeal community transcribe mcrA genes under flooded and drained conditions in Japanese paddy field soil, *Soil Biology & Biochemistry*, *41*(2), 276-285.
Webb, E. K. (1982), On the correction of flux measurements for effects of heat and water vapour transfer, *Boundary-Layer Meteorology*, *23*(2), 251-254.
Weiguo Liu, H. Y. (2008), Multiple controls for the variability of hydrogen isotopic compositions in higher plant n--alkanes from modern ecosystems, *Global Change Biology*, *14*(9), 2166-2177.
Werner, R. A., et al. (1999), ConFlo III – An Interface for High Precision δ13C and δ15N Analysis with an Extended Dynamic Range, *Rapid Communications in Mass Spectrometry*, *13*(13), 1237-1241.
White, J. (1988), *Stable hydrogen isotope ratios in plants: A review of current theory and some potential applications*, 142-162 pp., Springer-Verlag, Berlin.
Whiticar, M., and H. Schaefer (2007), Constraining past global tropospheric methane budgets with carbon and hydrogen isotope ratios in ice, *Phil. Trans. R. Soc. A*, *365*(1856), 1793-1828.
Whiticar, M. J. (1993), Atmospheric Methane: Sources, Sinks, and Role in Global Change, in *Atmospheric Methane: Sources, Sinks, and Role in Global Change*, edited by M. A. K. Khalil, pp. 138-167, Springer, Berlin.
Wille, C., et al. (2008), Methane emission from siberian arctic polygonal tundra: eddy covariance measurements and modeling, *Glob. Change Biol.*, *14*, 1395-1408.
Xie, M., et al. (2009), Methane emissions from terrestrial plants over China and their effects on methane concentrations in lower troposphere, *Chin. Sci. Bull.*, *54*(2, doi: 10.1007/s11434-008-0402-6), 304-310.
Yakir, D., and M. J. DeNiro (1990), Oxygen and Hydrogen Isotope Fractionation during Cellulose Metabolism in Lemna gibba L, *Plant Physiol.*, *93*(1), 325-332.
Yakir, D. (1992), Variations in the natural abundance of O18 and deuterium in plant carbohydrates, *Plant Cell and Environment*, *15*(9), 1005-1020.
Yamada, K., et al. (2006), Hydrogen and carbon isotopic measurements of methane from agricultural combustion: Implications for isotopic signatures of global biomass burning sources, *Journal of Geophysical Research-Atmospheres*, *111*(D16).
Zeikus, J. G., and W. J. C (1974), Methane formation in Living Trees: A Microbial Origin, *Science*, *184*(4142), 1181-1183.
Ziegler, H., et al. (1976), Hydrogen Isotope Discrimination in Higher Plants: Correlations with Photosynthetic Pathway and Environment, *Planta*, *128*, 85-92.
Zimmerman, P. R., et al. (1982), Termites: A Potentially Large Source of Atmospheric Methane, Carbon Dioxide, and Molecular Hydrogen, *Science*, *218*(4572), 563-565.
Zimmerman, P. R., and J. P. Greenberg (1983), Termites and methane, *Nature*, *302*(5906), 354-355.

Hartelijk bedankt!

I would like to thanks first of all the people who encouraged me to tear myself from the Alps, for taking a different adventure. Thanks to my father and mother, Mario and Fiorenza and my brother Mattia.

Vorrei ringraziare prima di tutto le persone che mi hanno incoraggiato a lasciare le Alpi per intreprendere questa avventura. Grazie a mio padre Mario, a mia madre Fiorenza e a mio fratello Mattia per esserci stati anche se a distanza.

Special thanks to Iryna, Zina and the Belorussian community who always believed in what I was doing.

Специальные спасибо к Iryna, Zina и белорусской общине которое всегда верили в чего я делал.

Thanks to Anna and Olga for their special support. Thanks to all my numerous friends of the "Compagnia dello Stadio" and "Chei de Berghem" for visiting me in Utrecht and bringing always pasta and wine from Italy. Thanks to all my friends from the Italian Alpine Club and from the School of Alpinism Leone Pellicioli.

I am indeed grateful to my supervisor Thomas Röckmann for hiring me in his Lab and accompanying me into the world of stable isotopes and for let me play with all the fantastic instruments. He has been really an excellent mind, always following my experiments and giving new ideas and tips in order to make the best out of the data. Special thanks to Marc Braß who taught me numerous secrets of the methane system BRETT. Thanks to my ex officemate and colleague, Rupert Holzinger for the great experience in California and for always carefully checking my results.

I left a piece of my heart in the Amazon forest and here I would like to mention some people from the Instituto Nacional de Pesquisas da Amazônia who I have been in touch. For the best days at the base camp in the forest: Gerardo, Tomé, Frans, Antonio, Giulio, Hermes, Amauri. For the scientific support: Carlos, Veber, Alessandro, Tota, and Lissandra. Thanks to Antonio Manzi, Paulo Artaxo and Luciana Gatti for giving us the possibility to work in such unique ecosystem.

Eu deixei uma parte de meu coração na floresta de Amazônia e aqui eu gostaria de mencionar alguns povos do Instituto Nacional de Pesquisas da Amazônia. Para os melhores dias no acampamento ZF2 na floresta: Gerardo, Tomé, Frans, Antonio, Giulio, Hermes, Amauri. Para a sustentação científica: Carlos, Veber, Alessandro, Tota, e Lissandra. Agradecimentos a Antonio Manzi, a Paulo Artaxo e a Luciana Gatti para dar-nos a possibilidade do trabalho em tal ecossistema original.

My life in Utrecht at the IMAU would have been not the same without having friends like my ex colleagues Francesco Spada, Motoki Sasakawa and with the other colleagues: Catalina, Adriaan, Leonie, Joralf, Pim, Sjoerd, Carlos, Celia, Sylvia, Joseph and Anneke. I am grateful to all Atmospheric Physic & Chemistry Group, especially the help from the technicians Carina and Michel, and to all IMAU staff for their warm welcome.

Very friendly people who I am particularly linked are Prof. Boros Mihaly and Prof. Miklos Ghyczy from the University of Szeged in Hungary. They invited me for short visit collaboration in their Institute of Surgical Research in which we found new interesting physiological results regarding the methane emitted from animals.

I would like to wish my acknowledgments to Giuseppe Etiope, Martin Schoell and the guys from the Istituto Naionale di Geofisica e Vulcanologia for their interest in my research, and for collaborating in the context of geological methane sources.

Thanks to Prof. Calin Baciu and all the geologists I met in Cluj Napoca in Romania for awarding my research as the most outstanding in gas geochemistry.

Thanks to the Benelux Association of Stable Isotopes (BASIS) for the grant as best young scientist in the field of stable isotopes.

How not to mention my friend Thomas Reerink, who spent with me the most adventurous climbing, expeditions around the Alps and not only. Thanks to Paul Leclercq for the fabulous ski tour in Aime (France) in the house of his parents.

Curriculum vitae

Ivan Vigano was born on 23rd December 1978 in Bergamo, Italy. In 1998 he took a Diploma from the high school Giulio Natta in industrial chemistry. The next year he entered the University of Milano-Bicocca to study Environmental Sciences where he spent 3 years plus 2 years of Master specialization in Atmospheric Sciences. After one an half year of Thesis, he graduated in 2004 with the title "The Alps: annual study of snow precipitations in remote locations". The research aimed to show for the first time the chemical and physical properties of the dust in snow precipitations along the alpine arc. During his University life he became instructor of Alpinism in the National School of Alpinism Leone Pellicioli where he attended several climbing courses. After the graduation he moved to London to take and advanced English course and to work as bartender. Thereafter he returned to Bergamo were he has done several jobs and volunteering for the Mato Grosso Operation which helps needy people in South America. In November 2005 he began his PhD in Atmospheric Chemistry under the supervision of the Prof. T.Röckmann on atmospheric stable isotopes applications. He was few months later involved in the project of methane emissions from plants. In 2006 he was involved with Marc Braß in the complete removal of the isotope lab, which was moved from the Max Planck Institute for Nuclear Physic in Heidelberg, Germany, to the IMAU (Institute for Marine and Atmospheric Research, Utrecht), The Netherlands. In 2007 he took part in a field campaign in Sierra Nevada (California, U.S.), in order to measure for the first time in U.S., methane fluxes with Eddy Covariance techniques. He was, from 2006, member of the Large Scale Biosphere-Atmosphere Experiment in Amazonia (LBA) where he was responsible for the organization of the Dutch team from the IMAU. He participated in November-December 2008 for the first part of the LBA project and in April 2009 for the second part. He also organized and supervised the installation of various equipments for methane measurements in the Amazon forest. He supervised and taught to local students how to operate sampling units for gas analyses. In 2008 he earned also a grant from the Benelux Association of Stable Isotopes (BASIS) as best young scientist in stable isotopes. In 2009 his research was awarded from the Cluj-Napoca University in Romania, as the most outstanding in gas geochemistry.
In 2009 he was also collaborating with Prof. Boros Mihaly and Prof. Miklos Ghyczy from the Institute of Surgical Research, University of Szeged (Hungary), for a project on methane formation in animals.
In the last months of his PhD project he was also collaborating with Dr. Giuseppe Etiope from the Italian institute for geophysics and volcanology (INGV, Istituto Nazionale di Geofisica e Vulcanologia) and with Prof. Dario Tedesco (Department of Environmental Sciences, University of Napoli 2) for measuring methane emissions and isotope values from different geological sources.
In this thesis are presented the main results of the research carried out in 4 years of PhD studies at the IMAU. The date of his PhD defense has been fixed in Utrecht the 8th of January 2010.

Publications

Vigano, I., van Weelden, H., Holzinger, R., Keppler, F., McLeod, A., and Röckmann, T., (2008), Effect of UV radiation and temperature on the emission of methane from plant biomass and structural components, *Biogeosciences, 5*(3), 937-947.

Vigano, I., Röckmann, T., Holzinger, R., van Dijk, A., Keppler, F., Greule, M., Brand, W.A., Geilmann, H., van Weelden, H., (2009), The stable isotope signature of methane emitted from plant material under UV irradiation, *Atmos. Environ.*, *doi:10.1016/j.atmosenv.2009.07.046*.

Vigano, I., Röckmann, T., Holzinger, R., van Dijk, A., Keppler, F., Greule, M., Brand, W.A., Geilmann, H., van Weelden, H., (2009), Water drives the deuterium content of the methane emitted from plants, *Geochim. Cosmochim. Acta*, *submitted manuscript*.

Smeets C. J. P. P., Holzinger R., Vigano I., Goldstein A. H., Röckmann, T., (2009), Eddy covariance methane measurements at a Ponderosa pine plantation in California, *Atmos. Chem. Phys*., 9(1), 5201-5229.

F. Keppler, F., Hamilton, J.T.G., McRoberts, W.C., Vigano, I., Braß, M., and Röckmann, T., (2008), Methoxyl groups of plant pectin as a precursor of atmospheric methane: evidence from deuterium labelling studies, *New Phytol.*, 178, 808-814, doi: 10.111/j.1469-8373.2008.02411.x, 2008.